Aalto-yliopisto
Insinööritieteiden
korkeakoulu

Vladimir Lopatinski

Vortex induced vibrations in high-rise buildings

Diplomityö, joka on jätetty opinnäytteenä tarkastettavaksi diplomi-insinöörin tutkintoa varten.

Espoossa 25.05.2020
Valvoja: professori Jarkko Niiranen
Ohjaaja: diplomi-insinööri Joona Tuikka

Aalto-yliopisto
Insinööritieteiden
korkeakoulu

Aalto-yliopisto, PL 11000, 00076 AALTO
www.aalto.fi

Diplomityön tiivistelmä

Tekijä Vladimir Lopatinski

Työn nimi Pyörteiden aiheuttama korkeiden rakennusten poikittaisvärähtely

Maisteriohjelma Rakennustekniikka **Koodi** ENG27

Työn valvoja professori Jarkko Niiranen

Työn ohjaaja diplomi-insinööri Joona Tuikka

Päivämäärä 25.05.2020 **Sivumäärä** 70+29 **Kieli** Englanti

Tiivistelmä

Tämän työn painopisteenä on käyttörajatilan tarkastelu korkeissa rakennuksissa. Tuulesta johtuva korkean rakennuksen värähtely saattaa aiheuttaa liikkeestä johtuvaa pahoinvointia sisällä olijoille. Jos rakennus on tarpeeksi hoikka, kuten suurin osa korkeista rakennuksista, tuulta vasten poikkisuuntainen värähtely on merkittävin tuulesta johtuva värähtely.

Tässä työssä esitellään tämänhetkiset työkalut poikkisuuntaisen värähtelyn arvioimiseksi projektin alkuvaiheessa. Standardit ja kirjallisuus tarjoavat käsinlaskentamenetelmiä kiihtyvyysvasteen arvioimiseksi. Tässä työssä esitellään tieteellisenä panoksena proseduuri, joka perustuu pyörrerataherätteen teoriaan, käyttäen elementtimenetelmää yhdessä pyörreratateorian kanssa poikkisuuntaisen kiihtyvyysvasteen arvioimiseksi.

Laskelmien tuloksissa oli hajontaa, mikä osoittaa, että pyörreratailmiö on monimutkainen ilmiö. Standardien ja kirjallisuuden tarjoamia kaavoja tulee käyttää vain alustavaan suunnitteluun. Erityisesti tulokset Eurokoodilla laskemalla ovat kertaluokkaa liian suuret, eikä niitä voi hyödyntää edes alustavaan korkeiden rakennuksien suunnitteluun.

Tässä työssä elementtimenetelmällä laskemalla tulokset olivat lähellä tuloksia, jotka oli laskettu standardeilla sekä kirjallisuudella pois lukien Eurokoodin avulla lasketut arvot, jotka olivat merkittävästi suuremmat. Vaikka elementtimenetelmässä oli tehty useampi konservatiivinen oletus, vaste oli lähes kaikissa tapauksissa pienempi kuin standardeilla laskemalla. Tämän menetelmän tarkkuutta täytyy vielä arvioida vertaamalla tuloksia täysimittaisiin mittauksiin.

Avainsanat korkea rakentaminen, aikahistoria-analyysi, pyörreratailmiö, standardi, kiihtyvyys

Aalto University
School of Engineering

Aalto University, P.O. BOX 11000, 00076 AALTO
www.aalto.fi

Abstract of master's thesis

Author Vladimir Lopatinski		
Title of thesis Vortex induced vibrations in high-rise buildings		
Master programme Building Technology		**Code** ENG27
Thesis supervisor Associate Professor Jarkko Niiranen		
Thesis advisor Master of Science Joona Tuikka		
Date 25.05.2020	**Number of pages** 70+29	**Language** English

Abstract

The focus of this study is on the serviceability limit state of high-rise buildings. Wind induced vibration in high-rise buildings may cause motion induced discomfort for the occupants. If a building is slender enough, which is the case in most high-rise buildings, across-wind acceleration due to vortex shedding is the leading cause of wind induced acceleration.

In this study current tools available are presented to evaluate acceleration response in the early stages of the project for preliminary design. Standards and literature provide hand calculation equations for evaluation. Based on the theory of vortex shedding phenomena, the finite element method is adopted in this study as a scientific contribution to evaluate across-wind response.

In this study it was discovered that current tools provide very scattered results and should not be used as a base for final design. Especially acceleration response results calculated by Eurocode are in the order of magnitude higher than the results by other standards and literature, making Eurocode insufficient for predicting acceleration response even for preliminary design.

Procedure based on finite element method was built by making multiple conservative assumptions and it was found to predict reasonably well, with results being near the predictions made by standards and literature. In most cases, results from standards were more conservative than predictions made by the procedure based on finite element method. This procedure needs further testing against full-scale measurements to evaluate its accuracy.

Keywords high-rise building, time history analysis, vortex shedding, standard, acceleration

Preface

Firstly, I would like to thank Ramboll Finland Oy for providing and funding this very interesting research. Special thanks go to my advisor Joona Tuikka from Ramboll, for steering the focus of this thesis in the right direction and answering all the questions I had. I would also like to thank my supervisor Associate Professor Jarkko Niiranen from Aalto University for helping with the organization of the content.

I would like to give my appreciation is given to the Lecturer from Aalto University Tommi Mikkola, for his in-depth explanation of fluid mechanics related to this study and for making me pay attention to the relevant information. Lastly, I would like to thank Nicky Lim from Ramboll for his time to help with the design standards interpretation and calculation.

Espoo 25.5.2020

Vladimir Lopatinski

Table of Contents

List of symbols

General symbols used in the study:

A	[-]	constant of roughness length for turbulence
A_{max}	[m/s^2]	peak acceleration
C_L	[-]	lift coefficient
$C_{L,rms}$	[-]	RMS of lift coefficient
F_L	[N]	lift force
I_u	[-]	turbulence intensity
K_a	[-]	aerodynamic parameter
R	[year]	return period
Re	[-]	Reynolds number
Sc	[-]	Scruton number
Sc_G	[-]	general non-dimensional mass-damping parameter
St	[-]	Strouhal number
T	[s]	sample size
$\overline{U}$	[m/s]	mean wind velocity
$\widehat{U}$	[m/s]	peak gust
b	[m]	width of the structure (the dimension perpendicular to the wind direction)
d	[m]	depth of the structure (the dimension parallel to the wind direction)
f	[Hz]	frequency
f_1	[Hz]	fundamental frequency of structure
f_e	[Hz]	natural frequency of structure
f_s	[Hz]	shedding frequency
f_s^L	[Hz]	lower boundary of shedding frequency
f_s^U	[Hz]	upper boundary of shedding frequency
g	[-]	peak gust factor
h	[m]	height of structure
k	[-]	mode shape parameter
k_p	[-]	peak factor
k_r	[-]	terrain factor
m_e	[kg/m]	mass of the structure per unit length
u, u'	[m/s]	turbulence wind component
u_*	[m/s]	friction velocity
$\ddot{u}_{max}$	[m/s^2]	horizontal peak acceleration
y_{max}	[m]	maximum across-wind amplitude at critical wind speed
z	[m]	height above the ground
z_0	[m]	roughness length
z_h	[m]	zero-plane displacement
z_{min}	[m]	minimum height above the ground
Δt	[s]	time-step
α	[-]	exponent of power law for wind profile
δ_s	[-]	structural logarithmic decrement of damping
ζ_a	[-]	aerodynamic damping ratio

η_j	[-]	critical damping ratio for *j*th mode
κ	[-]	von Karman's constant
ρ	[kg/m^3]	air density
σ_u	[m/s]	standard deviation of longitudinal wind velocity
$\sigma_{\ddot{u}}$	[m/s^2]	standard deviation of acceleration of structure
τ	[Hz]	upcrossing frequency
υ	[m^2/s]	kinematic viscosity

Symbols used in EN 1991-1-4:

C_c	[-]	aerodynamic constant
K	[-]	mode shape factor; shape parameter
K_a	[-]	aerodynamic damping parameter
K_w	[-]	correlation length factor
L_j	[m]	correlation length
Re	[-]	Reynolds number
Sc	[-]	Scruton number
St	[-]	Strouhal number
T	[year]	return period
a	[m/s^2]	peak structure across-wind acceleration
a_L	[-]	normalized limiting amplitude
b	[m]	width of the structure (the dimension perpendicular to the wind direction)
c_{dir}	[-]	directional factor
c_f	[-]	force coefficient
c_{lat}	[-]	aerodynamic exciting coefficient
c_{prob}	[-]	probability factor
c_r	[-]	roughness factor
c_o	[-]	orography factor
c_{season}	[-]	seasonal factor
d	[m]	depth of the structure (the dimension parallel to the wind direction)
h	[m]	height of structure
k_p	[-]	peak factor
k_r	[-]	terrain factor
m_b	[kg]	mass of the structure
m_z	[kg/m]	mass of the structure per unit length
$m_{i,e}$	[kg/m]	equivalent mass of the structure per unit length for mode *i*
n_i	[Hz]	natural frequency of the structure of the mode *i*
v_{crit}	[m/s]	critical wind velocity of the vortex shedding
v_m	[m/s]	mean wind velocity
$v_{b,0}$	[m/s]	fundamental value of the basic wind velocity
n_b	[m/s]	basic wind velocity
y_{max}	[m]	maximum across-wind amplitude at the critical wind speed
z	[m]	height above the ground
z_0	[m]	roughness length
Φ_1	[-]	fundamental modal shape
δ_s	[-]	structural logarithmic decrement of damping
λ	[-]	slenderness ratio

ρ	[kg/m^3]	air density
σ_y	[m]	standard deviation of deflection
ζ	[-]	exponent of mode shape

Symbols used in NBCC 2005:

B	[-]	background turbulence factor
C_e	[-]	exposure factor
D	[m]	depth of the structure (the dimension parallel to the wind direction)
F	[-]	gust energy ratio
H	[m]	height of structure
I_w	[-]	importance factor
T	[s]	sample time
V	[m/s]	reference wind velocity
V_H	[m/s]	mean wind velocity at top of the structure
W	[m]	width of the structure (the dimension perpendicular to the wind direction)
a_r	[m/s^2]	-
a_w	[m/s^2]	peak structure across-wind acceleration
g	[m/s^2]	gravity constant
g_p	[-]	peak factor
n_0	[Hz]	fundamental frequency of the structure
n_w	[Hz]	first modal frequency of the structure
s	[-]	size reduction factor
z	[m]	height of interest above the ground
z_{ref}	[m]	reference height above the ground
α	[-]	power exponent
β_D	[-]	ratio of critical damping in along-wind direction
β_W	[-]	ratio of critical damping in across-wind direction
ν	[Hz]	upcrossing frequency
ρ_b	[kg/m^3]	density of structure

Symbols used in AIJ:

B	[m]	width of the structure (the dimension perpendicular to the wind direction)
D	[m]	depth of the structure (the dimension parallel to the wind direction)
C'_L	[-]	RMS overturning moment coefficient
E_H	[-]	wind speed profile factor at reference height H
E_r	[-]	exposure factor of flat terrain categories
F_L	[-]	wind spectrum factor in across-wind direction
H	[m]	reference height
K_D	[-]	directionality factor
M_L	[kg]	generalized mass of building for across-wind vibration
R_L	[-]	resonance factor for across-wind vibration
U_0	[m/s]	basic wind speed

U_H	[m/s]	design wind speed
U^*_{Lcr}, U^*_{Tcr}	[m/s]	non-dimensional critical wind speed for aeroelastic instability in across-wind and torsional directions
Z	[m]	height above the ground
Z_b, Z_G	[m]	parameters determining exposure factor
a_{Lmax}	[m/s^2]	maximum response acceleration in across-wind direction at top of building.
f_L	[Hz]	natural frequency for first mode in across-wind direction
f_T	[Hz]	natural frequency for first mode in torsional direction
g_{aL}	[-]	peak factor in across-wind direction
k_{rW}	[-]	return period conversion factor
q_H	[N/m^2]	velocity pressure at height *H*
r	[year]	design return period
α	[-]	exponent of power law for wind profile
β	[-]	exponent of power law for vibration mode
ζ_L	[-]	critical damping ratio for first mode in across-wind direction
λ	[-]	mode correction factor of general wind force
λ_U	[-]	wind velocity return period ratio

Symbols used in AS/NZS 1170.2:

C	[-]	return period conversion factor
C_{fs}	[-]	across-wind force spectrum coefficient generalized for a linear mode shape
I_h	[-]	turbulence intensity
K_m	[-]	mode shape correction factor for across-wind acceleration
$M_{z,cat}$	[-]	terrain/height multiplier
V_{des}	[m/s]	design wind speed
V_n	[-]	reduced wind velocity
b	[m]	width of the structure (the dimension perpendicular to the wind direction)
g_R	[-]	peak factor for resonant response
g_v	[-]	peak factor for the upwind velocity fluctuations
h	[m]	height of structure
k	[-]	mode shape power exponent for the fundamental mode
m_0	[kg/m]	average mass per unit height
n_e	[Hz]	natural frequency for first mode in across-wind direction
$\ddot{y}_{max}$	[m/s^2]	peak acceleration at the top of a structure in across-wind direction
ρ	[kg/m^3]	air density
ζ	[-]	ratio of structural damping to critical damping of a structure

Symbols used in the method by Emil Simiu:

A	[m^2]	area of horizontal section of the building

B	[m]	width of the structure (the dimension perpendicular to the wind direction)
C, p	[-]	empirical constants
D	[m]	depth of the structure (the dimension parallel to the wind direction)
H	[m]	height of structure
$\bar{V}(H)$	[m/s]	mean hourly wind velocity at height H
n_1	[Hz]	fundamental natural frequency in across-wind direction
z	[m]	height above the ground
ρ	[kg/m^3]	air density
ρ_b	[kg/m^3]	mass of building per unit volume
ζ	[-]	damping ratio

Abbreviations

AIJ	Architectural Institute of Japan
ASCE	American Society of Civil Engineers
CoV	Coefficient of Variation
FEM	Finite Element Method
ISO	International Organization for Standardization
NBCC	National Building Code of Canada
RMS	Root Mean Square
VIV	Vortex Induced Vibration

1 Introduction

1.1 Background

Wind induced oscillations of high-rise buildings are directly affecting habitability, where across-wind vibration is more significant than along-wind vibration when the structure is slender enough. The leading cause of across-wind acceleration for conventional high-rise buildings is vortex shedding. Vortex shedding is an oscillating flow behind the long, prismatic bluff body. It may appear on slender structures like chimneys, buildings, or bridge decks. The phenomenon is also known as Von Karman vortex street for the vortex tail it leaves behind the bluff body. A full analytical solution for this problem is not yet available and the procedures predicting vortex-induced vibrations are not fully reliable (Dyrbye & Hansen 1997, Hansen 2007). Therefore, there are many different approaches to describe this phenomenon mathematically. Eurocode, for example, has two different approaches: vortex-resonance and spectral model.

1.2 Aim and objectives

The aim of this thesis is to investigate across-wind acceleration response due to wind load on high-rise buildings. Another objective is to present design tools that evaluate across-wind acceleration significance in the early stages of the project. The main goal of the study is to evaluate the reliability of different methods for across-wind acceleration prediction.

The objective is to find high risk areas in high-rise buildings early in the design process when changes in shape, length, slenderness or structural elements are easy to implement.

Another objective is to increase understanding of what factors are affecting vortex shedding and their weight between each other to make reliable design.

1.3 Limitations

This thesis is focused on vortex shedding phenomenon and on the resulting building response. Determination of total damping of the structure is out of scope as well as investigation of damping systems. Also, determination of natural periods of structure is out of scope and is taken as known information from the model. The impact of surrounding buildings is considered only broadly as terrain category, leaving direct effect of other surrounding high-rise buildings out of scope. Regarding to building shape, the focus of this study is on non-tapered, square cross-sectional buildings with sharp corners. Effects of aerodynamic improvements are out of scope in this study. Computational fluid dynamic analysis is also out of scope as well as fatigue analysis.

1.4 Outline of report

In the 2nd chapter relevant wind properties to the vortex shedding are presented. In the 3rd chapter, the relationship between building and vortex shedding is explained and habitability criteria are introduced. In the 4th chapter approaches of calculation prediction of acceleration by different standards and literature is presented. In the 5th chapter 2D

finite element method to evaluate equivalent force caused by shedding frequency is presented. In the 6th chapter results from the 2D finite element method are used in 3D finite element software to acquire building acceleration. In the 7th chapter results are discussed and methods for acceleration calculation are evaluated.

2 Wind load

Mathematically total wind load is determined by 3 components (Hansen 2007, Dyrbye & Hansen 1997):

1. Net gust wind load due to air turbulence
2. Net vortex shedding wind load
3. Motion induced wind load.

The focus in this thesis is on net vortex shedding load. In this chapter the main theory and properties related to wind load are discussed. Logarithmic and power law theories are explained. Wind velocity profile concept is introduced as well as terrain influence on the wind profile. Also, in this chapter the impact of wind turbulence on high-rise buildings in along- and across-wind directions is discussed.

2.1 Mean wind velocity

All design codes and standards base their response calculations on basic wind velocity, which is then transformed into design wind velocity. Basic wind velocity is obtained from local climate history analysis. The value is a maximum of X minutes/seconds mean wind velocity at 10 meters above the ground. For example, Eurocode uses characteristic 10-minute mean wind velocity at 10 meters height above the ground as basic wind velocity (SFS-EN 1991-1-4 2005).

Figure 1 presents wind velocity variation with averaging time. The presented chart can be used to calculate wind mean velocity of X seconds for given mean velocity and gust duration. This is a useful tool to transform basic wind speeds for different codes and standards since different gust duration are used for basic wind speeds.

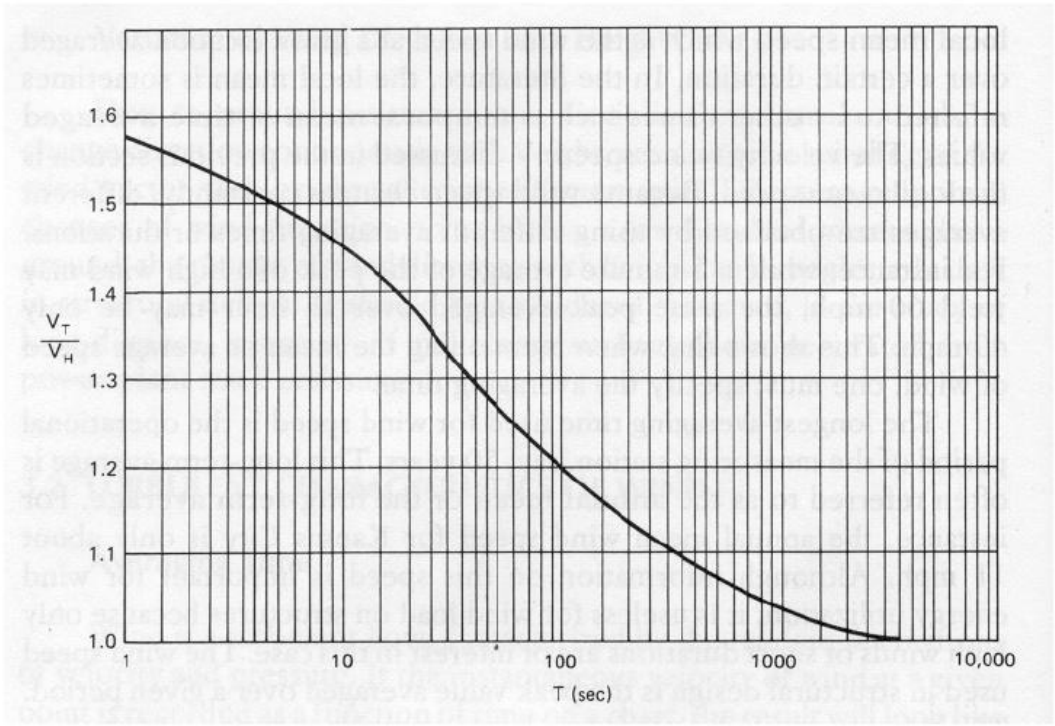

Figure 1. Wind velocity variation with averaging time for non-hurricane conditions (Liu 1991).

2.2 Wind velocity profile

In this section mean wind variation over height above ground near the surface is considered. Two leading mathematical expressions for wind profile are presented: 'Logarithmic law' and 'Power law'.

2.2.1 The 'Logarithmic law'

Logarithmic law is a semi-empirical relationship originally derived by Prandtl. This law has been found to predict the wind profile well in strong wind conditions in the atmospheric boundary near the surface (Holmes 2015.) Wind speed at height z is defined as:

$$\overline{U}(z) = \frac{u_*}{\kappa} \ln\left(\frac{z}{z_0}\right) \tag{1}$$

where u_* is friction velocity, z is height above the ground, z_0 is roughness length and κ is *von Karman's constant.* It has been found experimentally that constant k is about 0.4. Roughness length is measure of roughness of the ground surface. Constants depending on terrain type are presented in Table 1.

A useful way to apply logarithmic law is to solve desired wind speed at height z_1 with the help of reference wind speed at height z_2 by following expression:

$$\frac{U(z_1)}{U(z_2)} = \frac{\ln\left[\frac{(z_1 - z_h)}{z_0}\right]}{\ln\left[\frac{(z_2 - z_h)}{z_0}\right]} \tag{2}$$

where z_h is zero-plane displacement.

2.2.2 The 'Power law'

The Power law is purely empirical. It is easily integrated over a height, which is convenient for response calculation purposes (Holmes 2015.) Wind speed at height z is defined as:

$$\overline{U}(z) = \overline{U}_{10}\left(\frac{z}{10}\right)^{\alpha} \tag{3}$$

where $\overline{U}_{10}$ is mean wind speed at 10 m height, z is height above the ground and exponent α is dependent on terrain roughness. Table 1 presents the relation of exponent α to the roughness length.

Figure 2 presents comparison between power law and logarithmic law with z_{ref} = 100 m and terrain category I with defined reference wind velocity 30 m/s at z_{ref} height.

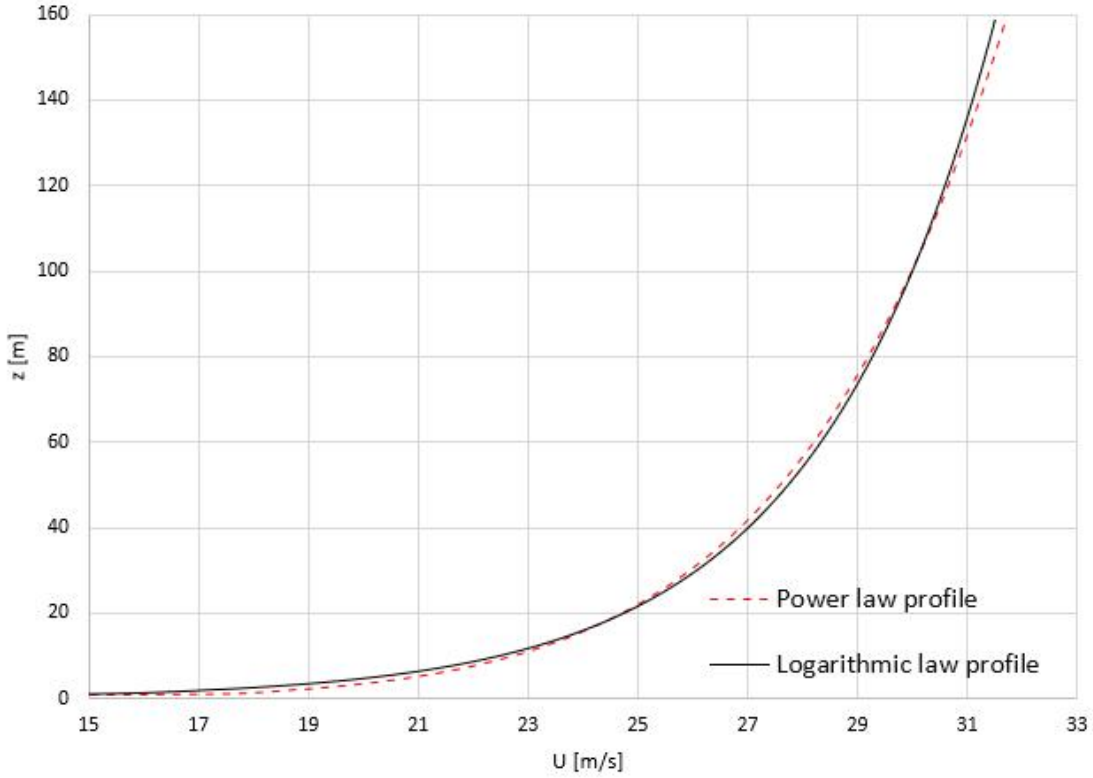

Figure 2. Comparison between power law and logarithmic law.

2.2.3 Terrain categories

Table 1. Terrain categories and parameters. Table 4.1 in EN 1991-1-4 and Table 3.2 in Dyrbye & Hansen (1997) combined.

	Terrain category	z_0[m]	z_{min}[m]	k_r[-]	α
0	Sea or coastal area exposed to open sea	0.003	1	0.16	-
I	Lakes or flat and horizontal area with negligible vegetation and without obstacles	0.01	1	0.17	0.12
II	Area with low vegetation such as grass and isolated obstacles (trees, buildings) with separations of at least 20 obstacle heights	0.05	2	0.19	0.16
III	Area with regular cover of vegetation or buildings or with isolated obstacles with separations of maximum 20 obstacle heights (such as villages, suburban terrain, permanent forest)	0.3	5	0.22	0.22
IV	Area in which at least 15% of the surface is covered with buildings and their average height exceeds 15 m	1.0	10	0.24	0.3

z_0 can be interpreted as the size of a characteristic vortex created by friction between air and terrain. z_{min} is the height below which wind velocity is assumed to be constant. k_r is terrain factor, which is proportional to roughness length and α is Power law exponent. Table 2 expresses different standards of terrain categories equivalent with each other.

Table 2. Terrain categories comparison between standards by Kwon & Kareem (2013).

ASCE	AS/NZS	AIJ	CNS	NBCC	EU	ISO	IWC
-	4	V	-	-	-	4	4
-	-	IV	D	C	IV	-	-
B	3	III	C	B	III	3	3
C	2	II	B	A	II	2	2
D	1	I	A	-	I	1	1
-	-	-	-	-	0	-	-

2.3 Wind turbulence

Natural wind profile can be expressed in two terms: mean component and fluctuating, turbulent component. Mathematically they can be expressed as:

$$U(z,t) = U(z) + u(x,y,z,t) \tag{4}$$

where *U(z,t)* is mean wind velocity component varying over height *z* and *u(x,y,z,t)* is turbulent component varying over height *z*, directions *x* and *y* and time *t*. Figure 3 illustrates the components.

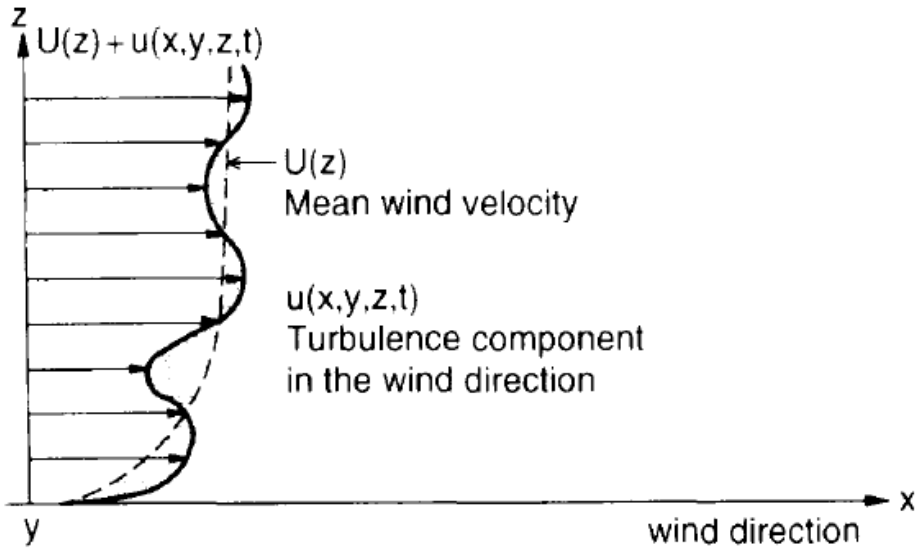

Figure 3. Wind field in along-wind direction (Dyrbye & Hansen 1997).

2.3.1 Mathematical expression

Turbulent wind flow is a complex, stochastic process and therefore it is convenient to describe it with a statistical approach (Dyrbye & Hansen 1997.) The ratio of standard deviation of the fluctuating component to mean value is known as *turbulence intensity* of that component. It is given as:

$$I_u = \frac{\sigma_u}{\overline{U}} \tag{5}$$

By full-scale measurements is has been found that standard deviation of longitudinal wind speed σ_u for roughness length z_0 = 0.05 m is equal to $2.5u_*$ (Dyrbye & Hansen 1997.) Hence, turbulence intensity can be expressed as a well-known formula, which is used in Eurocode:

$$I_u = \frac{2.5u_*}{\left(\frac{u_*}{0.4}\right)\ln\left(\frac{z}{z_0}\right)} = \frac{1}{\ln\left(\frac{z}{z_0}\right)} \tag{6}$$

Peak gust wind velocity is used in many design codes and standards as the basis for structural design. Since wind turbulence is random, peak gust of 10 minutes is also random (Holmes 2001.) Peak gust can be obtained by multiplying turbulent component with peak gust factor *g*. Peak factor is explained in detail in 4.2.5. Peak gust $\widehat{U}$ is given as:

$$\widehat{U} = \overline{U} + g\sigma_u \tag{7}$$

Peak gust factor depends on effective averaging time of gust τ and sample size *T*. However, Holmes (2001) notes that peak gust does not occur simultaneously along the whole height of the structure.

2.3.2 Impact on vortex shedding

According to Dyrbye & Hansen (1997), two turbulence conditions increase risk of violent across-wind vibrations:

1. Smooth, stratified wind flow occurring in a stable atmosphere. Topography or a low terrain category such as sea increase the risk of these conditions occurring. Smooth flow increases negative aerodynamic damping generated by vortex shedding. This is considered a rare, extreme event.

2. Small-scale turbulence, generated by a nearby structure of similar size, may increase lift coefficient. The effect of lift coefficient is explained in 3.1.5. This is considered a frequent event over structural life.

However, these conclusions are from chimney measurements, meaning that behavior of sharp-edged structures might be different. Experiments by Kawai (1992) were carried out for rectangular prisms with smooth and turbulent flow at 0^o angle of incidence. Various side ratios were considered. For example, on a cross-section with a side ratio of 1:2, it was observed that turbulent flow increased vortex-induced vibrations when compared to smooth flow. Figure 4 represents shedding frequency changes due to wind and structure type changes.

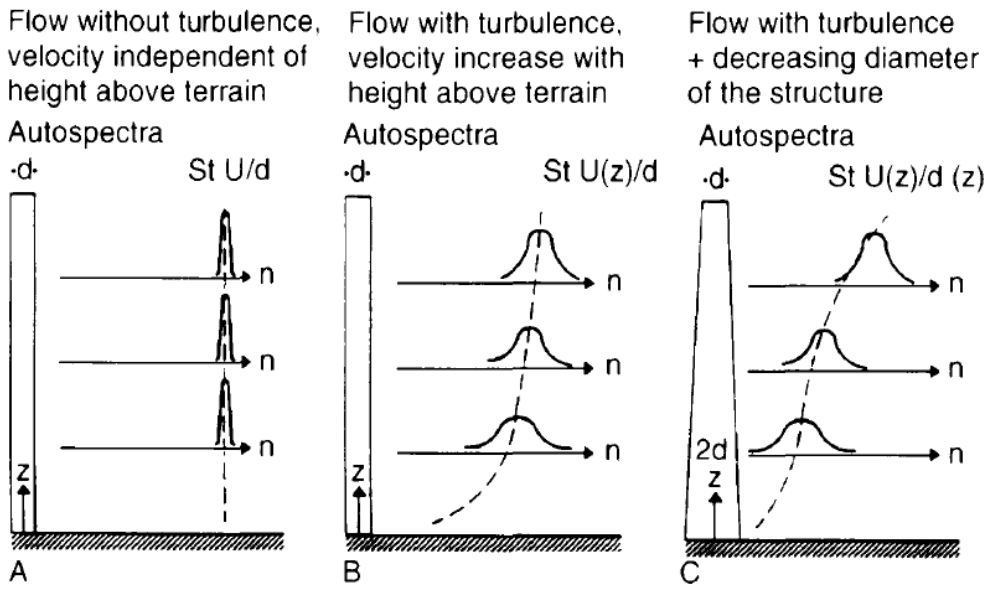

Figure 4. Sketch representing turbulence, velocity profile, height above the ground and diameter variation are affecting the auto spectrum of the lift load.

A. When diameter is constant, wind is smooth and velocity is independent of height above the ground, vortex shedding frequency is constant over height.

B. When wind velocity increases over height and diameter is constant, vortex shedding frequency increases over height.

C. When wind velocity increases over height and structure is tapered, vortex shedding frequency increases over height even more than in case B. (Dyrbye & Hansen 1997)

2.4 Angle of attack

Kawai (1995) investigated further the effect of the angle of attack on occurrence of VIV (vortex-induced vibration) and galloping. For square cross-section, most violent VIV response was at 0^{o} angle of attack in both smooth and turbulent flow. When the angle of attack increases, response amplitude decreases rapidly. For design purposes this means that 0^{o} angle of attack is most critical and strongly conservative.

3 Building vibration due to vortex shedding

This chapter explains the relationship between high-rise buildings vibration and vortex shedding. Vibration in slender high-rise buildings is a very important design aspect. In most cases, serviceability limit state is more critical than ultimate limit state in the structural design of high-rise buildings. The focus of this chapter is mainly on vortex shedding induced vibrations. First, interaction parameters related to vortex shedding are introduced. Then vortex shedding phenomenon is explained in detail. In conclusion, habitability of occupants is discussed.

3.1 Vortex shedding

Vortex shedding may occur when vortices are shed alternately behind the bluff body. This phenomenon may be interpreted in structural design as equivalent load on the sides of the structure in across-wind direction. Figure 5 illustrates how vortices are producing equivalent lateral load to the cladding.

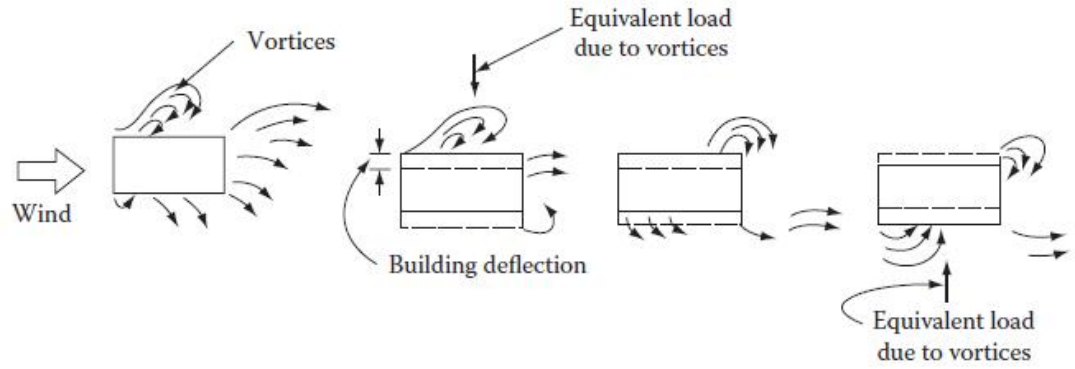

Figure 5. Periodic shedding of vortices generates building vibration transverse to the direction of wind.

3.1.1 Shedding frequency

As the vortices are shed alternatively on each side, harmonically varying load has the same frequency as vortices are shed. The frequency f_s of lateral load due to vortex shedding is defined as:

$$f_s = \frac{StU}{d} \tag{8}$$

where *St* is *Strouhal number*, *U* is mean velocity of wind and *d* is the across-wind dimension of the structure. Significant vibrations occur when f_s is near natural frequency f_e of the structure in across-wind direction.

3.1.2 Reynolds number

Reynolds number expresses the ratio between inertial and viscous forces. *Strouhal number* of different cross-sections of the structures is dependent on the *Reynolds number*. Yet, at critical and trans-critical regimes of *Re*, *St* of cross-sections with sharp edges is

not much dependent on *Re*, since separation tends to occur at the building corners (Pozzuoli 2012.) It is defined as:

$$Re = \frac{Ud}{\upsilon} \tag{9}$$

where υ is kinematic viscosity of the fluid. *Reynolds number* regimes (Giosan & Eng):

Sub-critical range: $Re < 3 \times 10^5$
Critical range: $3 \times 10^5 < Re < 3 \times 10^6$
Trans-critical range: $Re > 3 \times 10^6$

For a circular cross-section in the critical range of *Re*, vortices tend to occur irregularly, unless motion of the structure is large enough to cause a lock-in condition, which is described in detail in 3.1.3.

3.1.3 Lock-in

Structural motion may interact with the wind field in such a way that vortex shedding f_s synchronizes with natural frequency f_e of the structure. Shedding frequency remains constant over a certain range of wind velocities, being locked in natural frequency as illustrated in Figure 6. This condition is called a *lock-in*. Lower damping widens the range of wind velocities for a lock-in, since oscillation amplitude is larger. (Dyrbye & Hansen 1997, Pozzuoli 2012.)

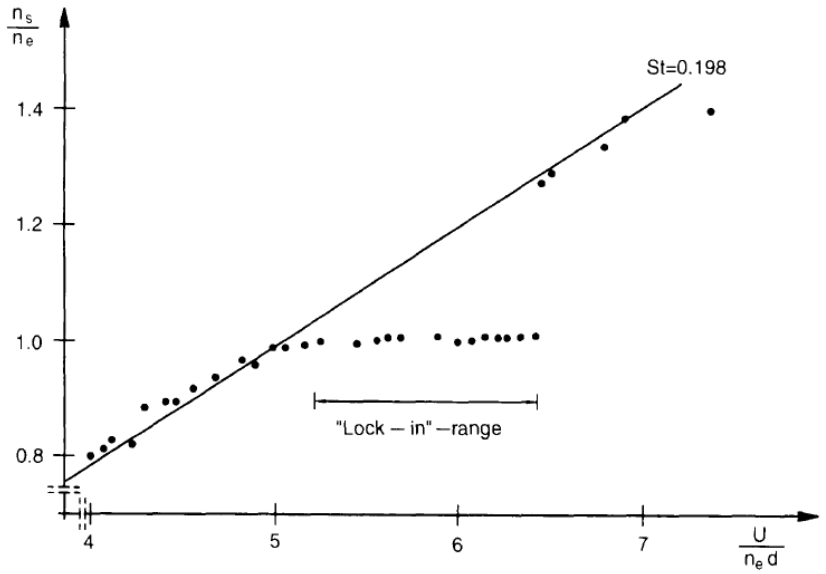

Figure 6. Experimental investigation of lock in after Feng (1968), from Dyrbye & Hansen (1997). X axis represents reduced wind velocity and Y axis represents frequency ratio, where n_s is shedding frequency, n_e is natural frequency, U is wind velocity and d is depth of the structure.

3.1.4 Vortex shedding significance

Strength of vortex-shedding induced equivalent forces may be significant for the structure when critical conditions are met. With low damping of a slender structure, high amplitude vibrations can occur if the frequency of shed vortices is near the natural frequency of the structure. The velocity at which this condition is met is called *critical velocity*. If the

critical velocity is much higher than the design wind speed, the resonant condition will not occur. On the other hand, if critical velocity is too low, there will be no problem because aerodynamic excitation forces will be low. However, significant vibration response may occur if critical velocity is in range of 10-40 m/s. (Holmes 2001.)

Codes and literature provide simple evaluations of vortex shedding significance based on slenderness. Taranath (2012) suggests that across-wind response is likely to be more significant than along-wind response when a building is slender about both axes and the following criteria is met:

$$\frac{H}{\sqrt{BD}} > 3 \tag{10}$$

The Japanese standard AIJ – RLB (2004) suggests checking across-wind response if the same criteria is met. In addition, for rectangular cross-sections AIJ suggests vortex-induced vibrations and aeroelasticity checks with appropriate wind tunnel tests when the following condition is met:

$$\frac{H}{\sqrt{BD}} \geq 4 \text{ and } \left(\frac{U_H}{f_L \sqrt{BD}} \geq 0.83 U^*_{Lcr} \text{ or } \frac{U_H}{f_L \sqrt{BD}} \geq 0.83 U^*_{Tcr} \right) \tag{11}$$

where U_H is design wind velocity, f_L and f_T are the first natural periods in across-wind and torsional direction, U^*_{Lcr} and U^*_{Tcr} are non-dimensional critical wind speeds for aeroelastic instability in across-wind, and torsional direction respectively. They are calculated from Table 6.1 and table 6.2 respectively in AIJ. Also, AIJ suggests that if non-dimensional wind speed is 0.83 times non-dimensional critical wind speed or closer, vortex-induced vibrations may occur.

Eurocode suggests that vortex shedding should be investigated for structures when:

$$\frac{H}{B} > 6 \tag{12}$$

where B is smallest across-wind dimension.

In terms of critical velocity, Eurocode suggests that vortex shedding effect does not have to be investigated when $v_{crit} > 1.25\, v_m$. Also, Eurocode suggests that aeroelastic response should be considered for flexible structures, which is typically defined as structures with their first natural frequency being under 1 Hz. Australian/New Zealand standard AS/NZS 1170.2:2011 (2011) suggests that the acceptable across-wind acceleration level may be exceeded if the following expression is satisfied:

$$\frac{h^{1.3}}{m_0} > 0.0016 \tag{13}$$

where h is average roof height above the ground and m_0 is average mass per unit height.

American standard ASCE/SEI 7-10 (2010) suggests that a building is susceptible to vortex-induced and/or torsional vibrations when any of these conditions is met:

- Building height is over 122 m
- *H/b* is bigger than 4, where *b* is the smallest cross-section dimension
- The lowest natural frequency of the building is under 0.25 Hz
- The reduced velocity $\frac{\bar{V}_z}{n_1 B_{min}} > 5$, where $\bar{V}_z$ is mean hourly velocity at $z = 0.6h$.

B_{min} is minimum effective width defined as minimum value of $\sum h_i B_i / \sum h_i$ considering all wind directions (ASCE/SEI 7-10 2010).

3.1.5 Lift coefficient

As illustrated in Figure 7, aerodynamic load acting perpendicular to the approaching wind direction is called lift force. Corresponding lift coefficient is defined as:

$$C_L(\mathrm{t}) = \frac{F_L(t)}{\frac{1}{2}\rho U^2 dh} \tag{14}$$

where $F_L(t)$ is lift force acting perpendicular to the surface area, e.g. equal to across-wind dimension times height dh, ρ is air density and U is wind velocity. As the structure is swaying, the lift coefficient is fluctuating, and it is common practice to use the RMS (root-mean-square) fluctuating lift coefficient value. Essentially, lift coefficient determines the magnitude of the load.

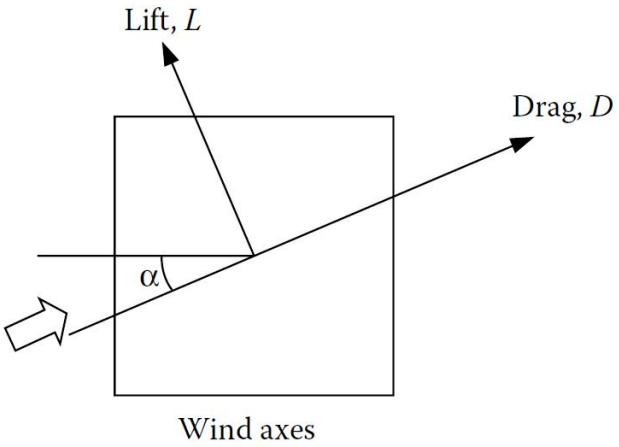

Figure 7. Lift and drag directions relative to incoming wind direction. (Holmes 2015)

Reynolds number is two or three orders of magnitude larger in full-scale than in wind tunnels, so it is hard to achieve *Re* similarity. In the case of rounded shapes, aerodynamic properties are strongly dependent on *Re*. However, in the case of sharp-edged bluff bodies in critical and trans-critical *Re* ranges, aerodynamic properties are much less sensitive to *Re*, but are more sensitive to the angle of attack. This happens because separation tends to occur at the building corners, whereas for rounded shapes the separation point varies. Therefore, influence of *Re* on flow around the building is not significant, especially in turbulent boundary layer flows. (Pozzuoli 2012.)

Joubert et al. (2015) did computational simulations on a 3D rectangular bluff body and it was found that the amplitude of lift coefficient fluctuation changes over height. Figure 8 illustrates time-averaged lift coefficient fluctuation over height. This also supports the

fact from Simiu (2011) that formation of vortices near the top of the building, where vortex shedding induced loads are most effective, is affected by the roof preventing the formation of regular vortices.

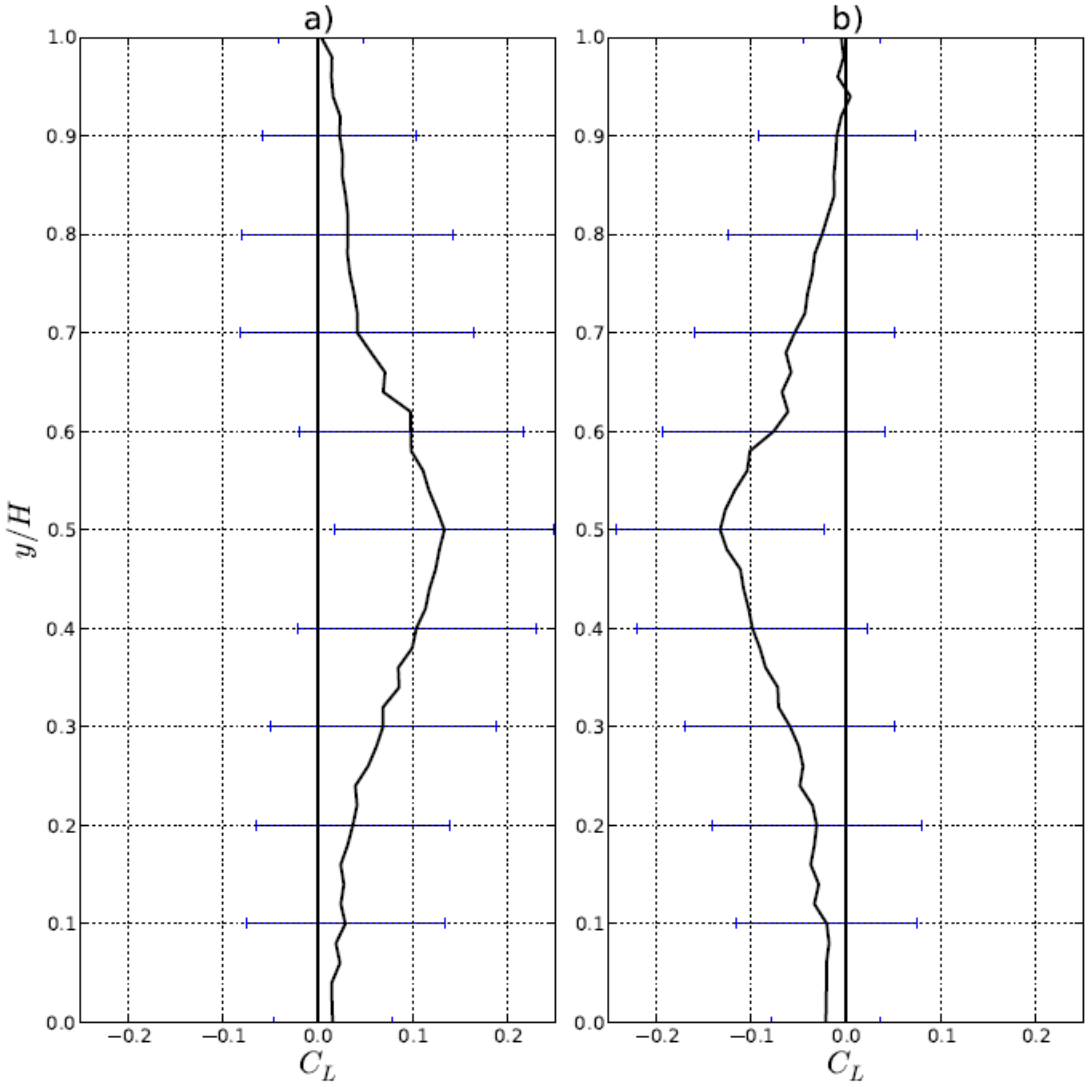

Figure 8. Time-averaged lift coefficient distribution over the height of the beam for the point of a) maximum and b) minimum lift during vortex shedding cycle with standard deviations (Joubert et al. 2015).

3.1.6 Strouhal number

Strouhal number varies for different bluff body shapes and aspect ratios in the case of a rectangular shape. Numerous experiments on square cross-sectional shapes have been conducted in wind tunnels. Table 3 presents *St* and $C_{L,\mathrm{rms}}$ from wind tunnel experiments, full scale measurements and standards.

Table 3. Comparison of Strouhal numbers for a single square cylinder.

	Research	Re x 10^4	Turbulence intensity	$C_{L,rms}$	St
Wind tunnel	Nakaguchi et al. (1968)	2-6	Smooth	-	0.125
	Vickery (1966)	4-16	Smooth	1.32	0.118
			10 %	0.67	0.12
	Bearman & Trueman (1972)	2-7	Smooth	-	0.125
	Reinhold et al. (1977)	1.4 x 10^2	Smooth	1.07	0.13
			12 %	0.86	0.12
	Lesage & Gartshore (1987)	3.3	-	1.33	0.13
	Knisely (1990)	2.2	0.5 %	1	0.13
	Norberg (1993)	1.3	Smooth	-	0.132
	Lyn et al. (1995)	2.14	2 %	-	0.132
	Tamura and Miyagi (1999)	3	0.4 %	1.05	0.128
			6,5/14,0%	0.37	0.116
	Sarioglu & Yavuz (2000)	20	-	-	0.12
	Noda & Nakayama (2003)	6.89	0.2 %	1.18	0.131
	Alam et al. (2011)	4.7	0.5 %	1.18	0.128
	Yen & Liu (2011)	2.1	0.4 %	-	0.132
	Liu et al. (2015)	4.58	0.7 %	1.1	0.135
	Andika et al. (2018)	10	-	-	0.126
Full scale	Xu et al. (2014)	3.8 x 10^3	-	-	0.106
	Li et al. (2018)	1.1 x 10^4	-	-	0.12
Standards	EN 1991-1-4	-	-	1.1	0.12
	Canadian Highway bridge design code	-	-	0.6	0.11

3.1.7 Scruton number

Scruton number, Sc, is a non-dimensional instability parameter also known as 'mass-damping parameter'. It is used to evaluate structure susceptibility to the occurrence of lock-in condition. *Sc* is defined as:

$$Sc = \frac{2\delta_s m_e}{\rho b^2} \tag{15}$$

where δ_s is structural damping expressed by the logarithmic decrement, m_e is mass per unit length, ρ is air density and b is the width of the structure. For different aspect ratios

Hansen (2013) suggests the use of a general non-dimensional mass-damping parameter. Sc_g is defined as:

$$Sc_G = \frac{2\delta_s m_e}{\rho b d} \tag{16}$$

where b is along-wind dimension and d is across-wind dimension of the structure. Hansen (2013) suggests adding a generalized version into future Eurocode revisions. The use of a generalized non-dimensional mass-damping parameter may reduce uncertainties related to predictions of vortex-induced and galloping induced vibrations.

Figure 9 represents the susceptibility of a rectangular cross-section to vortex-induced vibrations. Equation 11 mentioned in the Figure 9 refers to the equation (41) used in Eurocode.

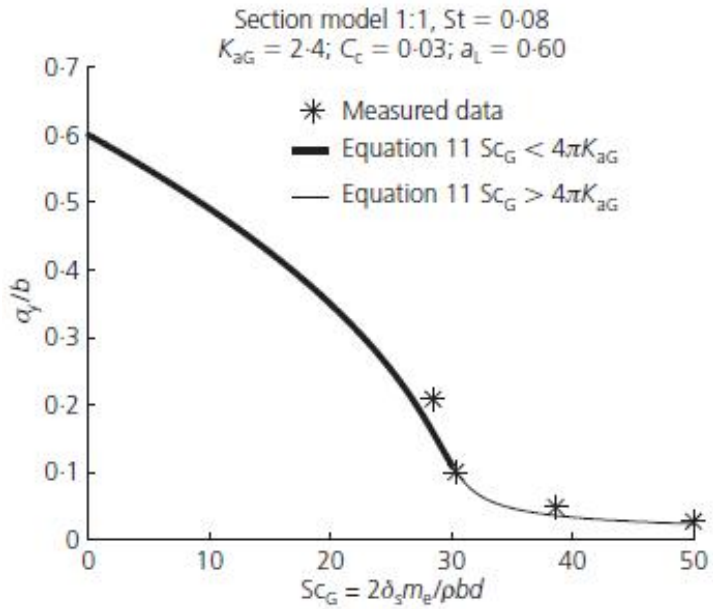

Figure 9. Square cross-section relative standard deviation of deflection over non-dimensional mass-damping parameter (Hansen 2013).

3.1.8 Angular dependence

As mentioned in chapter 2.4, aerodynamic characteristics of a square bluff body are dependent on the angle of attack. Figure 10 illustrates *St* dependence on angle of attack as well as negligible dependence on *Re*.

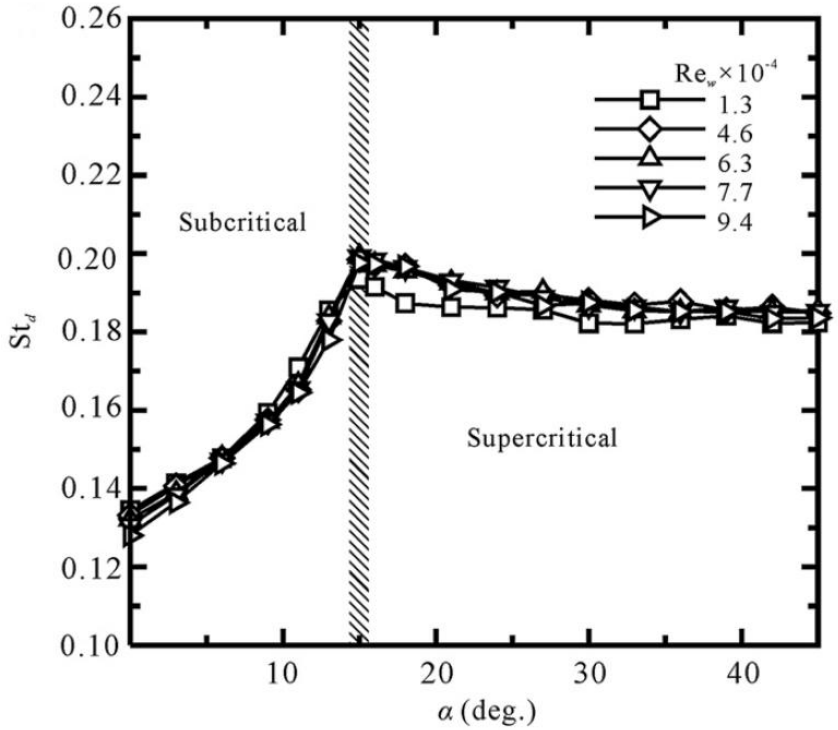

Figure 10. Strouhal number variation over the angle of attack with different Re (Huang et al. 2010).

3.2 Motion perception and human comfort

Perception of structural motion is highly dependent on a given activity. Depending on the task one is performing the threshold level of acceleration varies. Difference in that variation of the threshold level is in order of magnitude. Humans are more sensitive to acceleration when relaxing and less sensitive when performing tasks including movement. The wide variety of human activity in different kinds of facilities makes evaluation complicated. Therefore, common practice is to come into agreement with the customer of the allowed accelerations.

There is no international standard or agreement on the level of acceptable acceleration, but there are many guidelines given by research and codes, which help in the design process. To make a good design, acceleration limits for different return periods are to be considered. Acceleration may be considered as an RMS value, peak value or jerk. (Pozzuoli 2012.) Meaning of a *jerk* is the *rate of change of acceleration*, which may be primarily responsible for motion perception (McNamara et al. 2002). Debate on frequency dependence of motion perception is still open, but the usual approach is that motion perception is frequency dependent.

Research by Burton et al. (2006), Chen & Robertson (1972) and Irwin (1978) suggest that perception is frequency dependent. AIJ and ISO 6897:1984 (1984) standards follow the same principle. However, the National Building Code of Canada NBCC (2005), Chinese code JGJ 3-2002 and the Hong Kong Codes of Practice HKCOP 2004 suggest flat criteria of peak acceleration 15 milli-g for residential buildings and 25 milli-g for commercial buildings with a 10-year return period. ISO 10137:2007 (2007) standard's well-known curve in Figure 11 is for a one-year return period, but in the code there are also guidelines for vibrations with a return period of multiple times per day in the Annex C. AIJ gives 5 curves: H-10, H-30, H-50, H-70 and H-90, where the numbers mean 10%, 30%, 50%,

70% and 90% probability of perception respectively. Figure 11 shows comparison of these criteria.

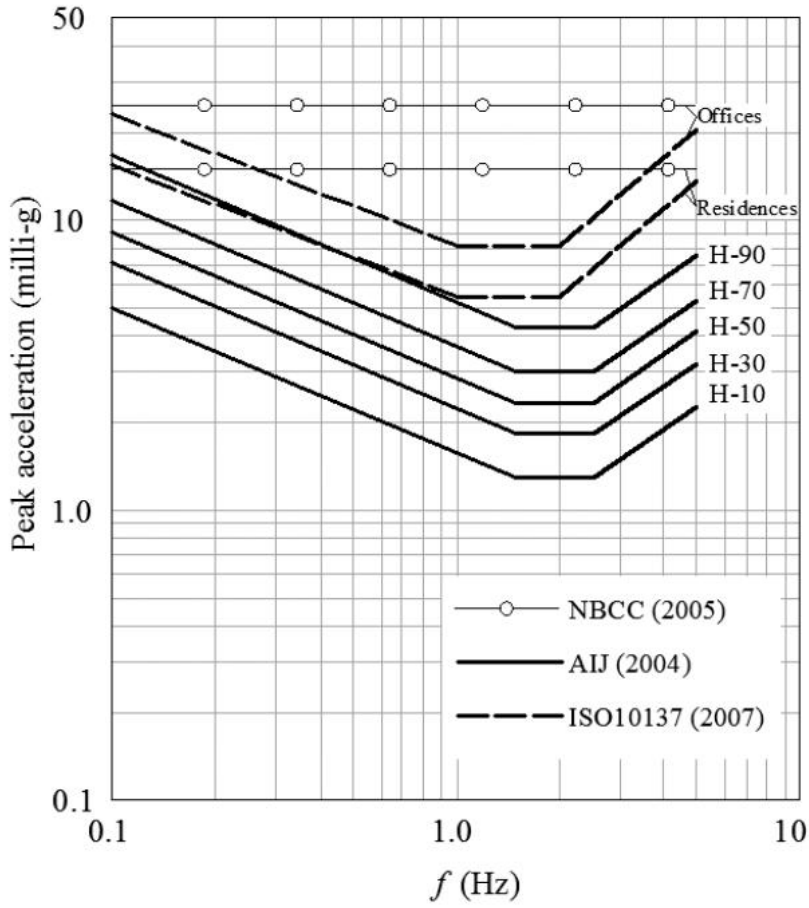

Figure 11. Comparison of different standards' perception limits of 10 minutes mean wind speed with 1-year return period (Pozos-Estrada et al. 2010).

Melbourne & Palmer (1992) have proposed acceleration limit criterion by equation (17) for frequency range $0.06 < f_e < 1.0$ and return period range $0.5 < R < 10$.

$$A_{max} = \sqrt{2\ln(f_e T)}\,(0.68 + 0.2\ln(R)\exp(-3.65 - 0.41\ln(f_e)) \qquad (17)$$

where A_{max} is peak acceleration, f_e is fundamental natural frequency, T is observation duration and R is return period.

4 International design standards and literature

In this chapter the application of Eurocode EN 1991-1-4 and other international major codes for acceleration prediction will be discussed. The selected codes are Eurocode EN 1991-1-4:2005 (2005) (Europe), NBCC (2005) (Canada), AIJ-RLB-2004 (2004) (Japan) and AS/NZS 1170.2:2011 (2011) (Australia/New Zealand). These standards are most frequently used in literature for the comparison and prediction of across-wind response. Also, the method by Simiu (2011) will be presented. Procedure of across-wind acceleration response calculations with each code will be presented and a comparative study between the codes will be made at the end of this chapter.

4.1 Example case

To make a comparison between different methods of calculating response acceleration, an example building must satisfy the limitations described in 4.2.1 provided by the standards. The selected building is non-tapered, with the dimensions of 30 x 30 x 200 m and equal mass distribution. The core and columns of the building are reinforced concrete, which usually gives the structure a structural damping ratio of 0.02. The building has a square cross-section with sharp corners and there are no openings.

4.2 Background for the codes

Two commonly used methods to estimate across-wind response due to vortex-shedding (Holmes 2001):

1. Sinusoidal excitation models
2. Random excitation models (Spectral model)

Majority of standards have adopted spectral models to the guidelines. The standards limitations, basic wind speed definition, peak factor and tip acceleration calculation will all be reviewed in this section.

4.2.1 Standards limitations

All across-wind response formulas provided are rough estimations and should be used for preliminary design. Also, the codes have various applicability limitations related to the formulas.

In terms of height of the structure, Eurocode and AS/NZS 1170.2 have a limit of 200 m above the ground. AIJ provides slenderness limit of $\frac{H}{\sqrt{BD}} \leq 6$ for rectangular shape.

In terms of how many modes are considered, Eurocode's first method is the only one that takes higher modes into account. Eurocode's second method, NBCC 2005, AIJ, AS/NZS 1170.2 and the method by Simiu are applicable only for a fundamental mode shape.

In terms of building shape, Eurocode's first method is applicable for rectangular, circular I, T, L and + shape. Eurocode's second method is applicable only for square or circular shapes of cantilever type structures with regular mass distribution. NBCC 2005 standard is applicable for a regular shape defined as "a building that has no unusual geometrical irregularity in spatial form". AIJ limits applicability to a rectangular cross-section with a

depth-to-width ratio range of $0.2 \leq D/B \leq 5$. AS/NZS 1170.2 limits applicability to the rectangular shapes that have the following dimension ratios: 3:1:1; 6:1:1 and 6:2:1 (h:b:d). Method provided by Simiu is limited to square cross-sectional shapes.

In terms of frequency range, all methods are applicable for flexible structures only, meaning that first natural period of the structure is under 1 Hz. AS/NZS 1170.2 has defined the lower limit as 0.2 Hz.

AIJ also provides an applicability limit as non-dimensional design wind speed for rectangular and circular cross-sections respectively:

$$\frac{U_H}{f_L\sqrt{BD}} \leq 10 \tag{18}$$

$$\frac{U_H}{f_L D} \leq 4.2 \tag{19}$$

In the method by Simiu there is a limitation in terms of deflection, which is an indication of aeroelastic instability. Maximum RMS across-wind deflection to the building depth σ_y/D for open terrain is 0.015; suburban terrain 0.025 and 0.045 for centers of large cities. AS/NZS 1170.2 does not cover structures which have frequencies of two fundamental modes that are within 10 % of each other and are both under 0.4 Hz. None of the procedures cover situations where wind channeling is possible due to surrounding buildings or topography.

4.2.2 Basic wind speed

To get comparable results between different standards, basic wind speed gust duration and the return period must be scaled accordingly, since the standards are using different initial conditions of the wind. It is noteworthy that Eurocode's method 2 does not use wind speed for calculation of across-wind response.

To get a response acceleration of, say a return period of 10 years, the input wind return period must also be 10 years. The basic wind speed given by the maps in the standards is not always a 10-year return period wind, so the standards have a method to scale wind velocity accordingly. However, the scaling method used in different standards varies slightly making their comparison inconsistent. In this study this problem will be studied as two separate wind velocity cases. In the first case, the return period will be scaled to 10 years by using Eurocode and that value will be used in all standards as input. In the second case, wind velocity will be scaled according to each standard separately.

In the first case the problem is that standards may be calibrated according to tests, and they are not purely based on local wind conditions, which will make the approach incorrect. In the second case calculation is based more on the local wind conditions of each country code, making results incomparable in that sense. The assumption is that these two methods do not have much difference and that no significant scatter will arise in response, since the change between methods is minor.

Return period conversion by different standards, T being defined as return period and V_{50} is defined as wind speed of 50 years return period:

Eurocode EN 1991-1-4:

$$U_T = U_{50}\left(\frac{1 - Kln\left(-\ln\left(1-\frac{1}{T}\right)\right)}{1 - Kln(-\ln(0.98))}\right)^n \quad (20)$$

where $K = 0.5$ and $n = 0.5$.

ASCE 7-10 for the method by Simiu:

$$U_T = U_{50}(0.36 + 0.1\ln(12T)) \quad (21)$$

AIJ:

$$U_T = U_{50}k_{rW} \quad (22)$$

where

$$k_{rW} = 0.63(\lambda_U - 1)\ln(T) - 2.9\lambda_U + 3.9 \quad (23)$$

where λ_U is approximated as 1.1 from Japanese wind maps: Figures 6.1 and 6.4 in AIJ.

NBCC 2005:

$$U_T = U_{50}I_w \quad (24)$$

where I_w is importance factor defined as 0.75 for SLS design in NBCC 2005 Table 4.1.7.1. It is assumed that the definition in NBCC 2005 for SLS condition is 10 years return period.

AS/NZS 1170.2:2011:

$$U_T = U_{50}C \quad (25)$$

where C is taken as the average of ratios between U_{10}- and U_{50}-values for non-cyclonic wind speeds defined in AS/NZS 1170.2:2011 Table 3.1. The value of C is 0.84.

The basic wind speed selected is 10 minutes mean peak at 10 meters above the ground in terrain category I. The value suggested by National Annex of Finland of SFS EN 1991-1-4:2005 (2016) is 21 m/s in a 50-year return period wind speed for terrain category II, which is used as the basic wind velocity for other standards in this study. It is assumed that topography, directionality, shielding and seasonal factors are 1.0.

The used peak gust durations in standards for calculation of across-wind acceleration response are listed in Table 4. Conversion of gust durations is made with the help of Figure 1 by Liu (1991). Converted wind velocities are listed also in Table 4. Converting return period by Eurocode is a conservative approach.

Table 4. Comparison of basic wind velocities for different standards.

		EC-1991-1-4		NBCC	AIJ	AS/NZ	Simiu
		Method 1	Method 2	2005		1770.2	
	Return period conversion factor	0.90	-	0.75	0.86	0.84	0.84
Basic wind velocity	50 years return period [m/s]	21.0	-	19.3	21.0	29.7	19.3
	10 years return period by Eurocode [m/s]	19.0	-	17.4	19.0	26.8	17.4
	10 years return period by each code separately [m/s]	19.0	-	14.4	18.0	25.1	16.2
	Response time	10-min	-	1-hr	10-min	3-s	1-hr

4.2.3 Sinusoidal model

The main assumption in sinusoidal model is that vortex-induced load is near-sinusoidal and therefore the responses are also sinusoidal. These models are deterministic rather than random. Sinusoidal models are good for situations where large oscillations occur, and the structure is in lock-in condition. Assumptions leading to this model are not very accurate for structures vibrating in turbulent wind conditions. However, the sinusoidal model is useful in the early stages of design to examine if vortex-induced vibrations are potentially occurring.

The ratio of vibration amplitude to the tower breath at the tip can be evaluated as (Holmes 2001):

$$\frac{y_{max}}{b} = \frac{kC_L}{4\pi ScSt^2} \tag{26}$$

where k is a parameter dependent on the model shape vibration, C_L is lift coefficient, Sc is *Scruton number*. *Scruton number* is a "mass-damping parameter", which evaluates how sensitive a structure is to lock-in due to vortex-shedding. Sc is defined as:

$$Sc = \frac{4\pi m\eta_j}{\rho b^2} \tag{27}$$

where m is average mass per unit length along the structure, η_j is critical damping ratio for jth mode and ρ is air density. For a *Scruton number* > 20 there is no risk of lock-in based on empirical experience. On the other hand, for Sc < 10, the risk of "lock-in" is apparent. For structures with a Sc of approximately 5-10 with the combination of stratification of air, wind direction and critical velocity, large vibrations may occur with a return period of 10-20 years. (Dyrbye & Hansen 1997.)

4.2.4 Spectral model

Spectral model considers wind as a random process, treating it as a power spectrum. Modal approach is used to obtain a response spectrum. Vickery & Clark (1972) originally

proposed the spectral model to predict vortex shedding induced vibrations. In the case of vortex-shedding frequency "locking in" to the natural frequency of the structure, the magnitude of fluctuating across-wind forces increases significantly. Aerodynamic damping can be described as a_y-b_y^3, where the first, linear term describes negative aerodynamic damping and the second nonlinear term describes positive damping related to self-limiting response. For amplitudes of 5-10 %, aerodynamic damping is described accurately enough with the first, linear term. (Hansen 2007.) The Aerodynamic damping ratio ζ_a is given by Vickery and Basu (1983):

$$\zeta_a = \frac{\rho b_{ref}^2}{m_e} K_{a,ref} \left(\gamma_K - \left(\frac{\sigma_{y,ref}}{\gamma_{aL} a_{L,ref} b_{ref}} \right)^2 \right) \tag{28}$$

Assuming reference velocity pressure as $q_{ref} = \frac{1}{2} \rho b_{ref}^2 n_e^2 / St^2$, where ρ is air density, the combined formula for standard deviation of the structural deflection (38) is then used in method 2 of Eurocode.

4.2.5 Peak factor

The peak factor k_p depends on the type of vibration. For a single harmonic sinusoidal vibration k_p equals $\sqrt{2}$ and for a stochastic type of response k_p equals approximately 4. The response type caused by vortex shedding is typically something between those two extremes. (Dyrbye & Hansen 1997.) The following expression was proposed by Ruscheweyh and Sedlacek (1988):

$$k_p = \sqrt{2} \left(1 + \frac{1.2}{\tan\left(0.75 \frac{Sc}{4\pi K_a} \right)} \right) \tag{29}$$

where K_a is an aerodynamic parameter.

In most of the standards peak factor for peak acceleration is similar to one another. The general expression of the peak factor is:

$$g = \sqrt{2 \ln(\tau T)} + \frac{0.5772}{\sqrt{2 \ln(\tau T)}} \tag{30}$$

where T is sample time and τ is average upcrossing frequency.

4.2.6 Input information for calculations

Wind speed is defined in 4.2.2. The following information is used for calculations:

- Building height: 200 m
- Building across-wind dimension: 30 m
- Building width: 30 m
- Building mass: 64115003 kg
- Damping ratio in across- and along-wind direction: 0.02

- Air density: 1.23 kg/m^3
- Fundamental frequency in across- and along-wind direction: 0.139 Hz
- Terrain category I in Eurocode.
- Return period: 10 years

4.2.7 Acceleration

Stochastic process is a process, in which the numerical outcome at any given moment of time or position in space is random and can only be predicted with certain probability. Horizontal acceleration and deflection of high-rise buildings are stochastic processes consisting of mean and fluctuating components. (Strømmen 2010.) In the case of across-wind response, the mean component is zero. (Holmes 2001.) Horizontal peak acceleration $\ddot{u}_{max}$ is proportional to the standard deviation of acceleration:

$$\ddot{u}_{max} = k_p \sigma_{\ddot{u}} \tag{31}$$

4.3 Eurocode EC-1991-1-4

Eurocode proposes two different methods to predict vortex-induced vibrations. Method 1, presented in EN 1991-1-4 Annex E, E.1.5.2 is based on vortex-resonance (sinusoidal) model. This model has been compared to full-scale measurements of chimneys in Denmark. In conclusion, that model overestimates frequent load, but underestimates rare, extreme events due to special meteorological events. (Dyrbye & Hansen 1997.) Method 2, presented in EN 1991-1-4, E.1.5.3 is based on the spectral (random excitation) model. It takes both rare and frequent events into account including turbulence effect in the vibration amplitudes predicted.

4.3.1 Method 1

Sinusoidal approach is adopted in Eurocode as follows:

$$\frac{y_{max}}{b} = \frac{K_w K C_{lat}}{ScSt^2} \tag{32}$$

where *Strouhal number St* is given in Figure E.1 in Eurocode. K_w is an effective correlation length factor given for cantilever type of structures as follows:

$$K_W = 3\frac{L_j/b}{\lambda}\left[1 - \frac{L_j/b}{\lambda} + \frac{1}{3}\left(\frac{L_j/b}{\lambda}\right)^2\right] \tag{33}$$

where λ is l/b and L_j is correlation length. L_j/b is function of vibration amplitude $y_F(s_j)/b$ and is given as:

$$\frac{L_j}{b} = \begin{cases} 6, & \frac{y_F(s_j)}{b} < 0.1 \\ 4.8 + 12\frac{y_F(s_j)}{b}, & 0.1 \leq \frac{y_F(s_j)}{b} \leq 0.6 \\ 12, & \frac{y_F(s_j)}{b} > 6 \end{cases} \tag{34}$$

This step is an iterative process, since the deflection is unknown at this point, meaning that the initial guess must be done in terms of deflection.

K is a mode shape factor given in Eurocode Table E.5. c_{lat} is a lateral force coefficient, which may be interpreted as lift coefficient. It is given as:

$$c_{lat} = \begin{cases} c_{lat,0}, & \frac{v_{crit,i}}{v_{m,Lj}} \leq 0.83 \\ c_{lat,0}\left(3 - 2.4\frac{v_{crit,i}}{v_{m,Lj}}\right), & 0.83 \leq \frac{v_{crit,i}}{v_{m,Lj}} < 1.25 \\ 0, & \frac{v_{crit,i}}{v_{m,Lj}} \geq 1.25 \end{cases} \tag{35}$$

where $v_{crit,i}$ is critical wind velocity for mode *i* and $v_{m,Lj}$ is mean wind velocity in the center of the effective correlation length L_j.

Scruton number Sc is given as:

$$Sc = \frac{2\delta_s m_{i,e}}{\rho b^2} \tag{36}$$

where δ_s is the structural logarithmic decrement of damping, ρ is air density, b is reference width of the cross-section and $m_{i,e}$ is equivalent mass m_e per unit length for mode *i* defined as:

$$m_{i,e} = \frac{\int_0^h m_z \Phi_1^2 dz}{\int_0^h \Phi_1^2 dz} \tag{37}$$

where m_z is mass per unit length and Φ_1 is the fundamental mode shape parameter defined as:

$$\Phi_1 = \left(\frac{z}{h}\right)^{\zeta} \tag{38}$$

where *z* is height above the ground and *h* is height of the structure.

Peak acceleration is not given in Eurocode directly, but it is solvable for both methods with the following formula:

$$a = (2\pi f_{n.i})^2 y_{max} \tag{39}$$

4.3.2 Method 2

The random excitation model is adopted in Eurocode as follows:

Maximum displacement at the point with the largest movement is given as:

$$y_{max} = \sigma_y k_p \tag{40}$$

where k_p is peak factor and σ_y is the standard deviation of deflection at the point where the mode shape has its largest deflection ($\Phi = 1$). σ_y is given as:

$$\frac{\sigma_y}{b} = \frac{1}{St^2} \frac{C_c}{\sqrt{\frac{Sc}{4\pi} - K_a\left(1 - \left(\frac{\sigma_{y,max}}{a_L b}\right)^2\right)}} \sqrt{\frac{\rho b^2}{m_e}} \sqrt{\frac{b}{h}} \tag{41}$$

where C_c is aerodynamic coefficient, K_a is the aerodynamic damping parameter and a_L is the normalized limiting amplitude, all given in Eurocode Table E.6. ρ is air density, m_e is effective mass per unit length and Sc is *Scruton number*, which is solvable from the equation (36). $K_{a,max}$, given in Eurocode Table E.6, is the parameter taking into account a rare, smooth air flow weather condition mentioned in 2.3.2 (Hansen 2007).

Solution to the equation (41) is given as:

$$\left(\frac{\sigma_y}{b}\right)^2 = c_1 + \sqrt{c_1^2 + c_2} \tag{42}$$

where c_1 and c_2 are given as:

$$c_1 = \frac{a_L^2}{2}\left(1 - \frac{Sc}{4\pi K_a}\right); \qquad c_2 = \frac{\rho b^2}{m_e} \frac{a_L^2}{K_a} \frac{C_c^2}{St^4} \frac{b}{h} \tag{43}$$

Peak factor k_p for intermediate amplitudes is solvable by the equation (29). Peak acceleration is solvable by the equation (31).

4.4 NBCC 2005

Essentially in NBCC 2005 the peak acceleration is calculated by multiplying peak factor by RMS of acceleration. Peak across-wind acceleration on top of the building is given as:

$$a_w = n_w^2 g_p \sqrt{WD}\left(\frac{a_r}{\rho_B g \sqrt{\beta_W}}\right) \tag{44}$$

where n_w is first modal frequency and β_W is the ratio of critical damping in across wind direction. g_p is peak factor, W is structure's across-wind dimension, D is structure's along-wind dimension, ρ_B is structure's density and g is gravity constant.

a_r is defined as:

$$a_r = 78.5x10^{-3}\left[\frac{V_H}{n_w\sqrt{WD}}\right]^{3.3} \tag{45}$$

where V_H is mean wind velocity at the top of the structure, which is calculated by:

$$V_H = V\sqrt{C_e} \tag{46}$$

where V is reference wind speed, C_e is exposure factor, which varies for each terrain category and is proportional to $\left(\frac{Z}{Z_{ref}}\right)^{\alpha}$ where Z_{ref} is reference height and α is power exponent, both dependent on terrain category.

Peak factor is defined as:

$$g_p = \sqrt{2\ln(\upsilon T)} + \frac{0.577}{\sqrt{2\ln(\upsilon T)}} \tag{47}$$

where T is taken as 3600 s and υ, the average fluctuation rate, is defined as:

$$\upsilon = n_0\sqrt{\frac{sF}{sF + \beta_D B}} \tag{48}$$

where n_0 is fundamental natural frequency and β_D is critical damping ratio in along-wind direction. B is defined from Figure 12 or by following equation:

$$B = \frac{4}{3}\int_0^{\frac{914}{H}}\left[\frac{1}{1+\frac{xH}{457}}\right]\left[\frac{1}{1+\frac{xW}{122}}\right]\left[\frac{x}{(1-x^2)^{\frac{4}{3}}}\right]dx \tag{49}$$

where H is height of the structure.

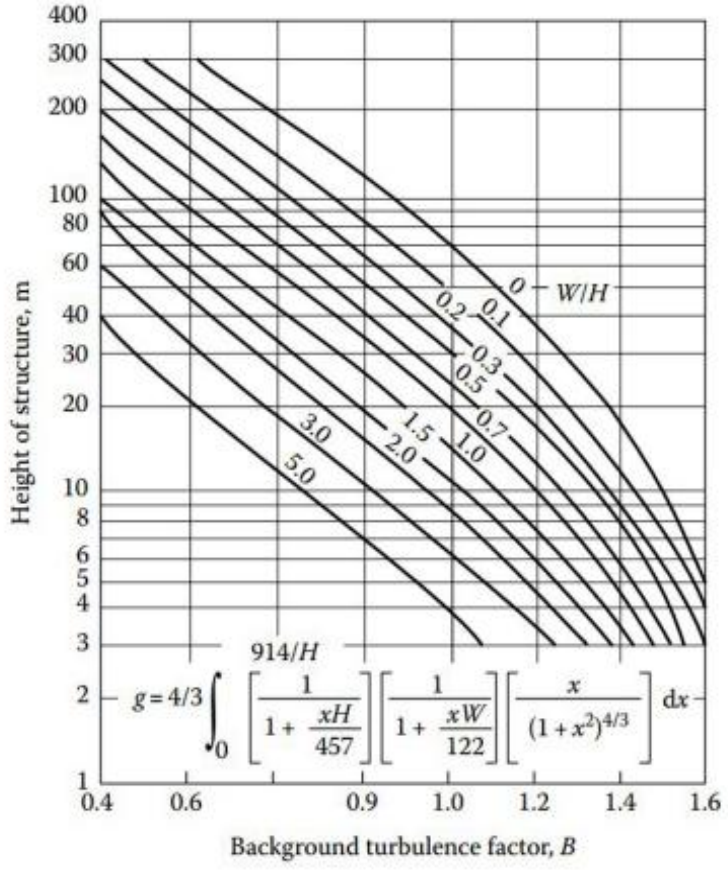

Figure 12. Background turbulence factor B.

Size reduction factor *s* is defined from Figure 13 or by following equation:

$$s = \frac{\pi}{3}\left[\frac{1}{1+\frac{8n_0H}{3V_H}}\right]\left[\frac{1}{1+\frac{10n_0W}{V_H}}\right] \tag{50}$$

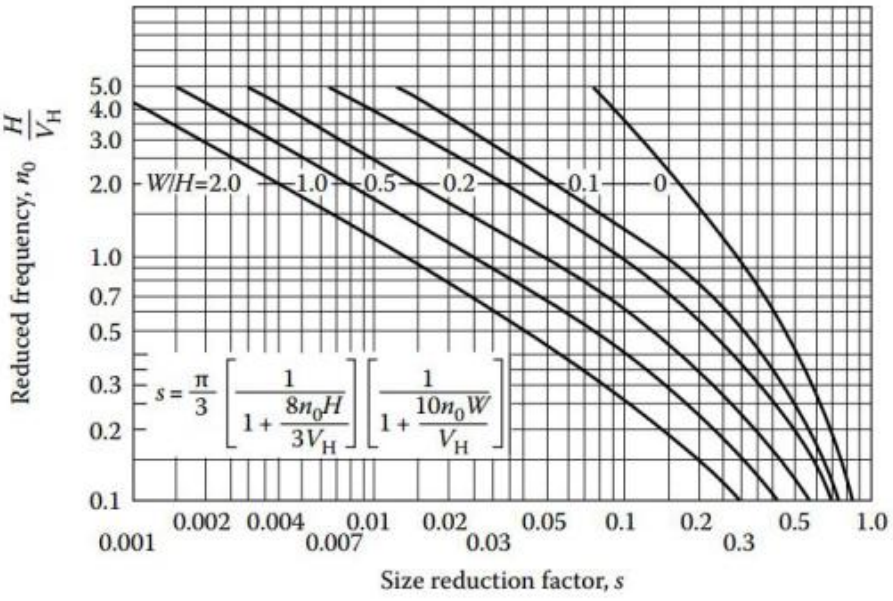

Figure 13. Size reduction factor s.

Gust energy ratio F is defined from Figure 14 or by following equations:

$$s = \frac{x_0^2}{(1 + x_0^2)^{\frac{4}{3}}} \tag{51}$$

$$x_0 = \left(\frac{1220 n_0}{V_H}\right) \tag{52}$$

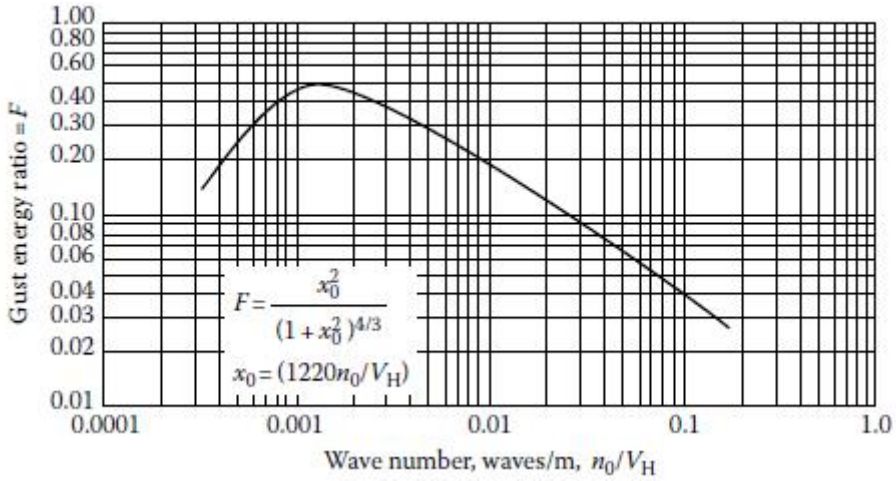

Figure 14. Gust energy ratio F.

4.5 AIJ

Derivations for wind load recommendations of AIJ are explained in detail by Tamura et al. (1996). The AIJ standard does a great job in providing explanations alongside the design procedure, helping the designer to understand phenomena and relations. Formula for across-wind acceleration is given as:

$$a_{Lmax} = \frac{q_H g_{aL} B H C'_L \lambda \sqrt{R_L}}{M_L} \tag{53}$$

where B is across-wind dimension of the building, H is building height and M_L is the generalized mass of the building in across-wind direction. Peak factor g_{aL} is given as:

$$g_{aL} = \sqrt{2 \ln(600 f_L) + 1.2} \tag{54}$$

where f_L is fundamental frequency for the first mode in across-wind direction.

q_H is wind velocity pressure given as:

$$q_H = \frac{1}{2} \rho U_H^2 \tag{55}$$

where ρ is air density and U_H is design wind speed.

C'_L is RMS overturning moment coefficient given as:

$$C'_L = 0.0082\left(\frac{D}{B}\right)^3 - 0.071\left(\frac{D}{B}\right)^2 + 0.22\left(\frac{D}{B}\right) \tag{56}$$

where D is along-wind dimension of the building.

λ is given as:

$$\lambda = 1 - 0.4\ln(\beta) \tag{57}$$

where $\beta = 1$ for conventional building and $\beta = 2$ for lattice structure.

Resonance factor R_L is given as:

$$R_L = \frac{\pi F_L}{4\zeta_L} \tag{58}$$

where ζ_L is critical damping ratio for the first mode in across-wind direction. F_L and required parameters for F_L are given as:

$$F_L = \sum_{j=1}^{m} \frac{4\kappa_j(1+0.6\beta_j)\beta_j}{\pi} \frac{\left(\frac{f_L}{f_{sj}}\right)^2}{\left\{1-\left(\frac{f_L}{f_{sj}}\right)^2\right\}^2 + 4\beta_j^2\left(\frac{f_L}{f_{sj}}\right)^2} \tag{59}$$

$$\kappa_1 = 0.85$$
$$\kappa_2 = 0.02$$

$$m = \begin{cases} 1, & D/B < 3 \\ 2, & D/B \geq 3 \end{cases} \tag{60}$$

$$f_{s1} = \frac{0.12}{\left\{1+0.38\left(\frac{D}{B}\right)^2\right\}^{0.89}} \frac{U_H}{B} \tag{61}$$

$$f_{s2} = \frac{0.56}{\left(\frac{D}{B}\right)^{0.85}} \frac{U_H}{B} \tag{62}$$

$$\beta_1 = \frac{\left(\frac{D}{B}\right)^4 + 2.3\left(\frac{D}{B}\right)^2}{\left\{2.4\left(\frac{D}{B}\right)^4 - 9.2\left(\frac{D}{B}\right)^3 + 18\left(\frac{D}{B}\right)^2 + 9.5\left(\frac{D}{B}\right) - 0.15\right\}} \frac{0.12}{\frac{D}{B}} \tag{63}$$

$$\beta_2 = \frac{0.28}{\left(\frac{D}{B}\right)^{0.34}} \tag{64}$$

4.6 AS/NZS 1170.2:2011

Australian/New-Zealand combined joint standard AS/NZS 1170.2:2011 provides the following equation for solving across-wind acceleration:

$$\ddot{y}_{max} = \frac{1.5 b g_R}{m_0}\left[\frac{0.5\rho_{air}\left[V_{des,\theta}\right]^2}{(1+g_v I_h)^2}\right] K_m \sqrt{\frac{\pi C_{fs}}{\zeta}} \tag{65}$$

where b is across-wind dimension of the building, m_0 is average mass per unit height, ρ_{air} is air density, $V_{des,\theta}$ is design wind speed, ζ is damping ratio and g_v is peak factor for upwind velocity fluctuations, which may be taken as 3.7.

g_r is peak factor given as:

$$g_R = \sqrt{2\ln(600 n_e)} \tag{66}$$

where n_e is fundamental frequency for the fundamental mode in across-wind direction.

K_m is mode shape correction factor given as:

$$K_m = 0.76 + 0.24k \tag{67}$$

where k is mode shape exponent taken as 1.5 for uniform cantilever structures.

I_h is turbulence intensity taken from Table 6.1 in AS/NZS 1170.2. C_{fs} is across-wind force spectrum coefficient generalized for a linear mode shape given in AS/NZS 1170.2 clause 6.3.2.3 and it is the function of reduced velocity given as:

$$V_n = \frac{V_{des,\theta}}{n_e b(1+g_v I_h)} \tag{68}$$

4.7 Method by Emil Simiu

Simiu (2011) provides procedure to estimate across-wind response. Formula for calculating across-wind acceleration is purely empirical based on wind tunnel tests and is restricted to square cross-section only, with no neighboring tall buildings. (Simiu 2011.) goes through wind design by ASCE/SEI 7-10 in detail and provides his own formulas for across-wind and torsional response. Peak deflection at height z is given as (Simiu 2011):

$$y_{pk}(z) = C\left[\frac{\bar{V}(H)}{n_1\sqrt{A}}\right]^p \frac{\sqrt{A}}{\zeta_1^{1/2}}\frac{\rho}{\rho_b}\frac{z}{H} \tag{69}$$

where C and p are empirical constants given as 0.00065 and 3.3 respectively from Simiu (2011). $\bar{V}(H)$ is mean hourly wind velocity at H above the ground, n_1 is fundamental frequency, A is area of the cross-section, ζ_1 is damping ratio for the first mode, ρ is air density, ρ_b is building mass per unit length and H is building height.

Peak acceleration in across-wind direction at height z is then calculated by:

$$\ddot{y}_{pk}(z) = (2\pi n_1)^2 y_{pk}(z) \tag{70}$$

4.8 Results and discussion

Tables 5 and 6 show the results for across-wind peak accelerations calculated by the standards. In Table 5 return period is converted by Eurocode for all standards and in Table 6 return period is converted by each standard separately.

It should be noted that acceleration response given by Eurocode is extremely high, being two to three magnitudes higher than acceleration response given by other standards. Similar results were found by Granroth (2019) and Kortelainen (2012). Results from Eurocode calculations will not be considered in the calculation of coefficient of variation.

By closer investigation in method 2, making a comparison with the study by Hansen (2013) referring to Figure 9, there was a difference in the used K_a factor, which has remarkable influence on the result. Eurocode suggests that the given value of $K_{a,max}$ is for 0% turbulence intensity scenario, and it is a very conservative assumption for calculations of higher turbulence intensity. Also, the method provided by Eurocode to evaluate across-wind response might be insufficient for conventional high-rise buildings since it is developed originally for stacks and chimneys.

Table 5. Serviceability results. Return period calculated by Eurocode.

	EC-1991-1-4		NBCC	AIJ	AS/NZ	Simiu
	Method 1	Method 2	2005		1770.2	
Basic wind velocity, 10 years return period [m/s]	19.0	-	17.4	19.0	26.8	17.4
Response time	10-min	-	1-hr	10-min	3-s	1-hr
Acceleration [m/s^2]	1.29	18.38	0.15	0.33	0.26	0.13
Acceleration [milli-g]	132	1874	15	34	26	14

Table 6. Serviceability results. Return period calculated by each code separately.

	EC-1991-1-4		NBCC	AIJ	AS/NZ	Simiu
	Method 1	Method 2	2005		1770.2	
Basic wind velocity, 10 years return period [m/s]	19.0	-	14.4	18.0	25.1	16.2
Response time	10-min	-	1-hr	10-min	3-s	1-hr
Acceleration [m/s^2]	1.29	18.38	0.08	0.27	0.19	0.10
Acceleration [milli-g]	132	1874	8	27	19	11

Coefficient of variation (CoV) for the results from Table 5 is 53.4% and for results from Table 6 it is 42.8%. Variation is much higher compared to other studies presented in 4.9. This might be due to different initial values of wind speed, which has a significant impact on the result. Gust duration conversions might differ slightly between the studies. It is also possible that the standard procedures have been interpreted in a different way.

Results are quite scattered, which points to a difficulty predicting the across-wind acceleration. It is mentioned in the literature and the standards that procedures provided by the standards are for rough, preliminary estimations and not for actual final design use. Wind tunnel tests are most appropriate to be used in design procedures, since they give the most accurate prediction of the response after full-scale measurements (Dyrbye & Hansen 1997, Irwin et al. 2013).

4.9 Studies on comparison

Many studies have been made to compare results of different country specific standards. In the study by Holmes et al. (2008) 8 different standards were used to compare across-wind acceleration response of high-rise buildings and a CoV of 17.6% (15.2% calculated by myself) was observed. Kwon & Kareem (2013) compared 5 international standards in terms of across-wind acceleration response with three cases. CoV in the cases were 27.9%, 15.4% and 17.7% and a bigger CoV was observed in across-wind responses compared to along-wind peak acceleration responses. In the study by Kijewski & Kareem (1998) 3 different standards were compared for 4 different wind speeds. The CoV for these velocities were 15.4%, 19.5%, 23.1% and 24.7%. In the study by Tozan et al. (2013) 5 different standards were compared and CoV was 56.9%.

The average CoV in these studies is 24.0%, meaning that there is quite some scatter in the prediction of across-wind acceleration response. Also, CoV tends to be smaller with higher wind speed. From the same series of studies, the average of CoV in along-wind acceleration is 20.8%, meaning that across-wind response is harder to predict. Vortex shedding phenomenon is more complex than along-wind oscillation, so the design process must consider that fact.

5 2D Finite element approach to estimate response

In this chapter 2D FEM (finite element method) design procedure will be proposed. This procedure will be used in conjunction with finite element analysis program RFEM. The first three natural frequency modes in x-direction are extracted from RFEM model. With this procedure the resulting dynamic equivalent force from vortex shedding acting on cladding is calculated. This force is then applied back to the RFEM model in chapter 6 and acceleration response of the structure will be obtained from RFEM calculations.

5.1 Model type

There are two fundamental options to model response in wind induced vibrations: the sinusoidal model and the band limited random forcing model. In the sinusoidal model load is harmonic rather than random. Canadian highway bridge design code (CSA S6-14 2014) suggests based on (Davenport et al., Vickery & Clark 1972, Harris & Crede 1976, Wootton 1969) that the random excitation model is considered more accurate than the harmonic, sinusoidal model. Sinusoidal oscillation happens when amplitude of the motion is large enough, in the order of 2.0% to 2.5%. On the other hand, the sinusoidal model leads to a more conservative estimation and it is easier to apply. The differences of these models are explained in sections 4.2.3 and 4.2.4. In this method presented the sinusoidal model will be used.

Assuming vortices are shed regularly, the formula for fluctuating time dependent lift load due to vortex shedding is (Dyrbye & Hansen 1997):

$$P_L(t) = \frac{1}{2}\rho D U^2 C_L \sin(2\pi f_n t) \tag{71}$$

where ρ is air density, U is mean wind velocity, t is time and f_n can be taken as natural vibration frequency of the structure or shedding frequency.

5.2 Frequency range for lock-in condition

From the lock-in theory it is assumed that there is a range of wind velocities over which the shedding frequency and the natural frequency of the structure lock-in into each other. The big challenge is to define the range of these frequencies over which lock-in occurs. Foley et al. (2004) and Dyrbye & Hansen (1997) recommends using lower f_s^L and upper f_s^U bound for frequencies over which shedding occurs in lock-in condition. They can be calculated by:

$$f_s^L = f_s - f_s' = \frac{St\overline{U}_z}{D} - \frac{St\bar{u}_z'}{D} = f_s\left[1 - \frac{u_z'}{\overline{U}_z}\right] \tag{72}$$

$$f_s^U = f_s + f_s' = \frac{St\overline{U}_z}{D} + \frac{St\bar{u}_z'}{D} = f_s\left[1 + \frac{u_z'}{\overline{U}_z}\right] \tag{73}$$

where U is the mean component of the wind at height z, and u_z' is the turbulent component at height z.

Turbulent component is assumed to be Gaussian distributed, zero-mean, random variable. Based on experiments standard deviation of the turbulent component is defined as (Dyrbye & Hansen 1997):

$$\sigma_u = Au_* \tag{74}$$

where A = 2.5 for roughness length z_0 = 0.05 m or A = 1.8 for roughness length z_0 = 0.3 m. The friction velocity u_* can be solved by (Dyrbye & Hansen 1997):

$$u_* = \frac{\bar{U}_z \kappa}{\ln\left(\frac{z}{z_0}\right)} \tag{75}$$

where k is von Karman's constant, which can be approximated as 0.4. An estimate of standard deviation of turbulent component at height z may be written as:

$$(\sigma_u)_z = \frac{A\bar{U}_z \kappa}{\ln\left(\frac{z}{z_0}\right)} \tag{76}$$

Frequency boundaries are assumed to be based on peak turbulent wind component variation from mean wind velocity U. Peak variation in turbulent wind component from the mean is assumed to be $1(\sigma_u)$. Upper and lower bound for shedding frequency may be rewritten as:

$$f_s^L = f_s\left[1 - \frac{u'_{z,max}}{\bar{U}_z}\right] = f_s\left[1 - \frac{1(\sigma_u)_z}{\bar{U}_z}\right] \tag{77}$$

$$f_s^U = f_s\left[1 + \frac{u'_{z,max}}{\bar{U}_z}\right] = f_s\left[1 + \frac{1(\sigma_u)_z}{\bar{U}_z}\right] \tag{78}$$

A range of 10-20% of the shedding frequency for the frequency range is commonly used by literature (Taranath 2012, Paidoussis et al. 2011).

Another challenge is to estimate longitudinal synchronization of vortex shedding. It may be approximated by correlation length, which is the length over which vortices act in phase. (Dyrbye & Hansen 1997.) A conservative solution is to apply a sinusoidal load on the length, determined by lower and upper boundaries of the frequency.

5.3 Design procedure

Design procedure is adopted from Foley et al. (2004) for square cross-section. This design procedure is strictly for square cross-section with sharp corners. In the case of a different cross-section, St, C_L and critical range of Re must be re-evaluated.

1. Determine wind velocities at the reference height 10 m that will be used for design.
2. Discretize the height of the structure into intervals suitable for evaluation. In a tapered case calculate average across-wind dimension d of each finite element.

3. Calculate wind velocity over the whole height at the center of each finite element for each reference wind velocity in range. Power law, logarithmic law or suitable standard may be chosen for this procedure.
4. Based on wind velocities calculated in step 3, calculate *Re* for each finite element with equation (9). Investigate what values of *St* and C_L should be used for a given *Re*.
5. Based on equation (8) calculate shedding frequency for each finite element.
6. For each velocity in step 1 and each shedding frequency defined in step 5 calculate the lower- and upper-range for shedding frequencies using equations (77) and (78).
7. Calculate sinusoidal load at each considered location for each vibration mode at the range from lower to upper shedding frequency for each element with equation (71).

1. 2. 3.) Velocities used at the reference height of 10 m are 5-35 m/s. The building is divided into 4 m long finite elements in vertical direction. Wind velocities were calculated for each finite element with logarithmic law equation (2). Only the calculations for a wind velocity range of 23-35 m/s is showed in this chapter. Full tables are shown in Appendix 7. (Table 7)

Table 7. Wind speed variation over height.

Elevation [m]	d(x) [m]	U(x)												
		23	24	25	26	27	28	29	30	31	32	33	34	35
200	30	33.0	34.4	35.8	37.3	38.7	40.1	41.6	43.0	44.4	45.9	47.3	48.7	50.2
196	30	32.9	34.3	35.8	37.2	38.6	40.1	41.5	42.9	44.4	45.8	47.2	48.6	50.1
192	30	32.8	34.3	35.7	37.1	38.5	40.0	41.4	42.8	44.3	45.7	47.1	48.5	50.0
188	30	32.8	34.2	35.6	37.0	38.5	39.9	41.3	42.7	44.2	45.6	47.0	48.4	49.9
184	30	32.7	34.1	35.5	37.0	38.4	39.8	41.2	42.6	44.1	45.5	46.9	48.3	49.8
180	30	32.6	34.0	35.5	36.9	38.3	39.7	41.1	42.6	44.0	45.4	46.8	48.2	49.6
176	30	32.5	34.0	35.4	36.8	38.2	39.6	41.0	42.5	43.9	45.3	46.7	48.1	49.5
172	30	32.5	33.9	35.3	36.7	38.1	39.5	40.9	42.4	43.8	45.2	46.6	48.0	49.4
168	30	32.4	33.8	35.2	36.6	38.0	39.4	40.8	42.3	43.7	45.1	46.5	47.9	49.3
164	30	32.3	33.7	35.1	36.5	37.9	39.3	40.7	42.1	43.6	45.0	46.4	47.8	49.2
160	30	32.2	33.6	35.0	36.4	37.8	39.2	40.6	42.0	43.4	44.8	46.2	47.6	49.0
156	30	32.1	33.5	34.9	36.3	37.7	39.1	40.5	41.9	43.3	44.7	46.1	47.5	48.9
152	30	32.1	33.5	34.8	36.2	37.6	39.0	40.4	41.8	43.2	44.6	46.0	47.4	48.8
148	30	32.0	33.4	34.8	36.1	37.5	38.9	40.3	41.7	43.1	44.5	45.9	47.3	48.7
144	30	31.9	33.3	34.7	36.0	37.4	38.8	40.2	41.6	43.0	44.4	45.7	47.1	48.5
140	30	31.8	33.2	34.6	35.9	37.3	38.7	40.1	41.5	42.8	44.2	45.6	47.0	48.4
136	30	31.7	33.1	34.4	35.8	37.2	38.6	40.0	41.3	42.7	44.1	45.5	46.8	48.2
132	30	31.6	33.0	34.3	35.7	37.1	38.5	39.8	41.2	42.6	44.0	45.3	46.7	48.1
128	30	31.5	32.9	34.2	35.6	37.0	38.3	39.7	41.1	42.4	43.8	45.2	46.5	47.9
124	30	31.4	32.7	34.1	35.5	36.8	38.2	39.6	40.9	42.3	43.7	45.0	46.4	47.8
120	30	31.3	32.6	34.0	35.4	36.7	38.1	39.4	40.8	42.2	43.5	44.9	46.2	47.6
116	30	31.2	32.5	33.9	35.2	36.6	37.9	39.3	40.6	42.0	43.4	44.7	46.1	47.4
112	30	31.0	32.4	33.7	35.1	36.4	37.8	39.1	40.5	41.8	43.2	44.5	45.9	47.2
108	30	30.9	32.3	33.6	35.0	36.3	37.6	39.0	40.3	41.7	43.0	44.4	45.7	47.1
104	30	30.8	32.1	33.5	34.8	36.2	37.5	38.8	40.2	41.5	42.8	44.2	45.5	46.9
100	30	30.7	32.0	33.3	34.7	36.0	37.3	38.7	40.0	41.3	42.7	44.0	45.3	46.7
96	30	30.5	31.9	33.2	34.5	35.8	37.2	38.5	39.8	41.2	42.5	43.8	45.1	46.5
92	30	30.4	31.7	33.0	34.4	35.7	37.0	38.3	39.6	41.0	42.3	43.6	44.9	46.2
88	30	30.2	31.6	32.9	34.2	35.5	36.8	38.1	39.4	40.8	42.1	43.4	44.7	46.0
84	30	30.1	31.4	32.7	34.0	35.3	36.6	37.9	39.2	40.6	41.9	43.2	44.5	45.8
80	30	29.9	31.2	32.5	33.8	35.1	36.4	37.7	39.0	40.3	41.6	42.9	44.2	45.5
76	30	29.8	31.0	32.3	33.6	34.9	36.2	37.5	38.8	40.1	41.4	42.7	44.0	45.3
72	30	29.6	30.9	32.1	33.4	34.7	36.0	37.3	38.6	39.9	41.1	42.4	43.7	45.0
68	30	29.4	30.7	31.9	33.2	34.5	35.8	37.0	38.3	39.6	40.9	42.2	43.4	44.7
64	30	29.2	30.4	31.7	33.0	34.3	35.5	36.8	38.1	39.3	40.6	41.9	43.1	44.4
60	30	29.0	30.2	31.5	32.7	34.0	35.3	36.5	37.8	39.0	40.3	41.6	42.8	44.1
56	30	28.7	30.0	31.2	32.5	33.7	35.0	36.2	37.5	38.7	40.0	41.2	42.5	43.7
52	30	28.5	29.7	31.0	32.2	33.4	34.7	35.9	37.2	38.4	39.6	40.9	42.1	43.4
48	30	28.2	29.4	30.7	31.9	33.1	34.4	35.6	36.8	38.0	39.3	40.5	41.7	42.9
44	30	27.9	29.1	30.4	31.6	32.8	34.0	35.2	36.4	37.6	38.9	40.1	41.3	42.5
40	30	27.6	28.8	30.0	31.2	32.4	33.6	34.8	36.0	37.2	38.4	39.6	40.8	42.0
36	30	27.3	28.5	29.6	30.8	32.0	33.2	34.4	35.6	36.7	37.9	39.1	40.3	41.5
32	30	26.9	28.0	29.2	30.4	31.5	32.7	33.9	35.1	36.2	37.4	38.6	39.7	40.9
28	30	26.4	27.6	28.7	29.9	31.0	32.2	33.3	34.5	35.6	36.8	37.9	39.1	40.2
24	30	25.9	27.0	28.2	29.3	30.4	31.5	32.7	33.8	34.9	36.1	37.2	38.3	39.4
20	30	25.3	26.4	27.5	28.6	29.7	30.8	31.9	33.0	34.1	35.2	36.3	37.4	38.5
16	30	24.6	25.6	26.7	27.8	28.8	29.9	31.0	32.0	33.1	34.2	35.2	36.3	37.4
12	30	23.6	24.6	25.7	26.7	27.7	28.7	29.8	30.8	31.8	32.8	33.9	34.9	35.9
10	30	23	24	25	26	27	28	29	30	31	32	33	34	35
8	30	22.3	23.2	24.2	25.2	26.1	27.1	28.1	29.0	30.0	31.0	31.9	32.9	33.9
4	30	19.9	20.8	21.7	22.6	23.4	24.3	25.2	26.0	26.9	27.8	28.6	29.5	30.4
0	30	19.9	20.8	21.7	22.6	23.4	24.3	25.2	26.0	26.9	27.8	28.6	29.5	30.4

4.) *Reynolds number* was calculated for each finite element with equation (9). Values of *Re* are all above 7 x 10^7 which means that $St = 0.11$ and $C_L = 1.1$ may be used for further calculations for every finite element (Table 8).

Table 8. Reynolds Numbers for wind speeds over height.

Elevation [m]	d(x) [m]	Re vs. wind speed and building height												
		23	24	25	26	27	28	29	30	31	32	33	34	35
200	30	6.6E+07	6.9E+07	7.2E+07	7.5E+07	7.7E+07	8.0E+07	8.3E+07	8.6E+07	8.9E+07	9.2E+07	9.5E+07	9.7E+07	1.0E+08
196	30	6.6E+07	6.9E+07	7.2E+07	7.4E+07	7.7E+07	8.0E+07	8.3E+07	8.6E+07	8.9E+07	9.2E+07	9.4E+07	9.7E+07	1.0E+08
192	30	6.6E+07	6.9E+07	7.1E+07	7.4E+07	7.7E+07	8.0E+07	8.3E+07	8.6E+07	8.9E+07	9.1E+07	9.4E+07	9.7E+07	1.0E+08
188	30	6.6E+07	6.8E+07	7.1E+07	7.4E+07	7.7E+07	8.0E+07	8.3E+07	8.5E+07	8.8E+07	9.1E+07	9.4E+07	9.7E+07	1.0E+08
184	30	6.5E+07	6.8E+07	7.1E+07	7.4E+07	7.7E+07	8.0E+07	8.2E+07	8.5E+07	8.8E+07	9.1E+07	9.4E+07	9.7E+07	1.0E+08
180	30	6.5E+07	6.8E+07	7.1E+07	7.4E+07	7.7E+07	7.9E+07	8.2E+07	8.5E+07	8.8E+07	9.1E+07	9.4E+07	9.6E+07	9.9E+07
176	30	6.5E+07	6.8E+07	7.1E+07	7.4E+07	7.6E+07	7.9E+07	8.2E+07	8.5E+07	8.8E+07	9.1E+07	9.3E+07	9.6E+07	9.9E+07
172	30	6.5E+07	6.8E+07	7.1E+07	7.3E+07	7.6E+07	7.9E+07	8.2E+07	8.5E+07	8.8E+07	9.0E+07	9.3E+07	9.6E+07	9.9E+07
168	30	6.5E+07	6.8E+07	7.0E+07	7.3E+07	7.6E+07	7.9E+07	8.2E+07	8.5E+07	8.7E+07	9.0E+07	9.3E+07	9.6E+07	9.9E+07
164	30	6.5E+07	6.7E+07	7.0E+07	7.3E+07	7.6E+07	7.9E+07	8.1E+07	8.4E+07	8.7E+07	9.0E+07	9.3E+07	9.6E+07	9.8E+07
160	30	6.4E+07	6.7E+07	7.0E+07	7.3E+07	7.6E+07	7.8E+07	8.1E+07	8.4E+07	8.7E+07	9.0E+07	9.2E+07	9.5E+07	9.8E+07
156	30	6.4E+07	6.7E+07	7.0E+07	7.3E+07	7.5E+07	7.8E+07	8.1E+07	8.4E+07	8.7E+07	8.9E+07	9.2E+07	9.5E+07	9.8E+07
152	30	6.4E+07	6.7E+07	7.0E+07	7.2E+07	7.5E+07	7.8E+07	8.1E+07	8.4E+07	8.6E+07	8.9E+07	9.2E+07	9.5E+07	9.8E+07
148	30	6.4E+07	6.7E+07	7.0E+07	7.2E+07	7.5E+07	7.8E+07	8.1E+07	8.3E+07	8.6E+07	8.9E+07	9.2E+07	9.5E+07	9.7E+07
144	30	6.4E+07	6.7E+07	6.9E+07	7.2E+07	7.5E+07	7.8E+07	8.0E+07	8.3E+07	8.6E+07	8.9E+07	9.1E+07	9.4E+07	9.7E+07
140	30	6.4E+07	6.6E+07	6.9E+07	7.2E+07	7.5E+07	7.7E+07	8.0E+07	8.3E+07	8.6E+07	8.8E+07	9.1E+07	9.4E+07	9.7E+07
136	30	6.3E+07	6.6E+07	6.9E+07	7.2E+07	7.4E+07	7.7E+07	8.0E+07	8.3E+07	8.5E+07	8.8E+07	9.1E+07	9.4E+07	9.6E+07
132	30	6.3E+07	6.6E+07	6.9E+07	7.1E+07	7.4E+07	7.7E+07	8.0E+07	8.2E+07	8.5E+07	8.8E+07	9.1E+07	9.3E+07	9.6E+07
128	30	6.3E+07	6.6E+07	6.8E+07	7.1E+07	7.4E+07	7.7E+07	7.9E+07	8.2E+07	8.5E+07	8.8E+07	9.0E+07	9.3E+07	9.6E+07
124	30	6.3E+07	6.5E+07	6.8E+07	7.1E+07	7.4E+07	7.6E+07	7.9E+07	8.2E+07	8.5E+07	8.7E+07	9.0E+07	9.3E+07	9.6E+07
120	30	6.3E+07	6.5E+07	6.8E+07	7.1E+07	7.3E+07	7.6E+07	7.9E+07	8.2E+07	8.4E+07	8.7E+07	9.0E+07	9.2E+07	9.5E+07
116	30	6.2E+07	6.5E+07	6.8E+07	7.0E+07	7.3E+07	7.6E+07	7.9E+07	8.1E+07	8.4E+07	8.7E+07	8.9E+07	9.2E+07	9.5E+07
112	30	6.2E+07	6.5E+07	6.7E+07	7.0E+07	7.3E+07	7.6E+07	7.8E+07	8.1E+07	8.4E+07	8.6E+07	8.9E+07	9.2E+07	9.4E+07
108	30	6.2E+07	6.5E+07	6.7E+07	7.0E+07	7.3E+07	7.5E+07	7.8E+07	8.1E+07	8.3E+07	8.6E+07	8.9E+07	9.1E+07	9.4E+07
104	30	6.2E+07	6.4E+07	6.7E+07	7.0E+07	7.2E+07	7.5E+07	7.8E+07	8.0E+07	8.3E+07	8.6E+07	8.8E+07	9.1E+07	9.4E+07
100	30	6.1E+07	6.4E+07	6.7E+07	6.9E+07	7.2E+07	7.5E+07	7.7E+07	8.0E+07	8.3E+07	8.5E+07	8.8E+07	9.1E+07	9.3E+07
96	30	6.1E+07	6.4E+07	6.6E+07	6.9E+07	7.2E+07	7.4E+07	7.7E+07	8.0E+07	8.2E+07	8.5E+07	8.8E+07	9.0E+07	9.3E+07
92	30	6.1E+07	6.3E+07	6.6E+07	6.9E+07	7.1E+07	7.4E+07	7.7E+07	7.9E+07	8.2E+07	8.5E+07	8.7E+07	9.0E+07	9.2E+07
88	30	6.0E+07	6.3E+07	6.6E+07	6.8E+07	7.1E+07	7.4E+07	7.6E+07	7.9E+07	8.2E+07	8.4E+07	8.7E+07	8.9E+07	9.2E+07
84	30	6.0E+07	6.3E+07	6.5E+07	6.8E+07	7.1E+07	7.3E+07	7.6E+07	7.8E+07	8.1E+07	8.4E+07	8.6E+07	8.9E+07	9.2E+07
80	30	6.0E+07	6.2E+07	6.5E+07	6.8E+07	7.0E+07	7.3E+07	7.5E+07	7.8E+07	8.1E+07	8.3E+07	8.6E+07	8.8E+07	9.1E+07
76	30	6.0E+07	6.2E+07	6.5E+07	6.7E+07	7.0E+07	7.2E+07	7.5E+07	7.8E+07	8.0E+07	8.3E+07	8.5E+07	8.8E+07	9.1E+07
72	30	5.9E+07	6.2E+07	6.4E+07	6.7E+07	6.9E+07	7.2E+07	7.5E+07	7.7E+07	8.0E+07	8.2E+07	8.5E+07	8.7E+07	9.0E+07
68	30	5.9E+07	6.1E+07	6.4E+07	6.6E+07	6.9E+07	7.2E+07	7.4E+07	7.7E+07	7.9E+07	8.2E+07	8.4E+07	8.7E+07	8.9E+07
64	30	5.8E+07	6.1E+07	6.3E+07	6.6E+07	6.9E+07	7.1E+07	7.4E+07	7.6E+07	7.9E+07	8.1E+07	8.4E+07	8.6E+07	8.9E+07
60	30	5.8E+07	6.0E+07	6.3E+07	6.5E+07	6.8E+07	7.1E+07	7.3E+07	7.6E+07	7.8E+07	8.1E+07	8.3E+07	8.6E+07	8.8E+07
56	30	5.7E+07	6.0E+07	6.2E+07	6.5E+07	6.7E+07	7.0E+07	7.2E+07	7.5E+07	7.7E+07	8.0E+07	8.2E+07	8.5E+07	8.7E+07
52	30	5.7E+07	5.9E+07	6.2E+07	6.4E+07	6.7E+07	6.9E+07	7.2E+07	7.4E+07	7.7E+07	7.9E+07	8.2E+07	8.4E+07	8.7E+07
48	30	5.6E+07	5.9E+07	6.1E+07	6.4E+07	6.6E+07	6.9E+07	7.1E+07	7.4E+07	7.6E+07	7.9E+07	8.1E+07	8.3E+07	8.6E+07
44	30	5.6E+07	5.8E+07	6.1E+07	6.3E+07	6.6E+07	6.8E+07	7.0E+07	7.3E+07	7.5E+07	7.8E+07	8.0E+07	8.3E+07	8.5E+07
40	30	5.5E+07	5.8E+07	6.0E+07	6.2E+07	6.5E+07	6.7E+07	7.0E+07	7.2E+07	7.4E+07	7.7E+07	7.9E+07	8.2E+07	8.4E+07
36	30	5.5E+07	5.7E+07	5.9E+07	6.2E+07	6.4E+07	6.6E+07	6.9E+07	7.1E+07	7.3E+07	7.6E+07	7.8E+07	8.1E+07	8.3E+07
32	30	5.4E+07	5.6E+07	5.8E+07	6.1E+07	6.3E+07	6.5E+07	6.8E+07	7.0E+07	7.2E+07	7.5E+07	7.7E+07	7.9E+07	8.2E+07
28	30	5.3E+07	5.5E+07	5.7E+07	6.0E+07	6.2E+07	6.4E+07	6.7E+07	6.9E+07	7.1E+07	7.4E+07	7.6E+07	7.8E+07	8.0E+07
24	30	5.2E+07	5.4E+07	5.6E+07	5.9E+07	6.1E+07	6.3E+07	6.5E+07	6.8E+07	7.0E+07	7.2E+07	7.4E+07	7.7E+07	7.9E+07
20	30	5.1E+07	5.3E+07	5.5E+07	5.7E+07	5.9E+07	6.2E+07	6.4E+07	6.6E+07	6.8E+07	7.0E+07	7.3E+07	7.5E+07	7.7E+07
16	30	4.9E+07	5.1E+07	5.3E+07	5.6E+07	5.8E+07	6.0E+07	6.2E+07	6.4E+07	6.6E+07	6.8E+07	7.0E+07	7.3E+07	7.5E+07
12	30	4.7E+07	4.9E+07	5.1E+07	5.3E+07	5.5E+07	5.7E+07	6.0E+07	6.2E+07	6.4E+07	6.6E+07	6.8E+07	7.0E+07	7.2E+07
10	30	4.6E+07	4.8E+07	5.0E+07	5.2E+07	5.4E+07	5.6E+07	5.8E+07	6.0E+07	6.2E+07	6.4E+07	6.6E+07	6.8E+07	7.0E+07
8	30	4.5E+07	4.6E+07	4.8E+07	5.0E+07	5.2E+07	5.4E+07	5.6E+07	5.8E+07	6.0E+07	6.2E+07	6.4E+07	6.6E+07	6.8E+07
4	30	4.0E+07	4.2E+07	4.3E+07	4.5E+07	4.7E+07	4.9E+07	5.0E+07	5.2E+07	5.4E+07	5.6E+07	5.7E+07	5.9E+07	6.1E+07
0	30	4.0E+07	4.2E+07	4.3E+07	4.5E+07	4.7E+07	4.9E+07	5.0E+07	5.2E+07	5.4E+07	5.6E+07	5.7E+07	5.9E+07	6.1E+07

5. and 6.) Shedding frequency was calculated for each finite element with equation (8). Red marked cells are of matching natural frequency of the structure with a range of ±0.001 and yellow marked cells are within frequency boundaries of the lock-in region (Table 9 and Table 10).

Table 9. Shedding frequency in each finite element.

Elevation [m]	d(x) [m]	Shedding frequency vs. wind speed and building height												
		23	24	25	26	27	28	29	30	31	32	33	34	35
200	30	0.121	0.126	0.131	0.137	0.142	0.147	0.152	0.158	0.163	0.168	0.173	0.179	0.184
196	30	0.121	0.126	0.131	0.136	0.142	0.147	0.152	0.157	0.163	0.168	0.173	0.178	0.184
192	30	0.120	0.126	0.131	0.136	0.141	0.147	0.152	0.157	0.162	0.168	0.173	0.178	0.183
188	30	0.120	0.125	0.131	0.136	0.141	0.146	0.151	0.157	0.162	0.167	0.172	0.178	0.183
184	30	0.120	0.125	0.130	0.136	0.141	0.146	0.151	0.156	0.162	0.167	0.172	0.177	0.182
180	30	0.120	0.125	0.130	0.135	0.140	0.146	0.151	0.156	0.161	0.166	0.172	0.177	0.182
176	30	0.119	0.125	0.130	0.135	0.140	0.145	0.150	0.156	0.161	0.166	0.171	0.176	0.182
172	30	0.119	0.124	0.129	0.135	0.140	0.145	0.150	0.155	0.160	0.166	0.171	0.176	0.181
168	30	0.119	0.124	0.129	0.134	0.139	0.145	0.150	0.155	0.160	0.165	0.170	0.176	0.181
164	30	0.118	0.124	0.129	0.134	0.139	0.144	0.149	0.155	0.160	0.165	0.170	0.175	0.180
160	30	0.118	0.123	0.128	0.134	0.139	0.144	0.149	0.154	0.159	0.164	0.170	0.175	0.180
156	30	0.118	0.123	0.128	0.133	0.138	0.143	0.149	0.154	0.159	0.164	0.169	0.174	0.179
152	30	0.118	0.123	0.128	0.133	0.138	0.143	0.148	0.153	0.158	0.164	0.169	0.174	0.179
148	30	0.117	0.122	0.127	0.133	0.138	0.143	0.148	0.153	0.158	0.163	0.168	0.173	0.178
144	30	0.117	0.122	0.127	0.132	0.137	0.142	0.147	0.152	0.158	0.163	0.168	0.173	0.178
140	30	0.117	0.122	0.127	0.132	0.137	0.142	0.147	0.152	0.157	0.162	0.167	0.172	0.177
136	30	0.116	0.121	0.126	0.131	0.136	0.141	0.147	0.152	0.157	0.162	0.167	0.172	0.177
132	30	0.116	0.121	0.126	0.131	0.136	0.141	0.146	0.151	0.156	0.161	0.166	0.171	0.176
128	30	0.115	0.120	0.125	0.131	0.136	0.141	0.146	0.151	0.156	0.161	0.166	0.171	0.176
124	30	0.115	0.120	0.125	0.130	0.135	0.140	0.145	0.150	0.155	0.160	0.165	0.170	0.175
120	30	0.115	0.120	0.125	0.130	0.135	0.140	0.145	0.150	0.155	0.160	0.165	0.170	0.174
116	30	0.114	0.119	0.124	0.129	0.134	0.139	0.144	0.149	0.154	0.159	0.164	0.169	0.174
112	30	0.114	0.119	0.124	0.129	0.134	0.139	0.144	0.148	0.153	0.158	0.163	0.168	0.173
108	30	0.113	0.118	0.123	0.128	0.133	0.138	0.143	0.148	0.153	0.158	0.163	0.168	0.173
104	30	0.113	0.118	0.123	0.128	0.133	0.137	0.142	0.147	0.152	0.157	0.162	0.167	0.172
100	30	0.112	0.117	0.122	0.127	0.132	0.137	0.142	0.147	0.152	0.156	0.161	0.166	0.171
96	30	0.112	0.117	0.122	0.127	0.131	0.136	0.141	0.146	0.151	0.156	0.161	0.165	0.170
92	30	0.111	0.116	0.121	0.126	0.131	0.136	0.140	0.145	0.150	0.155	0.160	0.165	0.170
88	30	0.111	0.116	0.121	0.125	0.130	0.135	0.140	0.145	0.149	0.154	0.159	0.164	0.169
84	30	0.110	0.115	0.120	0.125	0.130	0.134	0.139	0.144	0.149	0.153	0.158	0.163	0.168
80	30	0.110	0.114	0.119	0.124	0.129	0.134	0.138	0.143	0.148	0.153	0.157	0.162	0.167
76	30	0.109	0.114	0.119	0.123	0.128	0.133	0.138	0.142	0.147	0.152	0.157	0.161	0.166
72	30	0.108	0.113	0.118	0.123	0.127	0.132	0.137	0.141	0.146	0.151	0.156	0.160	0.165
68	30	0.108	0.112	0.117	0.122	0.126	0.131	0.136	0.141	0.145	0.150	0.155	0.159	0.164
64	30	0.107	0.112	0.116	0.121	0.126	0.130	0.135	0.140	0.144	0.149	0.154	0.158	0.163
60	30	0.106	0.111	0.115	0.120	0.125	0.129	0.134	0.139	0.143	0.148	0.152	0.157	0.162
56	30	0.105	0.110	0.115	0.119	0.124	0.128	0.133	0.137	0.142	0.147	0.151	0.156	0.160
52	30	0.104	0.109	0.114	0.118	0.123	0.127	0.132	0.136	0.141	0.145	0.150	0.154	0.159
48	30	0.103	0.108	0.112	0.117	0.121	0.126	0.130	0.135	0.139	0.144	0.148	0.153	0.157
44	30	0.102	0.107	0.111	0.116	0.120	0.125	0.129	0.134	0.138	0.142	0.147	0.151	0.156
40	30	0.101	0.106	0.110	0.114	0.119	0.123	0.128	0.132	0.136	0.141	0.145	0.150	0.154
36	30	0.100	0.104	0.109	0.113	0.117	0.122	0.126	0.130	0.135	0.139	0.143	0.148	0.152
32	30	0.099	0.103	0.107	0.111	0.116	0.120	0.124	0.129	0.133	0.137	0.141	0.146	0.150
28	30	0.097	0.101	0.105	0.110	0.114	0.118	0.122	0.126	0.131	0.135	0.139	0.143	0.147
24	30	0.095	0.099	0.103	0.107	0.112	0.116	0.120	0.124	0.128	0.132	0.136	0.140	0.145
20	30	0.093	0.097	0.101	0.105	0.109	0.113	0.117	0.121	0.125	0.129	0.133	0.137	0.141
16	30	0.090	0.094	0.098	0.102	0.106	0.110	0.114	0.117	0.121	0.125	0.129	0.133	0.137
12	30	0.087	0.090	0.094	0.098	0.102	0.105	0.109	0.113	0.117	0.120	0.124	0.128	0.132
10	30	0.084	0.088	0.092	0.095	0.099	0.103	0.106	0.110	0.114	0.117	0.121	0.125	0.128
8	30	0.082	0.085	0.089	0.092	0.096	0.099	0.103	0.106	0.110	0.114	0.117	0.121	0.124
4	30	0.073	0.076	0.080	0.083	0.086	0.089	0.092	0.095	0.099	0.102	0.105	0.108	0.111
0	30	0.073	0.076	0.080	0.083	0.086	0.089	0.092	0.095	0.099	0.102	0.105	0.108	0.111

Table 10. Shedding frequency upper and lower boundaries for the first natural frequency.

Mode	f_s [Hz]	z [m]	z_0 [m]	A	κ	$(\sigma_v)_z$	f_s^L [Hz]	f_s^U [Hz]
1	0.139	160	0.05	2.5	0.4	4.69	0.121	0.157

7.) There are vortex shedding induced forces acting on the center of each element for a specified frequency domain. In this example, in the wind speed domain of 27 m/s basic wind speed, shedding frequency matches the natural frequency of the structure at z = 160 m. (Table 11)

Table 11. Vortex shedding induced equivalent forces acting on each element for 15 m/s and 27 m/s basic wind velocities.

Height [m]	Wind velocity V = 15 m/s at 10 m [m/s]	Pressure at each element [N/m^2]	Line-load at each floor F(x) [kN/m]
200	21.5	156	0.626
196	21.5	312	1.246
192	21.4	310	1.241
188	21.4	309	1.236
184	21.3	308	1.230
180	21.3	306	1.225
176	21.2	305	1.219
172	21.2	303	1.214
168	21.1	302	1.208
164	21.1	300	1.202
160	21.0	299	1.196
156	21.0	297	1.189
152	20.9	296	1.183
148	20.9	294	1.177
144	20.8	292	1.170
140	20.7	291	1.163
136	20.7	289	1.156
132	20.6	287	1.149
128	20.5	285	1.141
124	20.5	283	1.134
120	20.4	281	1.126
116	20.3	279	1.118
112	20.2	277	1.109
108	20.2	275	1.101
104	20.1	273	1.092
100	20.0	271	1.082
96	19.9	268	1.073
92	19.8	266	1.063
88	19.7	263	1.053
84	19.6	260	1.042
80	19.5	258	1.031
76	19.4	255	1.019
72	19.3	252	1.007
68	19.2	248	0.994
64	19.0	245	0.980
60	18.9	241	0.966
56	18.7	238	0.950
52	18.6	234	0.934
48	18.4	229	0.917
44	18.2	225	0.898
40	18.0	219	0.878
36	17.8	214	0.856
32	17.5	208	0.831
28	17.2	201	0.804
24	16.9	193	0.773
20	16.5	184	0.737
16	16.0	174	0.695
12	15.4	160	0.321
10	15.0	152	0.304
8	14.5	143	0.570
4	13.0	115	0.458
0	13.0	115	0.000

Height [m]	Wind velocity V = 27 m/s at 10 m [m/s]	Pressure at each element [N/m^2]	Line-load at each floor F(x) [kN/m]
200	38.7	507	2.027
196	38.6	1010	4.038
192	38.5	1005	4.021
188	38.5	1001	4.004
184	38.4	997	3.987
180	38.3	992	3.969
176	38.2	988	3.951
172	38.1	983	3.932
168	38.0	978	3.913
164	37.9	973	3.894
160	37.8	969	3.874
156	37.7	963	3.854
152	37.6	958	3.833
148	37.5	953	3.812
144	37.4	948	3.790
140	37.3	942	3.768
136	37.2	936	3.745
132	37.1	930	3.722
128	37.0	924	3.697
124	36.8	918	3.673
120	36.7	912	3.647
116	36.6	905	3.621
112	36.4	898	3.594
108	36.3	891	3.566
104	36.2	884	3.537
100	36.0	877	3.507
96	35.8	869	3.476
92	35.7	861	3.444
88	35.5	853	3.410
84	35.3	844	3.375
80	35.1	835	3.339
76	34.9	825	3.301
72	34.7	815	3.261
68	34.5	805	3.219
64	34.3	794	3.175
60	34.0	782	3.129
56	33.7	770	3.079
52	33.4	757	3.027
48	33.1	743	2.970
44	32.8	727	2.910
40	32.4	711	2.844
36	32.0	693	2.772
32	31.5	673	2.693
28	31.0	651	2.605
24	30.4	626	2.504
20	29.7	597	2.388
16	28.8	563	2.250
12	27.7	520	1.039
10	27.0	493	0.986
8	26.1	462	1.847
4	23.4	371	1.484
0	23.4	371	0.000

5.4 Flowchart for design procedure of other shapes

Different cross-sectional shapes have a significant impact on the response of the structure. The following steps illustrate what information needs to be found in the case of a different shape:

1. Find *Strouhal number* for the shape investigated and its dependence on angle of attack and *Reynolds number*.
2. Find lift coefficient for the shape investigated and its dependence on angle of attack and *Reynolds number*. Investigate how lift coefficient varies between smooth and turbulent flow.

3. Find the critical range(s) of *Reynolds number*, where vortices are shed alternatively from the sides. There might be a region of *Re*, where vortices are shed chaotically behind the bluff body and therefore cannot create high amplitude vibration.
4. Find the critical angle of attack in terms of the biggest lift force. Investigate other angles of attack as well, since shedding frequency will change if *St* changes with angle of attack, and the zone of resonance might hit a more critical area.

Canadian highway bridge design code (CSA S6-14 2014) has a suggestion that in case of a tapered structure, the shedding frequency varies over the length of the structure. As the frequency increases, resonant vibration occurs first at the thinner part of the structure, distributing towards the wider part as the wind velocity increases. Effectively, critical wind velocity should be treated as a range, being directly dependent on cross-section dimension change. For the vibration mode *i*, maximum and minimum of the critical velocity can be expressed as:

$$\frac{f_i d_{min}}{St} \leq V_{cr} \leq \frac{f_i d_{max}}{St} \tag{79}$$

Tapered shape reduces continuity in longitudinal direction as the theoretical shedding frequency changes along the height as illustrated in Figure 4. (Simiu 2011.)

In the case of more complex shapes, such as non-symmetric, helical or corner cuts, the initial simplified procedure is unreliable, because there is very little research done for special shapes and it is hard to find basic parameters, which define the load magnitude. Davenport (1971) did wind tunnel experiments for six different building shapes with similar mechanical properties. A simplified illustration of the peak deflections of different shapes in comparison to each other is found in Figure 15.

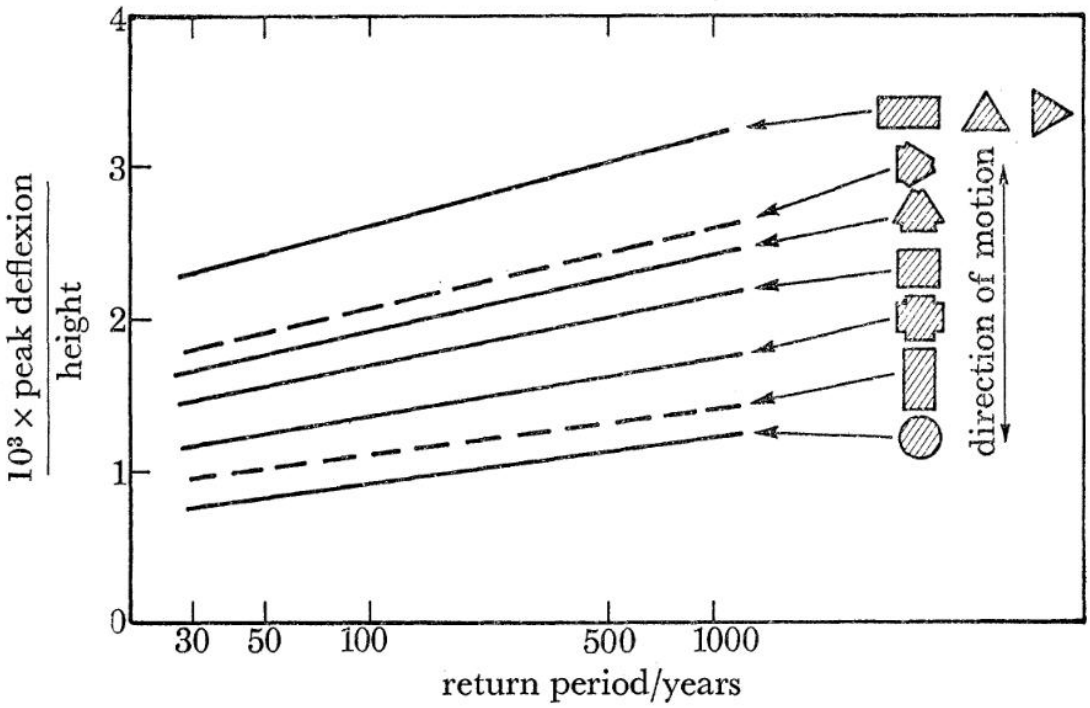

Figure 15. Effect of the shape of the cross-section on maximum deflection (Davenport 1971).

5.5 Contribution of higher modes

When only the contribution of the first vibration mode to acceleration is investigated, response may be corrected by increasing it to take higher modes into account. Li et al. (2009) suggests that the total increase of acceleration should be 6% in that case.

5.6 Accuracy of the model

There are two assumptions that make this model strongly conservative. Referring to Figure 8, assumption of a constant lift coefficient over the whole height may produce a total force around two times bigger. Assumption of vortices acting in phase over such a long distance over the height may produce two to ten times bigger force than in reality. Lock-in condition requires oscillations that are big enough to form vortices in phase over a long distance, which is much harder to achieve in the case of high-rise buildings in comparison with chimneys.

6 3D Finite element approach to estimate response

In this chapter a 3D FEM model will be made in Dlubal RFEM 5.22.01. The model is a 30 x 30 x 200 m simplified typical high-rise building. Modal properties are extracted from the model for 2D FEM analysis, from where obtained load history is used as input into the 3D model. Modal and mass properties obtained from RFEM will be used in the calculations by standards. Maximum acceleration will be obtained from this model as a result to be compared with the standards.

6.1 Building properties and configuration

The building is a basic reinforced concrete high-rise building with columns on the outer perimeter and a shear wall core in the center along the whole height. General floor plan is illustrated in Figure 16. The whole model is illustrated in Figure 17.

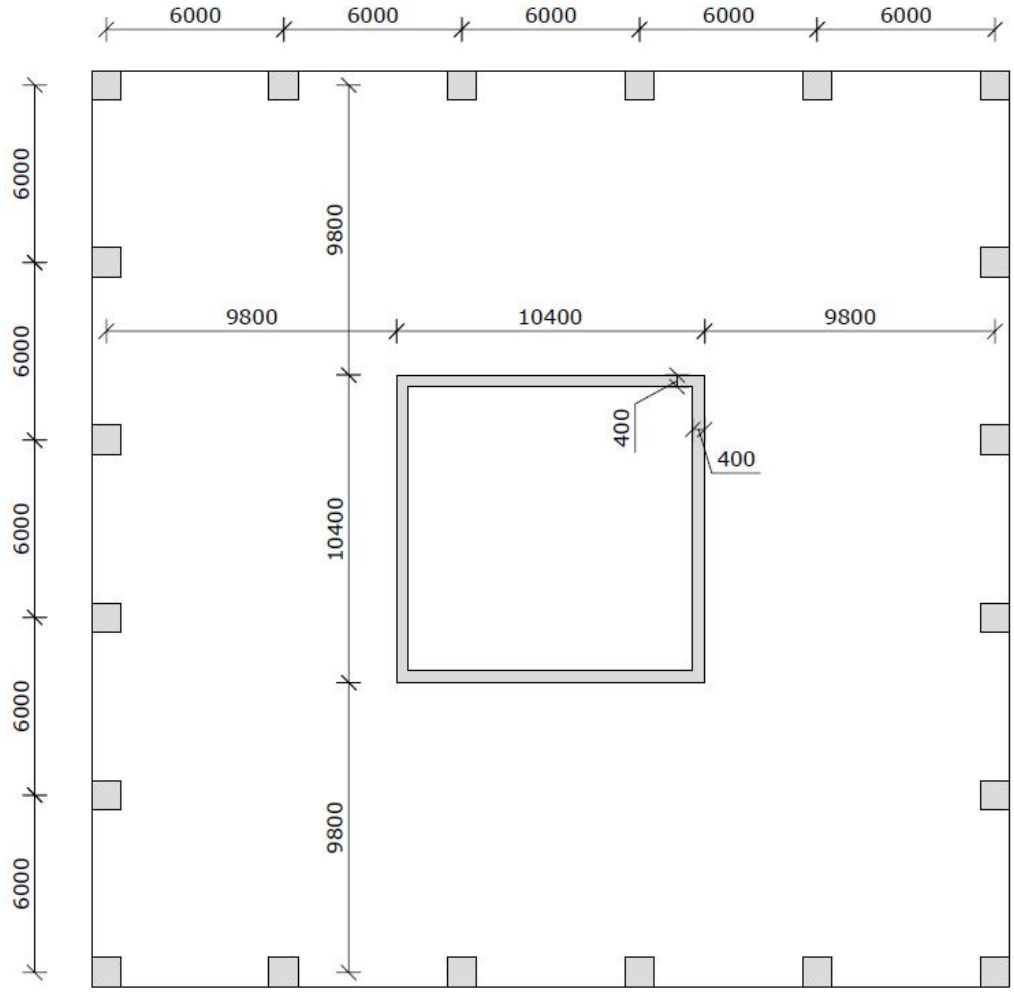

Figure 16. General floor plan and columns layout.

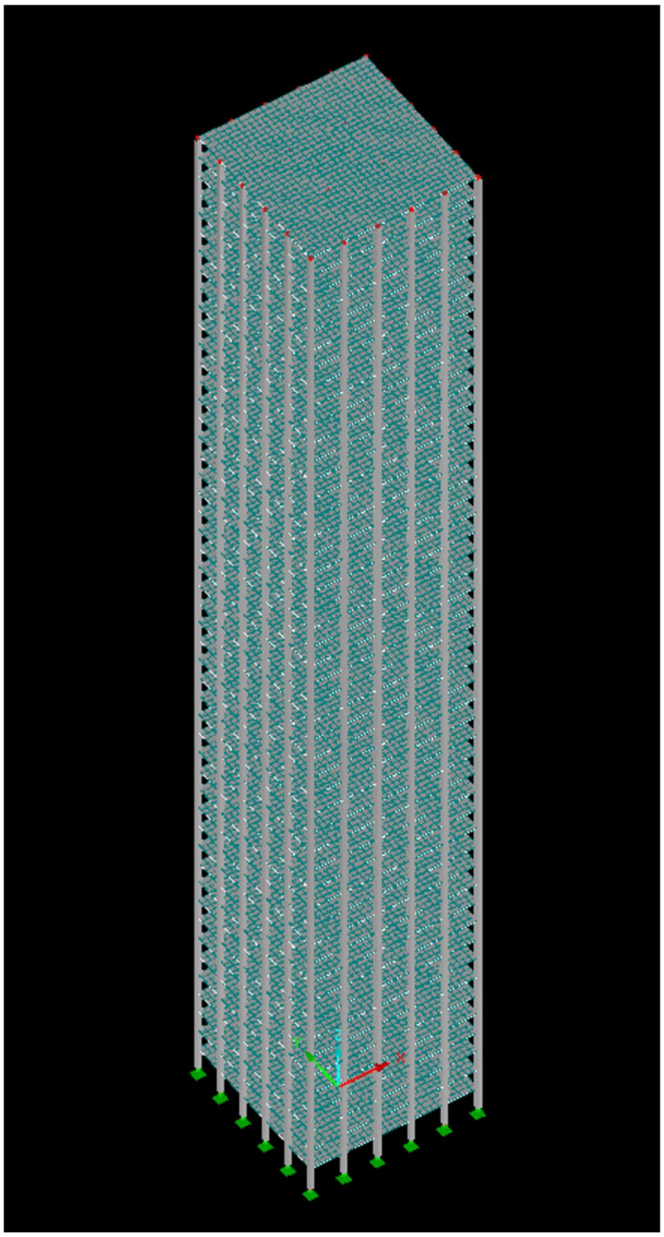

Figure 17. 3D view of the whole model.

The model was configured with the following properties:

- Reinforced concrete structure with walls at the core and columns at the perimeter.
- Building height is 200 m with a floor height of 4 m.
- Width in both directions is 30 m.
- Thickness of the slabs is 300 mm.
- Core wall thickness is 400 mm.
- The cross-section of the columns is 1000 x 1000 mm squared.
- Concrete of C70/85 strength was used for columns and shear walls and C35/45 was used for slabs.
- Vertical concrete structures are assumed to be uncracked.
- Bending and torsional stiffness of slabs is assumed to be 0.25.
- Damping is taken as 0.02.
- Loads used are self-weight, live load and wind load.
- Building is for office usage with a live load of 4 kN/m^2.
- Live load is reduced to 0.3 in load combination.

- The supports for the columns are modelled as fixed in translation in X, Y and Z directions and fixed rotation around Z axis.
- The supports for the shear walls are modelled as fixed in translation in X, Y and Z directions and free to rotate around all axes.

6.2 Modal analysis

Natural frequencies were calculated with a RF-DYNAM add-on module in RFEM. The building's first three natural vibration frequencies in X-direction are:

1. 0.139 Hz
2. 0.617 Hz
3. 1.511 Hz

6.3 Dynamic wind analysis

6.3.1 Settings setup

Dynamic wind analysis is performed with RF_DYNAM Pro add-on module in RFEM. The setup options are described in this section. The mass cases that were included in analysis were self-weight and live load. In the mass combination 100% of self-weight and 30% of live load were used for analysis. In the "Natural vibration cases" tab, the lowest 4 eigenvalues were selected. Figure 18 and Figure 19 shows other options related to mesh and solving parameters.

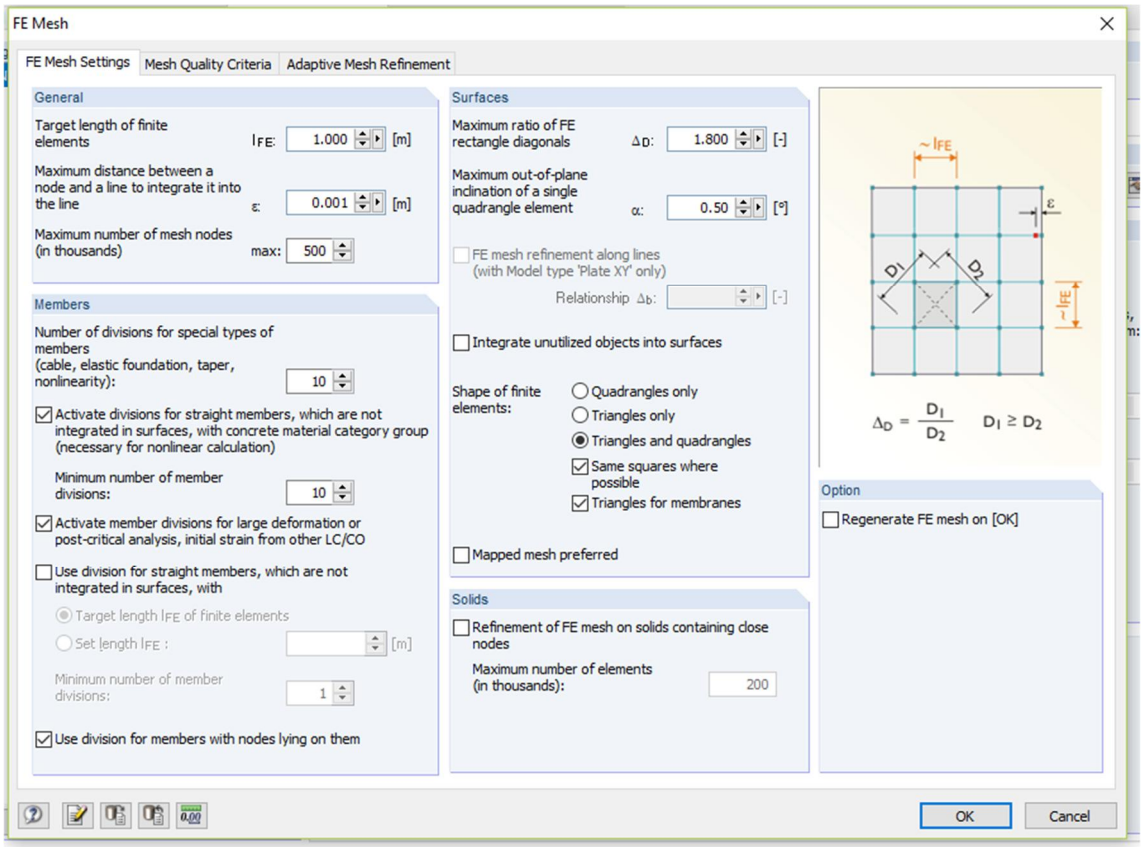

Figure 18. Mesh parameters.

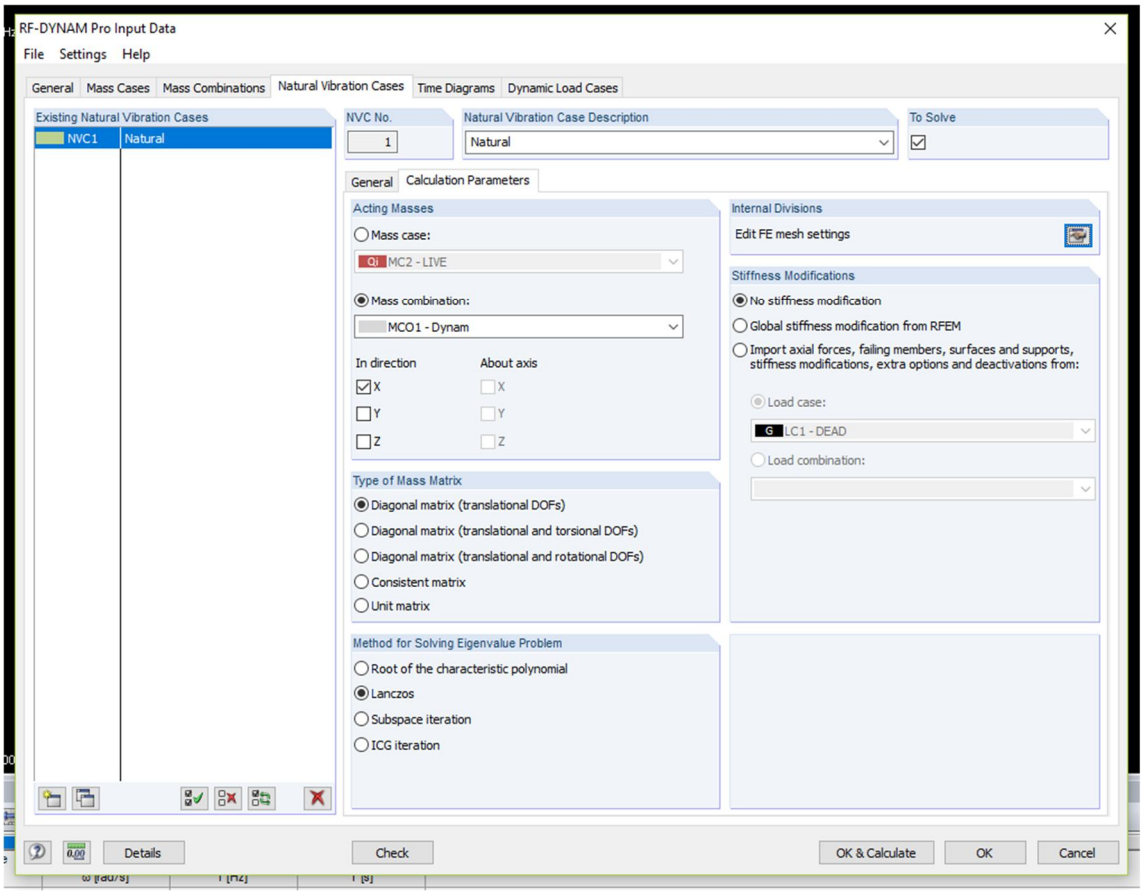

Figure 19. Calculation parameters.

Wind load is modelled based on 2D analysis and static values are taken from Table 11. Dynamic behavior is added in "Time diagrams" tab as a function. The function used is sinusoidal part of the equation (71):

$$k(t) = \sin(2\pi f_s t) \tag{80}$$

where f_s is shedding frequency. Recommended time-step size by Hernandez & Brebbia (2007) for sinusoidal simulation is:

$$\Delta t = \frac{1}{20f} \tag{81}$$

where f is the frequency examined. The examined period is defined by trial. Acceleration response is evened out after 250 s, so 300 s and 400 s examination times were used. Time history and dynamic load setups are shown in Figure 20 and Figure 21.

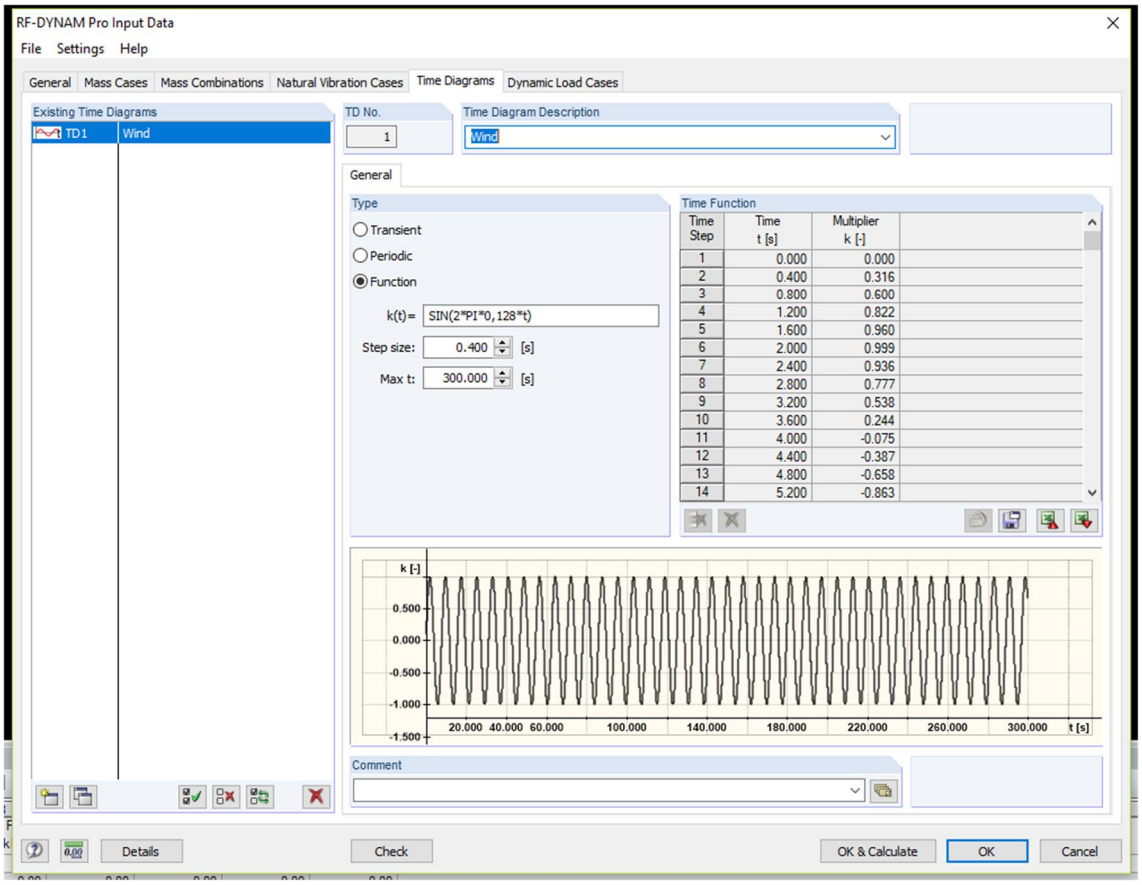

Figure 20. Time diagram setup.

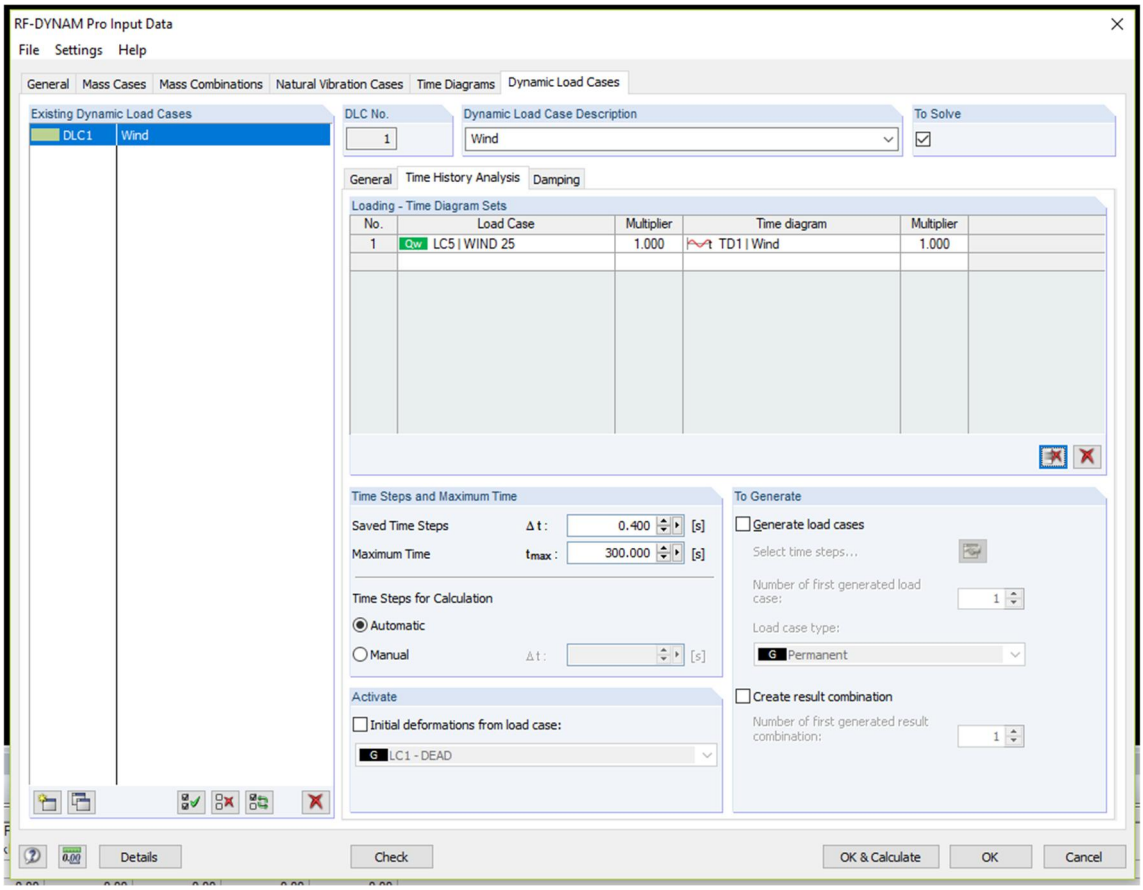

Figure 21. Dynamic load setup.

6.3.2 Load setup

Wind load is modelled as line load acting at each floor slab within the frequency range in height. Values are calculated by design procedure found in chapter 5.3, where the final used values are presented in Table 11.

Shedding frequency for non-resonant cases was selected to be at the same height as it would be for a resonant case, which is at 160 m in this case. The frequency range was calculated as presented in chapter 5.2. This method is not fully accurate since it is assumed that the vortices that formed, act in phase as it would be in a lock-in condition, which happens only at a region where the shedding frequency matches the natural frequency. This is a strongly conservative assumption in that sense.

In total 11 simulations were made for the range of basic wind velocities between 14-27 m/s. 14 m/s was selected as the lower boundary to compare the result with the codes that have has 1-hour average response times. 27 m/s was selected as the upper boundary since it is the lowest wind speed, where the shedding frequency meets the natural frequency of the building. Also, 27 m/s happens to be roughly equivalent to the maximum of 3-s gust, which is the gust duration used in AS/NZS 1170.2 standard as initial value. For the higher wind speeds, the resonant frequency height would be lower a height as can be seen from Table 9, making the results harder to compare. However, in a real design it would be necessary to check the response also at the higher wind speeds.

6.3.3 Results

The measured acceleration is at the top corner of the building. Accelerations seems to even out in all simulations at the latest after 250 seconds. In all simulations, except in the resonant simulation, fluctuation of acceleration with constant frequency is observed in the beginning of the simulation. However, that frequency varied between simulations, comparing Figure 22 and Figure 23 for example. Figure 24 shows a simulation at resonance frequency and an acceleration of 381 milli-g response was observed, which is extremely high.

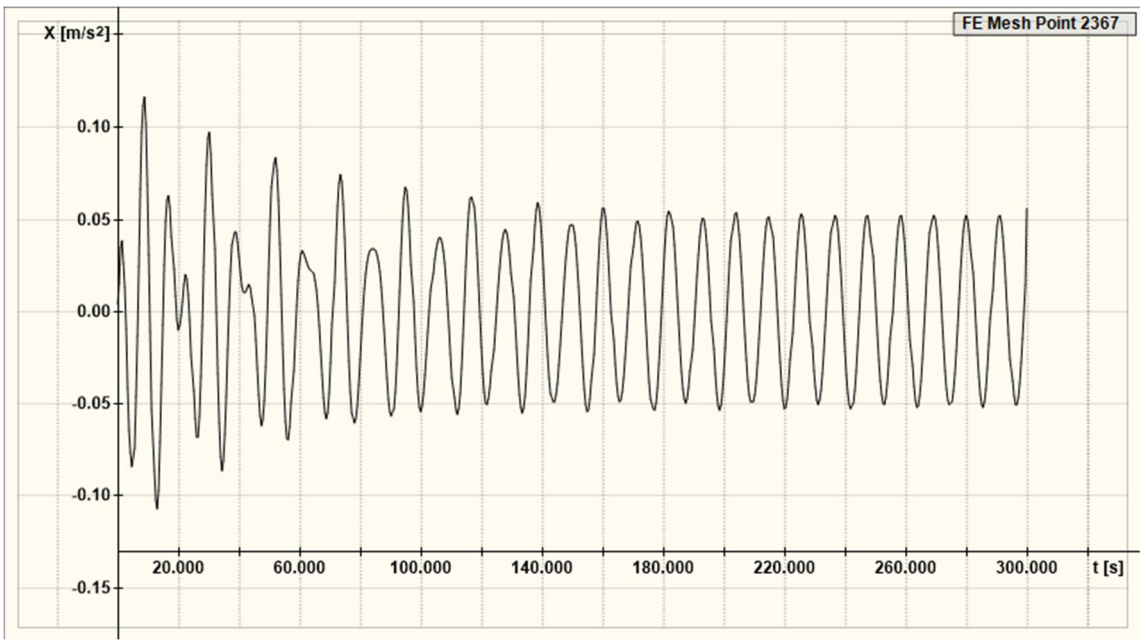

Figure 22. Acceleration response at the top of the building with 18 m/s basic wind speed.

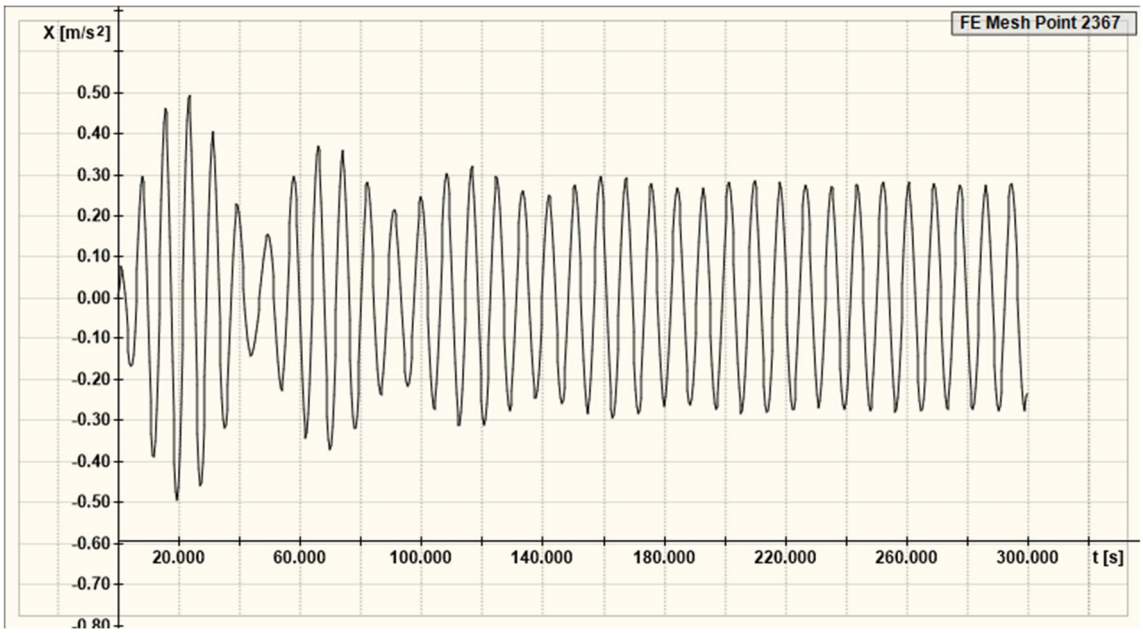

Figure 23. Acceleration response at the top of the building with 23 m/s basic wind speed.

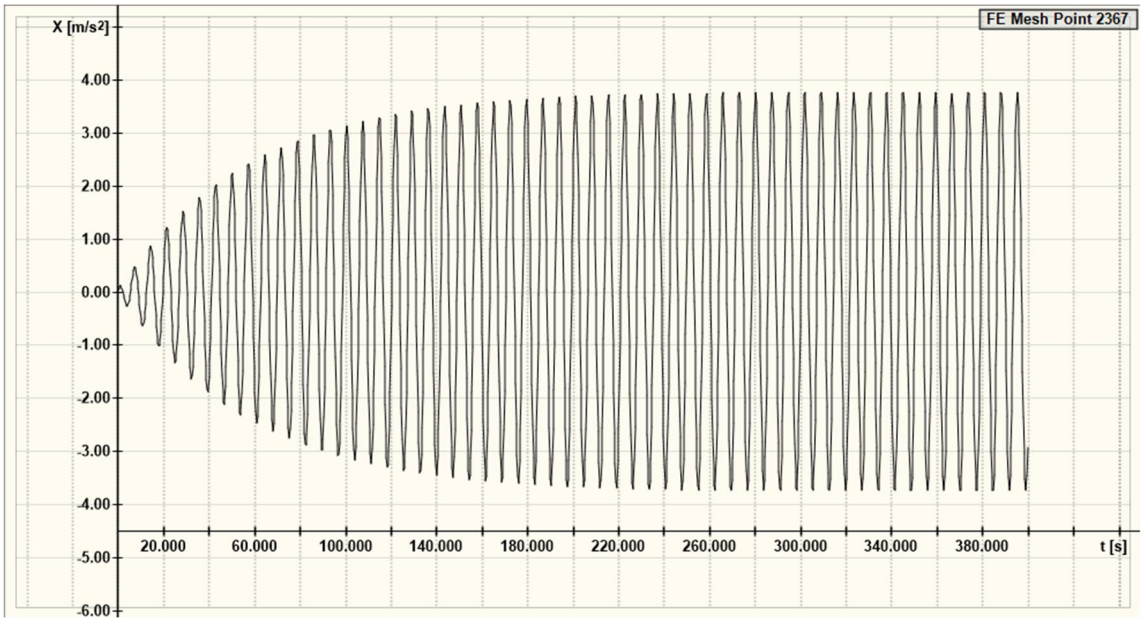

Figure 24. Acceleration response at the top of the building with 27 m/s basic wind speed.

Accelerations obtained for basic wind speeds of over 23 m/s are high, especially closer to the resonant frequency as seen in Figure 25. Since it is unrealistic to have an average basic wind speed of say 27 m/s for a long period of time, gust duration has a limiting effect on developed acceleration. Figure 25 presents response acceleration considering gust duration with a dashed line. This assumption is not fully realistic, since wind speed first develops and then decreases after its peak, producing an initial oscillation of the building, contributing to the peak acceleration.

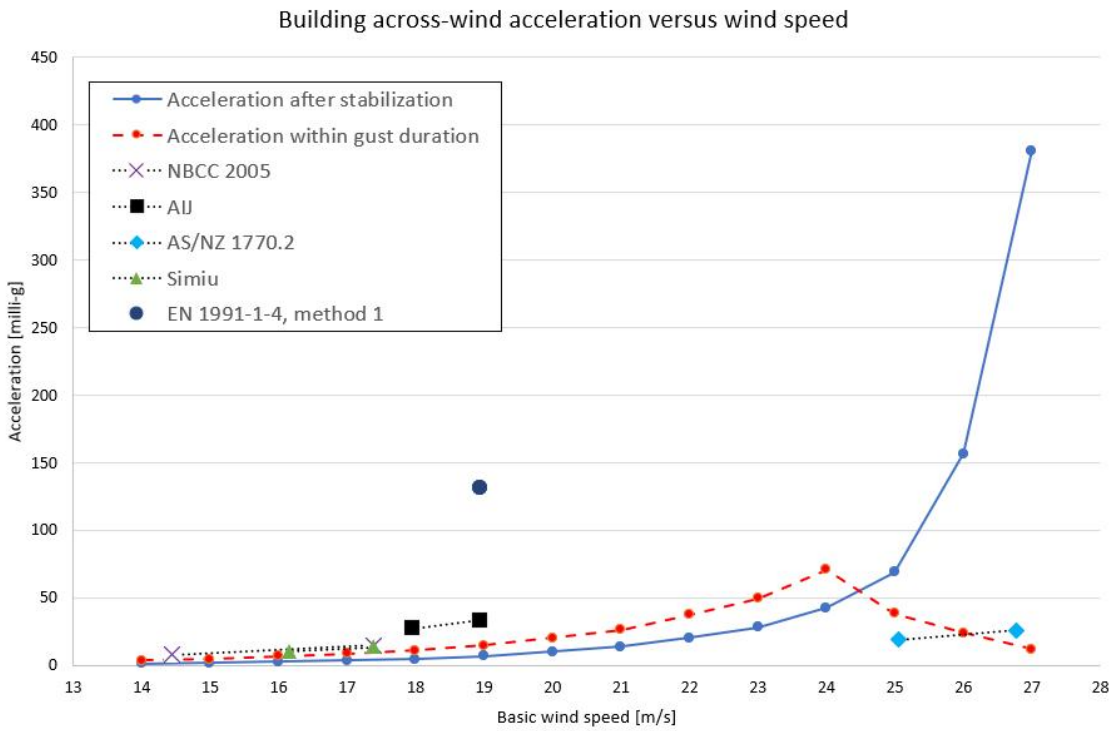

Figure 25. Acceleration response for different wind speeds and methods.

There are two results presented from each standard, one in which a higher acceleration is obtained by converting the return period by Eurocode's method and another where a lower value is obtained by converting the return period by each code's own procedures presented in 4.2.2.

Comparing the finite element method with the standards, the results are reasonably close to the response, considering gust duration except for the response calculated by Eurocode. It is worth mentioning that the standards are giving a higher value than the finite element method for across-wind acceleration response, except AS/NZS 1170.2 with return period scaling done by that code. Very conservative assumptions have been made in the 2D finite element method. However, it is still predicting lower acceleration values than the standards. Figure 26 presents a scaled region where the most relevant information about acceleration is presented, leaving out exceptionally high accelerations.

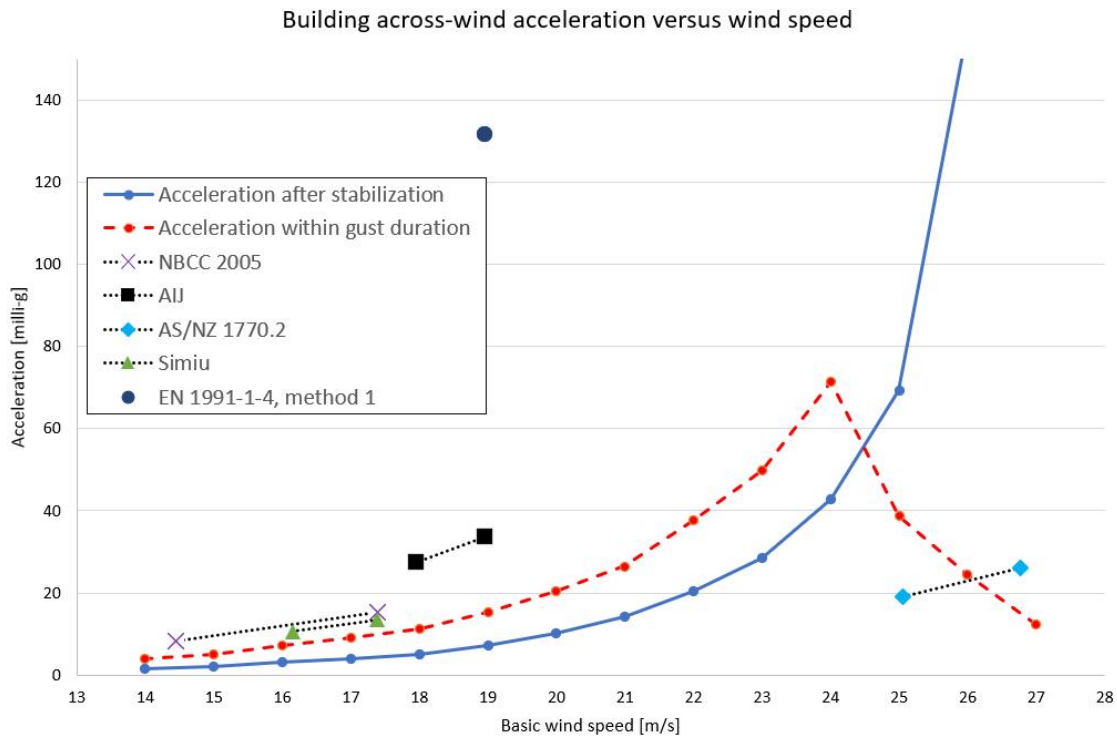

Figure 26. Acceleration response for different wind speeds and methods.

The finite element method might be useful as a tool to evaluate across-wind response acceleration, among others. This study shows that the response is reasonable and in the same order of magnitude with the calculations by standards if gust duration is considered. Also, with this tool it is easy to find out the resonant wind speeds, that could cause high-amplitude vibrations. This makes it easier to steer the design process towards a solution where resonance is very unlikely to happen in terms of wind return period.

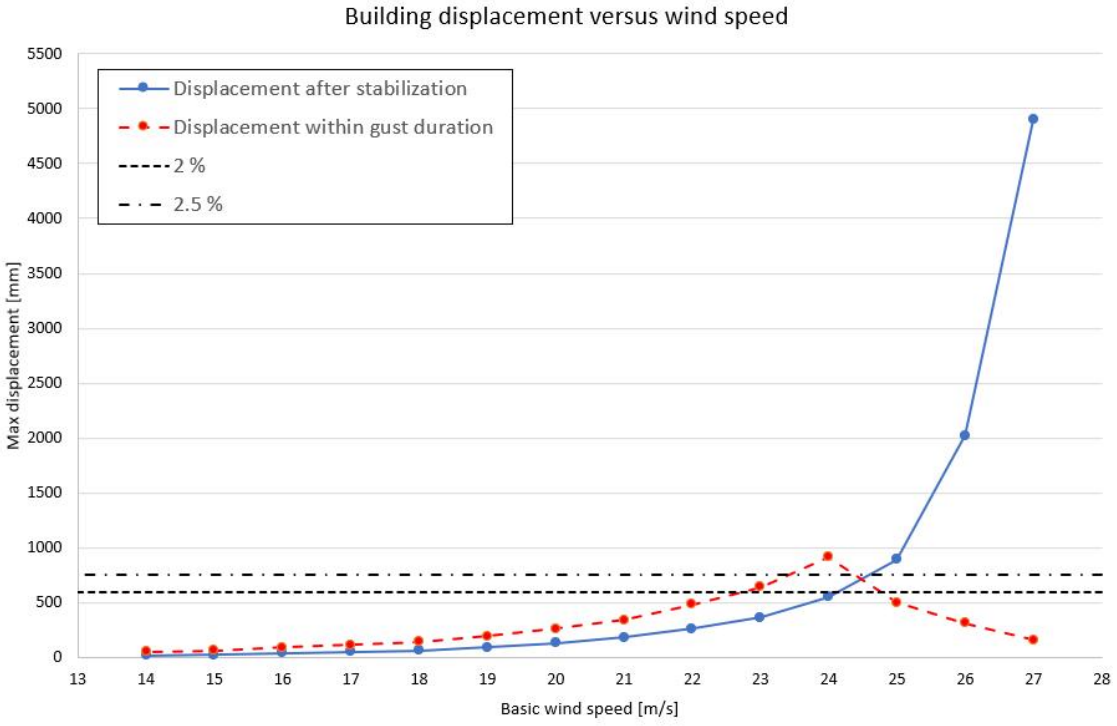

Figure 27. Displacement response for different wind speeds by finite element method.

Figure 27 shows maximum tip displacement compared to 2% and 2.5% relative displacement mentioned in chapter 5.1. This result indicates that an actual lock-in condition is possible to happen for this structure when basic wind speed is over 23 m/s.

This study is lacking comparison with full-scale measurements, which could show if the predictions by the finite element method, standards and literature are on the safe side or not. Also, the accuracy of the predictions would be valuable information from comparison with full-scale measurements.

Wind speeds for different gust durations were calculated based on a 10-year return period, and the 10-minutes mean peak wind speed 18.95 m/s was calculated by Eurocode. Wind speeds and related gust durations in Figure 28 were used to calculate the acceleration response within the gust duration presented in Figure 26.

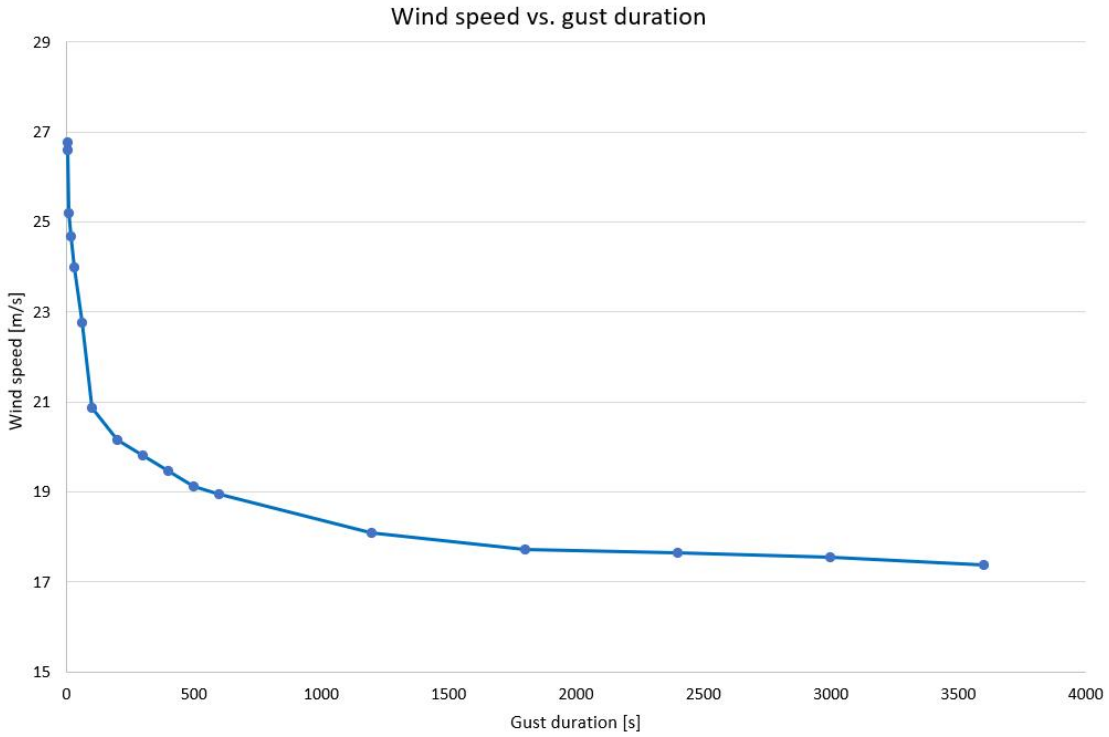

Figure 28. Wind speed versus gust duration based on basic wind speed 18.95 m/s.

7 Discussion and conclusions

The aim of this thesis was to investigate vortex shedding phenomenon and its predictability by calculations. Based on the calculations and current understanding of the phenomenon it is indeed hard to predict acceleration response without wind-tunnel tests. Acceleration results from the calculations by the standards, literature and procedure based on finite element method are scattered amongst each other, confirming the fact that vortex shedding phenomenon is hard to predict. Hence, wind tunnel testing is needed if there are any non-standard environments in the surroundings of the building or if the building itself is slender or unusually shaped. Wind tunnel testing is considered the most accurate prediction method for assessing building response to the wind.

Eurocode is not sufficient for predictions of across-wind accelerations and it is limited to 200 m high buildings. However, vortex shedding may occur also on lower buildings as well making an absolute height limit a poor measure for that. Slenderness of the building determines if across-wind acceleration is more critical than along-wind. Other international standards are predicting across-wind acceleration more accurately, but they are limited to building shape and some other aspects, making their usage very case specific.

Equations used in the calculations by Eurocode are reasonable and there is a good theoretical background combined with full-scale testing. However, assumptions of the parameters in the case of high-rise buildings are extremely conservative, making the predictions unusable. A suggestion arises that Eurocode should tweak EN 1991-1-4 Annex E to be usable for the design of high-rise buildings in future revisions.

A procedure based on finite element method to evaluate across-wind acceleration response was adopted in this study for use on high-rise buildings. The results with this procedure are close to the predictions done by the standards and literature, making it an additional simple tool to check for building susceptibility to the acceleration caused by vortex shedding. Also, the finite element method reveals if a building is susceptible to the vortices shedding at natural frequency. Testing the finite element method against full-scale measurements could give more evidence about the accuracy of the procedure.

Some questions were left out of this thesis, since only a basic square, non-tapered case was studied. For further studies, it might be useful to find out the lift coefficient, *Strouhal number* and *Reynolds* number combinations for the various cross-sections and shapes of high-rise buildings.

Many strongly conservative assumptions were made in the finite element method in order to maintain a position on the safe side of the design procedure. There is a lot of room for optimization in longitudinal vortex synchronization length, lift coefficient magnitude dependence on the relative height and vortex induced vibration outside the natural frequency range. For a non-resonant shedding frequency, the load was set for the upper 75% of the total height. It was not investigated if there is a more optimal option of where to apply the load, since lift coefficient is smaller the closer the load is to the top of the building.

References

AIJ-RLB-2004, 2004. *AIJ Recommendations for Loads on Buildings.* Tokyo, Japan: Architectural Institute of Japan.

AS/NZS 1170.2:2011, 2011. *Structural design actions – Part 2: Wind actions.* Standards Australia Ltd., Sydney / Standards New Zealand, Wellington.

ASCE/SEI 7-10, 2010. *Minimum Design Loads of Buildings and Other Structures.* Reston, Virginia, USA: American Society of Civil Engineers.

Burton, M.D., Kwok, K.C., Hitchcock, P.A. and Denoon, R.O., 2006. Frequency dependence of human response to wind-induced building motion. *Journal of Structural Engineering,* **132**(2), pp. 296-303. ISSN 0733-9445.

Chen, P.W. & Robertson, L.E., 1972. Human perception thresholds of horizontal motion. *Journal of the Structural Division, ASCE.* **92**(8), pp. 1681-1695.

CAN/CSA S6.1-14, 2014. *Commentaries to Canadian highway bridge design code.* Ontario, Canada: CSA Group.

Davenport, A.G., 1971. The Response of Six Building Shapes to Turbulent Wind, *Philosophical Transactions of the Royal Society of London. Series A, Mathematical and Physical Sciences,* **269**(1199), pp. 385-394.

Davenport, A. G et al., *New approaches to the design of the structures against wind action.* Faculty of Engineering Science, University of Western Ontario (unpublished).

Dyrbye, C. & Hansen, S.O., 1997. *Wind Loads on Structures.* Chichester, England: John Wiley & Sons Ltd. ISBN 0-471-95651-1.

Feng, C.C., 1968. *The measurement of vortex induced effects in flow past stationary and oscillating circular and D-section cylinders.* M.A. Sc. Thesis. University of British Columbia, Vancouver.

Foley, C.M., Ginal, S.J., Peronto, J.L. & Fournelle, R.A., 2004. *Structural analysis of sign bridge structures and luminaire supports.* Marquette University, Milwaukee, Wisconsin, USA.

Giosan, I. & Eng, P. *Vortex shedding induced loads on free standing structures.* Structural Vortex Shedding Response Estimation Methodology and Finite Element Simulation. Available at: http://citeseerx.ist.psu.edu/viewdoc/download?doi=10.1.1.582.3179&rep=rep1&type=pdf [cited 07.05.2020].

Granroth, S., 2019. *Utilizing FEM-programs time history analysis during wind caused vibrations in high-rise buildings*. M.A. Sc. Thesis. University of Oulu, Oulu.

Hansen, S.O., 2007. Vortex-induced vibrations of structures. *Structural Engineers World Congress*. Bangalore, India, November 2-7.

Hansen, S.O., 2013. Vortex-induced vibrations – the Scruton number revisited. *Proceedings of the Institution of Civil Engineers - Structures and Buildings,* **166**(10), pp. 560-571. ISSN 0965-0911.

Harris, C.M. & Crede, C.E., 1976. *Harris' Shock and vibration handbook.* 2nd edn. New York, USA: The McGraw-Hill Companies. ISBN 0-07-026799-5.

Hernandez, S. & Brebbia, C.A., 2007. *Computer Aided optimum Design in Engineering X.* Southampton, UK: WIT Press, pp. 203-204. ISBN: 978-1-84564-070-5.

Holmes, J.D., 2015. *Wind Loading of Structures.* 3rd edn. Florida, USA: Taylor & Francis Group, LLC. ISBN: 978-1482229196.

Holmes, J.D., Tamura, Y. & Krishna, P., 2008. Wind loads on low, medium and high-rise buildings by Asia-Pacific codes. *The Fourth International Conference on Advances in Wind and Structures (AWAS'08)*, Jeju, Korea, 29-31 May.

Holmes, J.D., 2001. *Wind Loading of Structures.* New York, USA: Spon Press. ISBN: 9780419246107.

Huang, R.F., Lin, B.H. & Yen, S.C., 2010. Time-averaged topological flow patterns and their influence on vortex shedding of a square cylinder in crossflow at incidence. *Journal of Fluids and Structures,* **26**(3), pp. 406-429.

ISO 10137:2007, 2007. *Bases for design of structures – Serviceability of buildings and walkways against vibrations*. 2nd edn. Geneva, Switzerland: International organization for standardization (ISO).

ISO 6897:1984, 1984. *Guidelines for the evaluation of the response of occupants of fixed structures, especially buildings and off-shore structures, to low-frequency horizontal motion (0,063 to 1 Hz)*. Geneva, Switzerland: International organization for standardization (ISO).

Irwin, A.W., 1978. Human response to dynamic motion of structures. *The Structural Engineer,* **56A**(9), pp. 237-243. ISSN: 1466-5123.

Irwin, P., Denoon, R., Scott, D., 2013. *Wind Tunnel Testing of High-Rise Buildings*: *An output of the CTBUH Wind Engineering Working Group*. Council on Tall Buildings and Urban Habitat: Chicago, USA.

Joubert, E.C., Harms, T.M. & Venter, G., 2015. Computational simulation of the turbulent flow around a surface mounted rectangular prism. *Journal of Wind Engineering & Industrial Aerodynamics,* **142**, pp. 173-187. ISSN: 0167-6105.

Kawai, H., 1995. Effects of angle of attack on vortex induced vibration and galloping of tall buildings in smooth and turbulent boundary layer flows. *Journal of Wind Engineering & Industrial Aerodynamics,* **54-55**, pp. 125-132.

Kawai, H., 1992. Vortex induced vibration of tall buildings. *Journal of Wind Engineering & Industrial Aerodynamics,* **41**(1-3), pp. 117-128.

Kijewski, T. & Kareem, A., 1998. Dynamic wind effects: a comparative study of provisions in codes and standards with wind tunnel data. *Wind and Structures,* **1**(1), pp. 77-109.

Kortelainen, P., 2012. *Korkeiden rakennusten vaste tuulikuormituksessa*. M.A. Thesis. Tampere University of Technology, Tampere.

Kwon, D.K. & Kareem, A., 2013. Comparative study of major international wind codes and standards for wind effects on tall buildings. *Engineering Structures,* **51**, pp. 23-35.

Li, Q.S., Xie, J., To, A. & Zhi, L.H., 2009. Wind tunnel studies and their validations with field measurements for a super-tall building. *The Seventh Asia-Pacific Conference on Wind Engineering*, Taipei, Taiwan, 8-12 November.

Liu, H., 1991. *Wind Engineering: A Handbook for Structural Engineers.* Englewood Cliffs, New Jersey, USA. ISBN: 978-0139602795.

McNamara, R., Kareem, A. & Kijewski, T., 2002. Ask the Experts...Perception of Motion Criteria for Tall Buildings Subjected to Wind: A Panel Discussion, *Proceedings of the Reflections from ASCE Structures Congress*, Denver, USA, 4-6 April.

Melbourne, W.H. & Palmer, T.R., 1992. Accelerations and comfort criteria for buildings undergoing complex motions. *Journal of Wind Engineering & Industrial Aerodynamics,* **41**(1-3), pp. 105-116.

National Annex of Finland of SFS EN 1991-1-4:2005, 2016. *Rakenteiden lujuus ja vakaus.* Helsinki, Finland: Ministry of the Environment.

NBCC, 2005. *National building code of Canada.* Associate Committee on the National Building Code. Ottawa, Canada: National Research Council of Canada (NRC).

Paidoussis, M.P., Price, S.J. & Langre, E., 2011. *Fluid-Structure Interactions.* New York, USA: Cambridge University Press. ISBN: 9780521119429.

Pozos-Estrada, A., Hong, H.P. & Galsworthy, J.K., 2010. Serviceability design factors for wind-sensitive structures. *Canadian Journal of Civil Engineering,* **37**(5), pp. 728-738.

Pozzuoli, C., 2012. *Aeroelastic Effects on Tall Buildings: Performance-Based Comfort Analysis*. Dr. thesis. University of Florence, Firenze.

Ruscheweyh, H. & Sedlacek, G., 1988. Crosswind vibrations of steel stacks. - critical comparison between some recently proposed codes -. *Journal of Wind Engineering & Industrial Aerodynamics,* **30**(1-3), pp. 173-183.

SFS-EN 1991-1-4:2005, 2005. *Eurocode 1: Actions on structures - General actions - Part 1-4: Wind actions.* Helsinki, Finland: Finnish standards association.

Simiu, E., 2011. *Design of buildings for wind.* 2nd edn. New Jersey, Canada: John Wiley & Sons Inc. ISBN: 9780470464922.

Strømmen, E.N., 2010. *Theory of Bridge Aerodynamics.* 2nd edn. Trondheim, Norway: Springer-Verlag Berlin Heidelberg. ISBN: 139783642136597.

Tamura, Y., Kawai, H., Uematsu, Y., Marukawa, H., Fujii, K. & Taniike, Y., 1996. Wind load and wind-induced response estimations in the Recommendations for Loads on Buildings, AIJ 1993. *Engineering Structures,* **18**(6), pp. 399-411.

Taranath, B.S., 2012. *Structural Analysis and Design of Tall Buildings.* Boca Raton, USA: CRC/Taylor & Francis Group. ISBN: 9781439850893.

Tozan, S., Güler, K. & Erkus, B., 2013. Wind comfort assessment of a tall building according to various structural codes. *Second Conference on Smart Monitoring, Assessment and Rehabilitation of Structures*, Istanbul, Turkey, 9-11 September.

Vickery, B.J. & Clark, A.W., 1972. Lift of across wind response of tapered stacks. *Journal of the Structural Division,* **98**(1), pp. 1-20.

Vickery, B.J. & Basu, R.I., 1983. Across-wind vibrations of structures of circular cross-section. Part I. Development of a mathematical model for two-dimensional conditions. *Journal of Wind Engineering & Industrial Aerodynamics,* **12**(1), pp. 49-73.

Wootton, L.R., 1969. The oscillation of large circular stacks in wind. *Proceedings of the Institution of Civil Engineers,* **43**(3), pp. 573-598.

Appendix 1. Across-wind acceleration according to EN 1991-1-4 E.1.5.2

Building height $h := 200\ m$

width $b := 30\ m$

depth $d := 30\ m$

Height of interest $z := 200\ m$

Building mass $m_b := 64115003\ kg$

Building mass per unit lenght $m_z := \frac{m_b}{h} = \left(3.206 \cdot 10^5\right)\ \frac{kg}{m}$

Air density $\rho := 1.23\ \frac{kg}{m^3}$

Fundamental frequency across-wind $n_1 := 0.139\ Hz$

Logarithmic decrement of damping of the first mode $\delta_s := 0.1$

Terrain category $Te := 1$

Rougness length, I

$$z_0 := \left\| \begin{array}{l} \text{if } Te = 0 \\ \quad \| \ 0.003\ m \\ \text{else if } Te = 1 \\ \quad \| \ 0.01\ m \\ \text{else if } Te = 2 \\ \quad \| \ 0.05\ m \\ \text{else if } Te = 3 \\ \quad \| \ 0.3\ m \\ \text{else} \\ \quad \| \ 1\ m \end{array} \right\| = 0.01\ m$$

Rougness length, II $z_{0.II} := 0.05\ m$

Directional factor $c_{dir} := 1$

Seasonal factor $c_{season} := 1$

Orography factor $c_o := 1$

Return period $T := 10$

Basic wind velocity $v_{b.0} := 21 \ \frac{m}{s}$

Strouhal number $St := 0.12$

Mode shape exponent $\zeta := 1.5$

$$\Phi_1 := \left(\frac{z}{h}\right)^{\zeta} = 1$$

$$m_{1.e} := \frac{\int_0^h m_z \cdot {\Phi_1}^2 \, dz}{\int_0^h {\Phi_1}^2 \, dz} = \left(3.206 \cdot 10^5\right) \ \frac{kg}{m}$$

$$Sc := \frac{2 \cdot \delta_s \cdot m_{1.e}}{\rho \cdot b^2} = 57.918$$

$K := 0.13$

Initial guess

$L_j := 6 \cdot b = 180 \ m$ Table E.4

$$\lambda := \frac{h}{b}$$

$$K_W := 3 \cdot \frac{\frac{L_j}{b}}{\lambda} \cdot \left(1 - \frac{\frac{L_j}{b}}{\lambda} + \frac{1}{3} \cdot \left(\frac{\frac{L_j}{b}}{\lambda}\right)^2\right) = 0.999$$

$$v_{crit.1} := \frac{b \cdot n_1}{St} = 34.75 \ \frac{m}{s}$$

Height above the ground of the center of effective correlation length

$$z_{Lj} := \frac{L_j}{2} + \left(h - L_j\right) = 110 \ m$$

$$k_r := 0.19 \cdot \left(\frac{z_0}{z_{0.II}}\right)^{0.07} = 0.17$$

$$c_{r.Lj} := k_r \cdot \ln\left(\frac{z_{Lj}}{z_0}\right) = 1.58$$

$n := 0.5$

$K := 0.2$

$$c_{prob} := \left(\frac{1 - K \cdot \ln\left(-\ln\left(1 - \frac{1}{T}\right)\right)}{1 - K \cdot \ln\left(-\ln(0.98)\right)} \right)^{n} = 0.902$$

$$v_b := c_{dir} \cdot c_{season} \cdot c_{prob} \cdot v_{b.0} = 18.952 \ \frac{m}{s}$$

$$v_{m.L1} := c_{r.Lj} \cdot c_o \cdot v_b = 29.938 \ \frac{m}{s}$$ Table E.3

$$\frac{v_{crit.1}}{v_{m.L1}} = 1.161$$

$c_{lat.0} := 1.1$

$$c_{lat} := \left\| \begin{array}{l} \text{if } \frac{v_{crit.1}}{v_{m.L1}} < 0.83 \\ \quad \left\| c_{lat.0} \right. \\ \text{else if } 0.83 \le \frac{v_{crit.1}}{v_{m.L1}} \le 1.25 \\ \quad \left\| \left(3 - 2.4 \cdot \frac{v_{crit.1}}{v_{m.L1}}\right) \cdot c_{lat.0} \right. \\ \text{else} \\ \quad \left\| 0 \right. \end{array} \right. = 0.236$$

$$y_{F.max} := b \cdot \frac{1}{St^2} \cdot \frac{1}{Sc} \cdot K \cdot K_W \cdot c_{lat} = 1.694 \ m$$

Check initial guess

$$\frac{y_{F.max}}{b} = 0.056$$ Check ok

$$a := \left(2 \cdot \pi \cdot n_1\right)^2 \cdot y_{F.max} = 1.292 \ \frac{m}{s^2}$$

$$a = 131.764 \ \frac{g}{1000}$$

Appendix 2. Across-wind acceleration according to EN 1991-1-4 E.1.5.3

Building height $h := 200\ m$

width $b := 30\ m$

depth $d := 30\ m$

Height of interest $z := 200\ m$

Building mass $m_b := 64115003\ kg$

Building mass per unit lenght $m_z := \frac{m_b}{h} = (3.206 \cdot 10^5)\ \frac{kg}{m}$

Air density $\rho := 1.23\ \frac{kg}{m^3}$

Fundamental frequency across-wind $n_1 := 0.139\ Hz$

Logarithmic decrement of damping of the first mode $\delta_s := 0.1$

Strouhal number $St := 0.12$

Mode shape exponent $\zeta := 1.5$

$$\Phi_1 := \left(\frac{z}{h}\right)^{\zeta} = 1$$

$$m_{1.e} := \frac{\int_0^h m_z \cdot {\Phi_1}^2\ dz}{\int_0^h {\Phi_1}^2\ dz} = (3.206 \cdot 10^5)\ \frac{kg}{m}$$

$$Sc := \frac{2 \cdot \delta_s \cdot m_{1.e}}{\rho \cdot b^2} = 57.918$$

$a_L := 0.4$

$K_{a.max} := 6$

$K_a := K_{a.max}$

$$c_1 := \frac{a_L^{\,2}}{2} \cdot \left(1 - \frac{Sc}{4 \cdot \pi \cdot K_a}\right) = 0.019$$

$$C_c := 0.04$$

$$c_2 := \frac{\rho \cdot b^2}{m_{1.e}} \cdot \frac{a_L^{\,2}}{K_a} \cdot \frac{C_c^{\,2}}{St^4} \cdot \frac{b}{h} = 1.066 \cdot 10^{-4}$$

$$\sigma_y := b \cdot \sqrt{c_1 + \sqrt{c_1^{\,2} + c_2}} = 5.983\ m$$

$$k_p := \sqrt{2} \cdot \left(1 + \frac{1.2}{\tan\left(0.75 \cdot \frac{Sc}{4 \cdot \pi \cdot K_a}\right)}\right) = 4.027$$

$$y_{max} := \sigma_y \cdot k_p = 24.091\ m$$

$$a := \left(2 \cdot \pi \cdot n_1\right)^2 \cdot y_{max} = 18.376\ \frac{m}{s^2}$$

$$a = \left(1.874 \cdot 10^3\right) \frac{g}{1000}$$

Appendix 3. Across-wind acceleration according to NBCC 2005

Basic wind speed return period conversion done by Eurocode.

Building height $H := 200\ m$

width $W := 30\ m$

depth $D := 30\ m$

Height of interest $Z := \frac{H}{m}$

Building mass $m_b := 64115003\ kg$

Air density $\rho := 1.23\ \frac{kg}{m^3}$

Bulding density $\rho_B := \frac{m_b}{H \cdot W \cdot D} = 356.194\ \frac{kg}{m^3}$

Fundamental frequency across-wind $n_w := 0.139\ Hz$

Damping ratio across-wind $\beta_W := 0.02$

Damping ratio along-wind $\beta_D := 0.02$

Terrain category $Te := 1$ (Category A)

Mean wind speed $V := \frac{18.95\ \frac{m}{s}}{1.09} = 17.385\ \frac{m}{s}$

$$C_e := \begin{cases} \left(\frac{Z}{10}\right)^{0.28} & \text{if } Te = 1 \\ 0.5 \cdot \left(\frac{Z}{12.7}\right)^{0.5} & \text{else if } Te = 2 \\ 0.4 \left(\frac{Z}{30}\right)^{0.72} & \text{else} \end{cases} = 2.314$$

$$V_H := V \cdot \sqrt{C_e} = 26.444\ \frac{m}{s}$$

$$S := \frac{\pi}{3} \cdot \left(\frac{1}{1 + \frac{8 \cdot n_w \cdot H}{3 \cdot V_H}}\right) \cdot \left(\frac{1}{1 + \frac{10 \cdot n_w \cdot W}{V_H}}\right) = 0.107$$

$$x_0 := \frac{1220 \cdot n_w}{V_H} \cdot m$$

$$F := \frac{{x_0}^2}{\left(1+{x_0}^2\right)^{\frac{4}{3}}} = 0.281$$

$$B := \frac{4}{3} \cdot \int_0^{\frac{914}{200}} \left(\frac{1}{1+\frac{x \cdot 200}{457}}\right) \cdot \left(\frac{1}{1+\frac{x \cdot 30}{122}}\right) \cdot \left(\frac{x}{\left(1+x^2\right)^{\frac{4}{3}}}\right) dx = 0.595$$

$$\nu := n_w \cdot \sqrt{\frac{S \cdot F}{S \cdot F + \beta_D \cdot B}} = 0.118 \ \frac{1}{s}$$

$$g_p := \sqrt{2 \cdot \ln\left(3600 \ s \cdot \nu\right)} + \frac{0.577}{\sqrt{2 \cdot \ln\left(3600 \ s \cdot \nu\right)}} = 3.644$$

$$a_r := 78.5 \cdot 10^{-3} \cdot \left(\frac{V_H}{n_w \cdot \sqrt{W \cdot D}}\right)^{3.3} \frac{m}{s^2} = 34.84 \ \frac{m}{s^2}$$

$$a_w := {n_w}^2 \cdot g_p \cdot \sqrt{W \cdot D} \cdot \left(\frac{a_r}{\rho_B \cdot g \cdot \sqrt{\beta_W}}\right) \cdot \frac{kg}{m^3} = 0.149 \ \frac{m}{s^2}$$

$$a_w = 15.191 \ \frac{g}{1000}$$

Basic wind speed return period conversion done by NBCC 2005.

Building height $H := 200\ m$

width $W := 30\ m$

depth $D := 30\ m$

Height of interest $Z := \frac{H}{m}$

Building mass $m_b := 64115003\ kg$

Air density $\rho := 1.23\ \frac{kg}{m^3}$

Bulding density $\rho_B := \frac{m_b}{H \cdot W \cdot D} = 356.194\ \frac{kg}{m^3}$

Fundamental frequency across-wind $n_w := 0.139\ Hz$

Damping ratio across-wind $\beta_W := 0.02$

Damping ratio along-wind $\beta_D := 0.02$

Terrain category $Te := 1$ (Category A)

Mean wind speed $V_{50} := \frac{21\ \frac{m}{s}}{1.09} = 19.266\ \frac{m}{s}$

SLS importance factor $I_w := 0.75$

$$V_{10} := V_{50} \cdot I_w = 14.45\ \frac{m}{s}$$

$$C_e := \begin{cases} \left(\frac{Z}{10}\right)^{0.28} & \text{if } Te = 1 \\ 0.5 \cdot \left(\frac{Z}{12.7}\right)^{0.5} & \text{else if } Te = 2 \\ 0.4 \left(\frac{Z}{30}\right)^{0.72} & \text{else} \end{cases} = 2.314$$

$$V_H := V_{10} \cdot \sqrt{C_e} = 21.979\ \frac{m}{s}$$

$$S := \frac{\pi}{3} \cdot \left(\frac{1}{1 + \frac{8 \cdot n_w \cdot H}{3 \cdot V_H}}\right) \cdot \left(\frac{1}{1 + \frac{10 \cdot n_w \cdot W}{V_H}}\right) = 0.083$$

$$x_0 := \frac{1220 \cdot n_w}{V_H} \cdot m$$

$$F := \frac{{x_0}^2}{\left(1+{x_0}^2\right)^{\frac{4}{3}}} = 0.25$$

$$B := \frac{4}{3} \cdot \int_0^{\frac{914}{200}} \left(\frac{1}{1+\frac{x \cdot 200}{457}}\right) \cdot \left(\frac{1}{1+\frac{x \cdot 30}{122}}\right) \cdot \left(\frac{x}{\left(1+x^2\right)^{\frac{4}{3}}}\right) dx = 0.595$$

$$\nu := n_w \cdot \sqrt{\frac{S \cdot F}{S \cdot F + \beta_D \cdot B}} = 0.111 \ \frac{1}{s}$$

$$g_p := \sqrt{2 \cdot \ln(3600 \ s \cdot \nu)} + \frac{0.577}{\sqrt{2 \cdot \ln(3600 \ s \cdot \nu)}} = 3.627$$

$$a_r := 78.5 \cdot 10^{-3} \cdot \left(\frac{V_H}{n_w \cdot \sqrt{W \cdot D}}\right)^{3.3} \frac{m}{s^2} = 18.92 \ \frac{m}{s^2}$$

$$a_w := {n_w}^2 \cdot g_p \cdot \sqrt{W \cdot D} \cdot \left(\frac{a_r}{\rho_B \cdot g \cdot \sqrt{\beta_W}}\right) \cdot \frac{kg}{m^3} = 0.081 \ \frac{m}{s^2}$$

$$a_w = 8.213 \ \frac{g}{1000}$$

Appendix 4. Across-wind acceleration according to AIJ

Basic wind speed return period conversion done by Eurocode.

Building height $H := 200\ m$

width $B := 30\ m$

depth $D := 30\ m$

Height of interest $Z := H$

Building mass $m_b := 64115003\ kg$

Building mass per unit height $m_Z := \frac{m_b}{H} = (3.206 \cdot 10^5)\ \frac{kg}{m}$

Air density $\rho := 1.23\ \frac{kg}{m^3}$

Fundamental frequency across-wind $f_L := 0.139\ Hz$

Damping ratio across-wind $\zeta_L := 0.02$

Mean 10-min wind speed $U_0 := 18.95\ \frac{m}{s}$

Terrain category $Te := 1$

Topography factor $E_g := 1$

Directionality factor $K_D := 1$

$$Z_b := \begin{cases} 5\ m & \text{if } Te = 1 \\ 5\ m & \text{else if } Te = 2 \\ 10\ m & \text{else if } Te = 3 \\ 20\ m & \text{else if } Te = 4 \\ 30\ m & \text{else} \end{cases} = 5\ m$$

$$Z_G := \begin{cases} 250\ m & \text{if } Te = 1 \\ 350\ m & \text{else if } Te = 2 \\ 450\ m & \text{else if } Te = 3 \\ 550\ m & \text{else if } Te = 4 \\ 650\ m & \text{else} \end{cases} = 250\ m$$

$$\alpha := \begin{cases} 0.1 & \text{if } Te = 1 \\ 0.15 & \text{else if } Te = 2 \\ 0.2 & \text{else if } Te = 3 \\ 0.27 & \text{else if } Te = 4 \\ 0.35 & \text{else} \end{cases} = 0.1$$

$$E_r := \begin{cases} 1.7 \cdot \left(\frac{Z}{Z_G}\right)^{\alpha} & \text{if } Z_b \le Z \le Z_G \\ 1.7 \cdot \left(\frac{Z_b}{Z_G}\right)^{\alpha} & \text{else} \end{cases} = 1.662$$

$$E_H := E_r \cdot E_g$$

$$U_H := U_0 \cdot K_D \cdot E_H = 31.504 \ \frac{m}{s}$$

$$m := \left\| \begin{array}{l} \text{if } \frac{D}{B} < 3 \\ \quad \| \ 1 \\ \text{else} \\ \quad \| \ 2 \end{array} \right\| = 1$$

$$f_{s1} := \frac{0.12}{\left(1 + 0.38 \cdot \left(\frac{D}{B}\right)^2\right)^{0.89}} \cdot \frac{U_H}{B}$$

$$f_{s2} := \frac{0.56}{\left(\frac{D}{B}\right)^{0.85}} \cdot \frac{U_H}{B}$$

$$\beta_1 := \frac{\left(\frac{D}{B}\right)^4 + 2.3 \cdot \left(\frac{D}{B}\right)^2}{2.4 \cdot \left(\frac{D}{B}\right)^4 - 9.2 \cdot \left(\frac{D}{B}\right)^3 + 18 \cdot \left(\frac{D}{B}\right)^2 + 9.5 \cdot \left(\frac{D}{B}\right) - 0.15} + \frac{0.12}{\left(\frac{D}{B}\right)}$$

$$\beta_2 := \frac{0.28}{\left(\frac{D}{B}\right)^{0.34}} = 0.28$$

$$\kappa_1 := 0.85$$
$$\kappa_2 := 0.02$$

$$F_{L1} := \frac{4 \cdot \kappa_1 \cdot \left(1 + 0.6 \cdot \beta_1\right) \cdot \beta_1}{\pi} \cdot \frac{\left(\frac{f_L}{f_{s1}}\right)^2}{\left(1 - \left(\frac{f_L}{f_{s1}}\right)^2\right)^2 + 4 \cdot {\beta_1}^2 \cdot \left(\frac{f_L}{f_{s1}}\right)^2} = 0.379$$

$$F_{L2} := \frac{4 \cdot \kappa_2 \cdot \left(1 + 0.6 \cdot \beta_2\right) \cdot \beta_2}{\pi} \cdot \frac{\left(\frac{f_L}{f_{s2}}\right)^2}{\left(1 - \left(\frac{f_L}{f_{s2}}\right)^2\right)^2 + 4 \cdot {\beta_2}^2 \cdot \left(\frac{f_L}{f_{s2}}\right)^2} = 5.119 \cdot 10^{-4}$$

$$F_L := \left\| \begin{array}{l} \text{if } m = 1 \\ \quad \| \ F_{L1} \\ \text{else} \\ \quad \| \ F_{L1} + F_{L2} \end{array} \right\| = 0.379$$

$$R_L := \frac{\pi \cdot F_L}{4 \cdot \zeta_L} = 14.873$$

$$\beta := 1$$

$$\lambda := 1 - 0.4 \cdot \ln(\beta)$$

$$C'_L := 0.0082 \cdot \left(\frac{D}{B}\right)^3 - 0.071 \cdot \left(\frac{D}{B}\right)^2 + 0.22 \cdot \frac{D}{B} = 0.157$$

$$g_{aL} := \sqrt{2 \cdot \ln(600\ s \cdot f_L) + 1.2} = 3.17$$

$$q_H := \frac{1}{2} \cdot \rho \cdot {U_H}^2 = 610.393\ Pa$$

$$M_L := \int_0^H m_Z \cdot \left(\frac{Z}{H}\right)^{2 \cdot \beta} dZ = \left(2.137 \cdot 10^7\right)\ kg$$

$$a_{Lmax} := \frac{q_H \cdot g_{aL} \cdot B \cdot H \cdot C'_L \cdot \lambda \cdot \sqrt{R_L}}{M_L} = 0.329\ \frac{m}{s^2}$$

$$a_{Lmax} = 33.58\ \frac{g}{1000}$$

Basic wind speed return period conversion done by AIJ.

Building height	$H := 200\ m$
width	$B := 30\ m$
depth	$D := 30\ m$
Height of interest	$Z := H$
Building mass	$m_b := 64115003\ kg$
Building mass per unit height	$m_Z := \frac{m_b}{H} = (3.206 \cdot 10^5)\ \frac{kg}{m}$
Air density	$\rho := 1.23\ \frac{kg}{m^3}$
Fundamental frequency across-wind	$f_L := 0.139\ Hz$
Damping ratio across-wind	$\zeta_L := 0.02$
Mean 10-min wind speed	$U_{50} := 21\ \frac{m}{s}$
Return period	$r := 10$
Terrain category	$Te := 1$
Topography factor	$E_g := 1$
Directionality factor	$K_D := 1$

$\lambda_U := 1.1$

$k_{rW} := 0.63 \cdot (\lambda_U - 1) \cdot \ln(r) - 2.9 \cdot \lambda_U + 3.9$

$U_{10} := U_{50} \cdot k_{rW} = 17.956\ \frac{m}{s}$

$$Z_b := \begin{cases} 5\ m & \text{if } Te = 1 \\ 5\ m & \text{else if } Te = 2 \\ 10\ m & \text{else if } Te = 3 \\ 20\ m & \text{else if } Te = 4 \\ 30\ m & \text{else} \end{cases} = 5\ m$$

$$Z_G := \begin{cases} 250\ m & \text{if } Te = 1 \\ 350\ m & \text{else if } Te = 2 \\ 450\ m & \text{else if } Te = 3 \\ 550\ m & \text{else if } Te = 4 \\ 650\ m & \text{else} \end{cases} = 250\ m$$

$$\alpha := \begin{cases} 0.1 & \text{if } Te = 1 \\ 0.15 & \text{else if } Te = 2 \\ 0.2 & \text{else if } Te = 3 \\ 0.27 & \text{else if } Te = 4 \\ 0.35 & \text{else} \end{cases} = 0.1$$

$$E_r := \left\| \begin{array}{l} \text{if } Z_b \le Z \le Z_G \\ \quad \left\| 1.7 \cdot \left(\frac{Z}{Z_G}\right)^{\alpha} \right. \\ \text{else} \\ \quad \left\| 1.7 \cdot \left(\frac{Z_b}{Z_G}\right)^{\alpha} \right. \end{array} \right. = 1.662$$

$$E_H := E_r \cdot E_g$$

$$U_H := U_{10} \cdot K_D \cdot E_H = 29.852 \ \frac{m}{s}$$

$$m := \left\| \begin{array}{l} \text{if } \frac{D}{B} < 3 \\ \quad \| 1 \\ \text{else} \\ \quad \| 2 \end{array} \right. = 1$$

$$f_{s1} := \frac{0.12}{\left(1 + 0.38 \cdot \left(\frac{D}{B}\right)^2\right)^{0.89}} \cdot \frac{U_H}{B}$$

$$f_{s2} := \frac{0.56}{\left(\frac{D}{B}\right)^{0.85}} \cdot \frac{U_H}{B}$$

$$\beta_1 := \frac{\left(\frac{D}{B}\right)^4 + 2.3 \cdot \left(\frac{D}{B}\right)^2}{2.4 \cdot \left(\frac{D}{B}\right)^4 - 9.2 \cdot \left(\frac{D}{B}\right)^3 + 18 \cdot \left(\frac{D}{B}\right)^2 + 9.5 \cdot \left(\frac{D}{B}\right) - 0.15} + \frac{0.12}{\left(\frac{D}{B}\right)}$$

$$\beta_2 := \frac{0.28}{\left(\frac{D}{B}\right)^{0.34}} = 0.28$$

$$\kappa_1 := 0.85$$
$$\kappa_2 := 0.02$$

$$F_{L1} := \frac{4 \cdot \kappa_1 \cdot (1 + 0.6 \cdot \beta_1) \cdot \beta_1}{\pi} \cdot \frac{\left(\frac{f_L}{f_{s1}}\right)^2}{\left(1 - \left(\frac{f_L}{f_{s1}}\right)^2\right)^2 + 4 \cdot {\beta_1}^2 \cdot \left(\frac{f_L}{f_{s1}}\right)^2} = 0.313$$

$$F_{L2} := \frac{4 \cdot \kappa_2 \cdot (1 + 0.6 \cdot \beta_2) \cdot \beta_2}{\pi} \cdot \frac{\left(\frac{f_L}{f_{s2}}\right)^2}{\left(1 - \left(\frac{f_L}{f_{s2}}\right)^2\right)^2 + 4 \cdot {\beta_2}^2 \cdot \left(\frac{f_L}{f_{s2}}\right)^2} = 5.764 \cdot 10^{-4}$$

$$F_L := \left\| \begin{array}{l} \text{if } m = 1 \\ \quad \| F_{L1} \\ \text{else} \\ \quad \| F_{L1} + F_{L2} \end{array} \right\| = 0.313$$

$$R_L := \frac{\pi \cdot F_L}{4 \cdot \zeta_L} = 12.276$$

$$\beta := 1$$

$$\lambda := 1 - 0.4 \cdot \ln(\beta)$$

$$C'_L := 0.0082 \cdot \left(\frac{D}{B}\right)^3 - 0.071 \cdot \left(\frac{D}{B}\right)^2 + 0.22 \cdot \frac{D}{B} = 0.157$$

$$g_{aL} := \sqrt{2 \cdot \ln\left(600\ s \cdot f_L\right) + 1.2} = 3.17$$

$$q_H := \frac{1}{2} \cdot \rho \cdot {U_H}^2 = 548.057\ Pa$$

$$M_L := \int_0^H m_Z \cdot \left(\frac{Z}{H}\right)^{2 \cdot \beta} dZ = \left(2.137 \cdot 10^7\right)\ kg$$

$$a_{Lmax} := \frac{q_H \cdot g_{aL} \cdot B \cdot H \cdot C'_L \cdot \lambda \cdot \sqrt{R_L}}{M_L} = 0.269\ \frac{m}{s^2}$$

$$a_{Lmax} = 27.392\ \frac{g}{1000}$$

Appendix 5. Across-wind acceleration according to AS/NZS 1170.2:2011

Basic wind speed return period conversion done by Eurocode.

Building height	$h := 200\ m$
width	$b := 30\ m$
depth	$d := 30\ m$
Height of interest	$z := h$
Building mass	$m_b := 64115003\ kg$
Building mass per unit height	$m_0 := \frac{m_b}{h} = (3.206 \cdot 10^5)\ \frac{kg}{m}$
Air density	$\rho := 1.23\ \frac{kg}{m^3}$
Fundamental frequency across-wind	$n_e := 0.139\ Hz$
Damping ratio across-wind	$\zeta_1 := 0.02$
Terrain/height multiplier	$M_{200.cat.1} := 1.32$
Mean 3-s gust wind speed	$V := \frac{18.95\ \frac{m}{s}}{1.09} \cdot 1.54 = 26.773\ \frac{m}{s}$

$$V_{des} := V \cdot M_{200.cat.1} = 35.341\ \frac{m}{s}$$

$$g_R := \sqrt{2 \cdot \ln(600\ s \cdot n_e)} = 2.974$$

$$g_v := 3.7$$

$$I_h := 0.085$$

$$k := 1.5$$

$$K_m := 0.76 + 0.24 \cdot k = 1.12$$

$$V_n := \frac{V_{des}}{n_e \cdot b \cdot (1 + g_v \cdot I_h)} = 6.447$$

$$I_{h.0.66} := 0.1$$

$$C_{fs} := 10^{\left(0.000406 \cdot V_n^{\ 4} - 0.0165 \cdot V_n^{\ 3} + 0.201 \cdot V_n^{\ 2} - 0.603 \cdot V_n - 2.76\right)} = 0.01$$

$$a := \frac{1.5 \cdot b \cdot g_R}{m_0} \cdot \left(\frac{0.5 \cdot \rho \cdot V_{des}^{\ 2}}{\left(1 + g_v \cdot I_h\right)^2} \right) \cdot K_m \cdot \sqrt{\frac{\pi \cdot C_{fs}}{\zeta_1}} = 0.257 \ \frac{m}{s^2}$$

$$a = 26.171 \ \frac{g}{1000}$$

Basic wind speed return period conversion done by AS/NZS 1170.2:2011.

Building height	$h := 200\ m$
width	$b := 30\ m$
depth	$d := 30\ m$
Height of interest	$z := h$
Building mass	$m_b := 64115003\ kg$
Building mass per unit height	$m_0 := \frac{m_b}{h} = (3.206 \cdot 10^5)\ \frac{kg}{m}$
Air density	$\rho := 1.23\ \frac{kg}{m^3}$
Fundamental frequency across-wind	$n_e := 0.139\ Hz$
Damping ratio across-wind	$\zeta_1 := 0.02$
Terrain/height multiplier	$M_{200.cat.1} := 1.32$
Mean 3-s gust wind speed	$V_{50} := \frac{21\ \frac{m}{s}}{1.09} \cdot 1.54 = 29.67\ \frac{m}{s}$

$$C := \frac{\frac{34}{39} + \frac{41}{45} + \frac{33}{44}}{3} = 0.844$$

$$V_{10} := V_{50} \cdot C = 25.05\ \frac{m}{s}$$

$$V_{des} := V_{10} \cdot M_{200.cat.1} = 33.066\ \frac{m}{s}$$

$$g_R := \sqrt{2 \cdot \ln(600\ s \cdot n_e)} = 2.974$$

$$g_v := 3.7$$

$$I_h := 0.085$$

$$k := 1.5$$

$$K_m := 0.76 + 0.24 \cdot k = 1.12$$

$$V_n := \frac{V_{des}}{n_e \cdot b \cdot \left(1 + g_v \cdot I_h\right)} = 6.032$$

$$I_{h.0.66} := 0.1$$

$$C_{fs} := 10^{\left(0.000406 \cdot V_n^{\ 4} - 0.0165 \cdot V_n^{\ 3} + 0.201 \cdot V_n^{\ 2} - 0.603 \cdot V_n - 2.76\right)} = 0.007$$

$$a := \frac{1.5 \cdot b \cdot g_R}{m_0} \cdot \left(\frac{0.5 \cdot \rho \cdot V_{des}^{\ 2}}{\left(1 + g_v \cdot I_h\right)^2}\right) \cdot K_m \cdot \sqrt{\frac{\pi \cdot C_{fs}}{\zeta_1}} = 0.188 \ \frac{m}{s^2}$$

$$a = 19.177 \ \frac{g}{1000}$$

Appendix 6. Across-wind acceleration according to Emil Simiu

Basic wind speed return period conversion done by Eurocode.

Building height $H := 200\ m$

width $B := 30\ m$

depth $D := 30\ m$

Height of interest $z := H$

Building mass $m_b := 64115003\ kg$

Building mass per unit volume $\rho_b := \frac{m_b}{H \cdot B \cdot D} = 356.194\ \frac{kg}{m^3}$

Air density $\rho := 1.23\ \frac{kg}{m^3}$

Fundamental frequency across $n_1 := 0.139\ Hz$

Damping ratio across-wind $\zeta_1 := 0.02$

Mean hourly wind speed $V_{zref} := \frac{18.95\ \frac{m}{s}}{1.09} = 17.385\ \frac{m}{s}$

Terrain roughness $z_0 := 0.01\ m$

Mean hourly wind speed height $z_{ref} := 10\ m$

$$V_H := V_{zref} \cdot \frac{\ln\left(\frac{z}{z_0}\right)}{\ln\left(\frac{z_{ref}}{z_0}\right)} = 24.925\ \frac{m}{s}$$

$A := B \cdot D = 900\ m^2$

$C := 0.00065$

$p := 3.3$

$$y_{pk} := C \cdot \left(\frac{V_H}{n_1 \cdot \sqrt{A}}\right)^p \cdot \frac{\sqrt{A}}{\sqrt{\zeta_1}} \cdot \frac{\rho}{\rho_b} \cdot \frac{z}{H} = 173.852\ mm$$

$$a := \left(2 \cdot \pi \cdot n_1\right)^2 \cdot y_{pk} = 0.133\ \frac{m}{s^2}$$

$$a = 13.522\ \frac{g}{1000}$$

Basic wind speed return period conversion done by ASCE-10.

Building height	$H := 200\ m$
width	$B := 30\ m$
depth	$D := 30\ m$
Height of interest	$z := H$
Building mass	$m_b := 64115003\ kg$
Building mass per unit volume	$\rho_b := \frac{m_b}{H \cdot B \cdot D} = 356.194\ \frac{kg}{m^3}$
Air density	$\rho := 1.23\ \frac{kg}{m^3}$
Fundamental frequency across	$n_1 := 0.139\ Hz$
Damping ratio across-wind	$\zeta_1 := 0.02$
Mean hourly wind speed	$V_{zref.50} := \frac{21\ \frac{m}{s}}{1.09} = 19.266\ \frac{m}{s}$
Terrain roughness	$z_0 := 0.01\ m$
Mean hourly wind speed height	$z_{ref} := 10\ m$
Return period	$T := 10$

$$V_{zref.10} := V_{zref.50} \cdot (0.36 + 0.1 \cdot \ln(12 \cdot T)) = 16.159\ \frac{m}{s}$$

$$V_H := V_{zref.10} \cdot \frac{\ln\left(\frac{z}{z_0}\right)}{\ln\left(\frac{z_{ref}}{z_0}\right)} = 23.167\ \frac{m}{s}$$

$$A := B \cdot D = 900\ m^2$$

$$C := 0.00065$$

$$p := 3.3$$

$$y_{pk} := C \cdot \left(\frac{V_H}{n_1 \cdot \sqrt{A}}\right)^p \cdot \frac{\sqrt{A}}{\sqrt{\zeta_1}} \cdot \frac{\rho}{\rho_b} \cdot \frac{z}{H} = 136.578\ mm$$

$$a := (2 \cdot \pi \cdot n_1)^2 \cdot y_{pk} = 0.104\ \frac{m}{s^2}$$

$$a = 10.623\ \frac{g}{1000}$$

Appendix 7. 2D finite element method table

Table 7.1. Wind speeds.

Elevation [m]	dl(x) [m]	U(x)																												
		5	6	7	8	9	10	11	12	13	14	15	16	17	18	19	20	21	22	23	24	25	26	27	28	29	30	31	32	33	34	35
200	30	7.2	8.6	10.0	11.5	12.9	14.3	15.8	17.2	18.6	20.1	21.5	22.9	24.4	25.8	27.2	28.7	30.1	31.5	33.0	34.4	35.8	37.3	38.7	40.1	41.6	43.0	44.4	45.9	47.3	48.7	50.2
196	30	7.2	8.6	10.0	11.4	12.9	14.3	15.7	17.2	18.6	20.0	21.5	22.9	24.3	25.8	27.2	28.6	30.0	31.5	32.9	34.3	35.8	37.2	38.6	40.1	41.5	42.9	44.4	45.8	47.2	48.6	50.1
192	30	7.1	8.6	10.0	11.4	12.8	14.3	15.7	17.1	18.6	20.0	21.4	22.8	24.3	25.7	27.1	28.5	29.9	31.4	32.8	34.3	35.7	37.1	38.5	39.9	41.4	42.8	44.3	45.7	47.1	48.5	50.0
188	30	7.1	8.5	10.0	11.4	12.8	14.2	15.7	17.1	18.5	19.9	21.4	22.8	24.2	25.6	27.1	28.5	29.9	31.3	32.8	34.2	35.6	37.0	38.5	39.9	41.3	42.7	44.2	45.6	47.0	48.4	49.9
184	30	7.1	8.5	10.0	11.4	12.8	14.2	15.6	17.1	18.5	19.9	21.3	22.7	24.2	25.6	27.0	28.4	29.9	31.3	32.7	34.1	35.5	37.0	38.4	39.8	41.2	42.6	44.1	45.5	46.9	48.3	49.8
180	30	7.1	8.5	9.9	11.3	12.8	14.2	15.6	17.0	18.4	19.9	21.3	22.7	24.1	25.5	27.0	28.4	29.8	31.2	32.6	34.0	35.5	36.9	38.3	39.7	41.1	42.6	44.0	45.4	46.8	48.2	49.6
176	30	7.1	8.5	9.9	11.3	12.7	14.2	15.6	17.0	18.4	19.8	21.2	22.6	24.1	25.5	26.9	28.3	29.7	31.1	32.5	34.0	35.4	36.8	38.2	39.6	41.0	42.5	43.9	45.3	46.7	48.1	49.5
172	30	7.1	8.5	9.9	11.3	12.7	14.1	15.5	16.9	18.4	19.8	21.2	22.6	24.0	25.4	26.8	28.2	29.6	31.1	32.5	33.9	35.3	36.7	38.1	39.5	40.9	42.4	43.8	45.2	46.6	48.0	49.4
168	30	7.0	8.5	9.9	11.3	12.7	14.1	15.5	16.9	18.3	19.7	21.1	22.5	23.9	25.4	26.8	28.2	29.6	31.0	32.4	33.8	35.2	36.6	38.0	39.4	40.8	42.3	43.7	45.1	46.5	47.9	49.3
164	30	7.0	8.4	9.8	11.2	12.6	14.0	15.5	16.9	18.3	19.7	21.1	22.5	23.9	25.3	26.7	28.1	29.5	30.9	32.3	33.7	35.1	36.5	37.9	39.3	40.7	42.1	43.6	45.0	46.4	47.8	49.2
160	30	7.0	8.4	9.8	11.2	12.6	14.0	15.4	16.8	18.2	19.6	21.0	22.4	23.8	25.2	26.6	28.0	29.4	30.8	32.2	33.6	35.0	36.4	37.8	39.2	40.6	42.0	43.4	44.8	46.2	47.6	49.0
156	30	7.0	8.4	9.8	11.2	12.6	14.0	15.4	16.8	18.2	19.6	21.0	22.4	23.8	25.2	26.6	28.0	29.4	30.7	32.1	33.5	34.9	36.3	37.7	39.1	40.5	41.9	43.3	44.7	46.1	47.5	48.9
152	30	7.0	8.4	9.8	11.2	12.5	13.9	15.3	16.7	18.1	19.5	20.9	22.3	23.7	25.1	26.5	27.9	29.3	30.7	32.1	33.5	34.8	36.2	37.6	39.0	40.4	41.8	43.2	44.6	46.0	47.3	48.8
148	30	7.0	8.3	9.7	11.1	12.5	13.9	15.3	16.7	18.1	19.5	20.9	22.2	23.6	25.0	26.4	27.8	29.2	30.6	32.0	33.4	34.8	36.1	37.5	38.9	40.3	41.7	43.1	44.5	45.9	47.3	48.7
144	30	6.9	8.3	9.7	11.1	12.5	13.9	15.2	16.6	18.0	19.4	20.8	22.2	23.6	25.0	26.3	27.7	29.1	30.5	31.9	33.3	34.7	36.0	37.4	38.8	40.2	41.6	43.0	44.4	45.8	47.1	48.5
140	30	6.9	8.3	9.7	11.1	12.4	13.8	15.2	16.6	18.0	19.3	20.7	22.1	23.5	24.9	26.3	27.6	29.0	30.4	31.8	33.2	34.6	35.9	37.3	38.7	40.1	41.5	42.8	44.2	45.6	47.0	48.4
136	30	6.9	8.3	9.6	11.0	12.4	13.8	15.2	16.5	17.9	19.3	20.7	22.0	23.4	24.8	26.2	27.6	28.9	30.3	31.7	33.1	34.4	35.8	37.2	38.6	40.0	41.3	42.7	44.1	45.5	46.8	48.2
132	30	6.9	8.2	9.6	11.0	12.4	13.7	15.1	16.5	17.9	19.2	20.6	22.0	23.3	24.7	26.1	27.5	28.8	30.2	31.6	33.0	34.3	35.7	37.1	38.5	39.8	41.2	42.6	44.0	45.3	46.7	48.1
128	30	6.8	8.2	9.6	10.9	12.3	13.7	15.1	16.4	17.8	19.2	20.5	21.9	23.3	24.6	26.0	27.4	28.8	30.1	31.5	32.9	34.2	35.6	37.0	38.3	39.7	41.1	42.4	43.8	45.2	46.5	47.9
124	30	6.8	8.2	9.5	10.9	12.3	13.6	15.0	16.4	17.7	19.1	20.4	21.8	23.1	24.5	25.8	27.3	28.6	29.9	31.4	32.7	34.1	35.4	36.8	38.2	39.4	40.9	42.3	43.7	45.0	46.4	47.8
120	30	6.8	8.1	9.5	10.8	12.2	13.5	14.9	16.3	17.6	19.0	20.3	21.7	23.0	24.4	25.7	27.1	28.5	29.8	31.2	32.5	33.9	35.2	36.6	37.9	39.3	40.6	42.0	43.4	44.7	46.1	47.4
116	30	6.7	8.1	9.4	10.8	12.1	13.5	14.8	16.2	17.5	18.9	20.2	21.6	22.9	24.3	25.6	27.0	28.3	29.7	31.0	32.4	33.7	35.1	36.4	37.8	39.1	40.5	41.8	43.2	44.5	45.9	47.2
112	30	6.7	8.1	9.4	10.8	12.1	13.4	14.8	16.1	17.5	18.8	20.2	21.5	22.9	24.2	25.5	26.9	28.2	29.6	30.9	32.3	33.6	35.0	36.3	37.6	39.0	40.3	41.7	43.0	44.4	45.7	47.1
108	30	6.7	8.0	9.4	10.7	12.1	13.4	14.7	16.1	17.4	18.7	20.1	21.4	22.8	24.1	25.4	26.8	28.1	29.5	30.8	32.1	33.5	34.8	36.2	37.5	38.8	40.2	41.5	42.8	44.2	45.5	46.9
104	30	6.7	8.0	9.3	10.7	12.0	13.3	14.7	16.0	17.3	18.7	20.0	21.3	22.6	24.0	25.3	26.7	28.0	29.3	30.7	32.0	33.3	34.7	36.0	37.3	38.7	40.0	41.3	42.7	44.0	45.3	46.7
100	30	6.7	8.0	9.3	10.6	11.9	13.3	14.6	15.9	17.3	18.6	19.9	21.2	22.6	23.9	25.2	26.5	27.9	29.2	30.5	31.9	33.2	34.5	35.8	37.2	38.5	39.8	41.2	42.5	43.8	45.1	46.5
96	30	6.6	7.9	9.2	10.6	11.9	13.2	14.5	15.9	17.2	18.5	19.8	21.1	22.5	23.8	25.1	26.4	27.7	29.1	30.4	31.7	33.0	34.4	35.7	37.0	38.3	39.6	41.0	42.3	43.6	44.9	46.2
92	30	6.6	7.9	9.2	10.5	11.8	13.1	14.5	15.8	17.1	18.4	19.7	21.0	22.4	23.7	25.0	26.3	27.6	28.9	30.2	31.6	32.9	34.2	35.5	36.8	38.1	39.4	40.8	42.1	43.4	44.7	46.0
88	30	6.5	7.8	9.2	10.5	11.8	13.1	14.4	15.7	17.0	18.3	19.6	20.9	22.2	23.5	24.9	26.2	27.5	28.8	30.1	31.4	32.7	34.0	35.3	36.6	37.9	39.2	40.6	41.9	43.2	44.5	45.8
84	30	6.5	7.8	9.1	10.4	11.7	13.0	14.3	15.6	16.9	18.2	19.5	20.8	22.1	23.4	24.7	26.0	27.3	28.6	29.9	31.2	32.5	33.8	35.1	36.4	37.7	39.0	40.3	41.6	42.9	44.2	45.5
80	30	6.5	7.8	9.1	10.3	11.6	12.9	14.2	15.5	16.8	18.1	19.4	20.7	22.0	23.3	24.6	25.9	27.2	28.5	29.8	31.0	32.3	33.6	34.9	36.2	37.5	38.8	40.1	41.4	42.7	44.0	45.3
76	30	6.5	7.8	9.1	10.3	11.6	12.9	14.1	15.4	16.7	18.0	19.3	20.6	21.9	23.1	24.4	25.7	27.0	28.3	29.6	30.9	32.1	33.4	34.7	36.0	37.3	38.6	39.9	41.1	42.4	43.7	45.0
72	30	6.4	7.7	8.9	10.2	11.5	12.8	14.1	15.3	16.6	17.9	19.2	20.4	21.7	23.0	24.3	25.6	26.8	28.1	29.4	30.7	31.9	33.2	34.5	35.8	37.0	38.3	39.6	40.9	42.2	43.4	44.7
68	30	6.3	7.6	8.9	10.1	11.4	12.7	14.0	15.2	16.5	17.8	19.0	20.3	21.6	22.8	24.1	25.4	26.6	27.9	29.2	30.4	31.7	33.0	34.3	35.5	36.8	38.1	39.3	40.6	41.9	43.1	44.4
64	30	6.3	7.6	8.8	10.1	11.3	12.6	13.9	15.1	16.4	17.6	18.9	20.2	21.4	22.7	23.9	25.2	26.4	27.7	29.0	30.2	31.5	32.7	34.0	35.3	36.5	37.8	39.0	40.3	41.6	42.8	44.1
60	30	6.3	7.5	8.7	9.9	11.1	12.4	13.6	14.9	16.1	17.4	18.6	19.8	21.1	22.3	23.5	24.8	26.0	27.3	28.5	29.7	31.0	32.2	33.4	34.7	35.9	37.2	38.4	39.6	40.9	42.1	43.4
56	30	6.2	7.4	8.7	9.9	11.1	12.4	13.6	14.9	16.1	17.3	18.6	19.8	20.9	22.1	23.3	24.5	25.8	27.0	28.2	29.4	30.7	31.9	33.1	34.4	35.6	36.8	38.0	39.3	40.5	41.7	42.9
52	30	6.2	7.4	8.6	9.8	11.0	12.3	13.5	14.7	16.0	17.2	18.4	19.6	20.9	22.1	23.1	24.3	25.5	26.7	27.9	29.1	30.4	31.6	32.8	34.0	35.2	36.4	37.6	38.9	40.1	41.3	42.5
48	30	6.1	7.4	8.6	9.8	11.0	12.3	13.5	14.7	16.0	17.2	18.4	19.6	20.9	22.1	23.1	24.3	25.5	26.7	27.9	29.1	30.4	31.6	32.8	34.0	35.2	36.4	37.6	38.9	40.1	41.3	42.5
44	30	6.1	7.3	8.5	9.7	10.9	12.1	13.4	14.6	15.8	17.0	18.2	19.4	20.6	21.9	23.1	24.3	25.5	26.7	27.9	29.1	30.4	31.6	32.8	34.0	35.2	36.4	37.6	38.9	40.1	41.3	42.5
40	30	6.0	7.2	8.4	9.6	10.8	12.0	13.2	14.4	15.6	16.8	18.0	19.2	20.4	21.6	22.8	24.0	25.2	26.4	27.6	28.8	30.0	31.2	32.4	33.6	34.8	36.0	37.2	38.4	39.6	40.8	42.0
36	30	5.9	7.1	8.3	9.5	10.7	11.9	13.0	14.2	15.4	16.6	17.8	19.0	20.2	21.3	22.5	23.7	24.9	26.1	27.3	28.5	29.6	30.8	32.0	33.2	34.4	35.6	36.7	37.9	39.1	40.3	41.5
32	30	5.8	7.0	8.2	9.3	10.5	11.7	12.9	14.0	15.2	16.4	17.5	18.7	19.9	21.0	22.2	23.4	24.5	25.7	26.9	28.0	29.2	30.4	31.5	32.7	33.9	35.1	36.2	37.4	38.6	39.7	40.9
28	30	5.7	6.9	8.0	9.2	10.3	11.5	12.6	13.8	14.9	16.1	17.2	18.4	19.5	20.7	21.8	23.0	24.1	25.3	26.4	27.6	28.7	29.9	31.0	32.2	33.3	34.5	35.6	36.8	37.9	39.1	40.2
24	30	5.6	6.8	7.9	9.0	10.1	11.3	12.4	13.5	14.6	15.8	16.9	18.0	19.2	20.3	21.4	22.5	23.7	24.8	25.9	27.0	28.2	29.3	30.4	31.5	32.7	33.8	34.9	36.1	37.2	38.3	39.4
20	30	5.5	6.6	7.7	8.8	9.9	11.0	12.1	13.2	14.3	15.4	16.5	17.6	18.7	19.8	20.9	22.0	23.1	24.2	25.3	26.4	27.5	28.6	29.7	30.8	31.9	33.0	34.1	35.2	36.3	37.4	38.5
16	30	5.3	6.4	7.5	8.5	9.6	10.7	11.7	12.8	13.9	15.0	16.0	17.1	18.2	19.2	20.3	21.4	22.4	23.5	24.6	25.6	26.7	27.8	28.8	29.9	31.0	32.0	33.1	34.2	35.2	36.3	37.4
12	30	5.1	6.2	7.2	8.2	9.2	10.3	11.3	12.3	13.3	14.4	15.4	16.4	17.4	18.5	19.5	20.5	21.6	22.6	23.6	24.6	25.7	26.7	27.7	28.7	29.8	30.8	31.8	32.8	33.9	34.9	35.9
10	30	5.0	6	7	8	9	10	11	12	13	14	15	16	17	18	19	20	21	22	23	24	25	26	27	28	29	30	31	32	33	34	35
8	30	4.8	5.8	6.8	7.7	8.7	9.7	10.6	11.6	12.6	13.5	14.5	15.5	16.5	17.4	18.4	19.4	20.3	21.3	22.3	23.2	24.2	25.2	26.1	27.1	28.1	29.0	30.0	31.0	31.9	32.9	33.9
4	30	4.3	5.2	6.1	6.9	7.8	8.7	9.5	10.4	11.3	12.1	13.0	13.9	14.7	15.6	16.5	17.3	18.2	19.1	19.9	20.8	21.7	22.6	23.4	24.3	25.2	26.0	26.9	27.8	28.6	29.5	30.4
0	30	4.3	5.2	6.1	6.9	7.8	8.7	9.5	10.4	11.3	12.1	13.0	13.9	14.7	15.6	16.5	17.3	18.2	19.1	19.9	20.8	21.7	22.6	23.4	24.3	25.2	26.0	26.9	27.8	28.6	29.5	30.4

Table 7.2. Reynolds numbers.

Elevation [m]	d(k) [m]	Re vs. wind speed and building height																													
		5	6	7	8	9	10	11	12	13	14	15	16	17	18	19	20	21	22	23	24	25	26	27	28	29	30	31	32	33	34	35
200	30	1.4E+07	1.7E+07	2.0E+07	2.3E+07	2.6E+07	2.9E+07	3.2E+07	3.4E+07	3.7E+07	4.0E+07	4.3E+07	4.6E+07	4.9E+07	5.2E+07	5.4E+07	5.7E+07	6.0E+07	6.3E+07	6.6E+07	6.9E+07	7.2E+07	7.5E+07	7.7E+07	8.0E+07	8.3E+07	8.6E+07	8.9E+07	9.2E+07	9.5E+07	9.7E+07	1.0E+08
196	30	1.4E+07	1.7E+07	2.0E+07	2.3E+07	2.6E+07	2.9E+07	3.1E+07	3.4E+07	3.7E+07	4.0E+07	4.3E+07	4.6E+07	4.9E+07	5.2E+07	5.4E+07	5.7E+07	6.0E+07	6.3E+07	6.6E+07	6.9E+07	7.2E+07	7.4E+07	7.7E+07	8.0E+07	8.3E+07	8.6E+07	8.9E+07	9.2E+07	9.4E+07	9.7E+07	1.0E+08
192	30	1.4E+07	1.7E+07	2.0E+07	2.3E+07	2.6E+07	2.9E+07	3.1E+07	3.4E+07	3.7E+07	4.0E+07	4.3E+07	4.6E+07	4.9E+07	5.1E+07	5.4E+07	5.7E+07	6.0E+07	6.3E+07	6.6E+07	6.9E+07	7.1E+07	7.4E+07	7.7E+07	8.0E+07	8.3E+07	8.6E+07	8.9E+07	9.1E+07	9.4E+07	9.7E+07	1.0E+08
188	30	1.4E+07	1.7E+07	2.0E+07	2.3E+07	2.6E+07	2.8E+07	3.1E+07	3.4E+07	3.7E+07	4.0E+07	4.3E+07	4.6E+07	4.8E+07	5.1E+07	5.4E+07	5.7E+07	6.0E+07	6.3E+07	6.6E+07	6.8E+07	7.1E+07	7.4E+07	7.7E+07	8.0E+07	8.3E+07	8.5E+07	8.8E+07	9.1E+07	9.4E+07	9.7E+07	1.0E+08
184	30	1.4E+07	1.7E+07	2.0E+07	2.3E+07	2.6E+07	2.8E+07	3.1E+07	3.4E+07	3.7E+07	4.0E+07	4.3E+07	4.5E+07	4.8E+07	5.1E+07	5.4E+07	5.7E+07	6.0E+07	6.3E+07	6.5E+07	6.8E+07	7.1E+07	7.4E+07	7.7E+07	7.9E+07	8.2E+07	8.5E+07	8.8E+07	9.1E+07	9.4E+07	9.7E+07	1.0E+08
180	30	1.4E+07	1.7E+07	2.0E+07	2.3E+07	2.6E+07	2.8E+07	3.1E+07	3.4E+07	3.7E+07	4.0E+07	4.3E+07	4.5E+07	4.8E+07	5.1E+07	5.4E+07	5.7E+07	6.0E+07	6.2E+07	6.5E+07	6.8E+07	7.1E+07	7.4E+07	7.7E+07	7.9E+07	8.2E+07	8.5E+07	8.8E+07	9.1E+07	9.4E+07	9.6E+07	9.9E+07
176	30	1.4E+07	1.7E+07	2.0E+07	2.3E+07	2.5E+07	2.8E+07	3.1E+07	3.4E+07	3.7E+07	4.0E+07	4.2E+07	4.5E+07	4.8E+07	5.1E+07	5.4E+07	5.7E+07	5.9E+07	6.2E+07	6.5E+07	6.8E+07	7.1E+07	7.4E+07	7.6E+07	7.9E+07	8.2E+07	8.5E+07	8.8E+07	9.1E+07	9.3E+07	9.6E+07	9.9E+07
172	30	1.4E+07	1.7E+07	2.0E+07	2.3E+07	2.5E+07	2.8E+07	3.1E+07	3.4E+07	3.7E+07	4.0E+07	4.2E+07	4.5E+07	4.8E+07	5.1E+07	5.4E+07	5.6E+07	5.9E+07	6.2E+07	6.5E+07	6.8E+07	7.1E+07	7.3E+07	7.6E+07	7.9E+07	8.2E+07	8.5E+07	8.8E+07	9.0E+07	9.3E+07	9.6E+07	9.9E+07
168	30	1.4E+07	1.7E+07	2.0E+07	2.3E+07	2.5E+07	2.8E+07	3.1E+07	3.4E+07	3.7E+07	3.9E+07	4.2E+07	4.5E+07	4.8E+07	5.1E+07	5.4E+07	5.6E+07	5.9E+07	6.2E+07	6.5E+07	6.8E+07	7.0E+07	7.3E+07	7.6E+07	7.9E+07	8.2E+07	8.5E+07	8.7E+07	9.0E+07	9.3E+07	9.6E+07	9.9E+07
164	30	1.4E+07	1.7E+07	2.0E+07	2.2E+07	2.5E+07	2.8E+07	3.1E+07	3.4E+07	3.7E+07	3.9E+07	4.2E+07	4.5E+07	4.8E+07	5.1E+07	5.3E+07	5.6E+07	5.9E+07	6.2E+07	6.5E+07	6.7E+07	7.0E+07	7.3E+07	7.6E+07	7.9E+07	8.1E+07	8.4E+07	8.7E+07	9.0E+07	9.3E+07	9.6E+07	9.8E+07
160	30	1.4E+07	1.7E+07	2.0E+07	2.2E+07	2.5E+07	2.8E+07	3.1E+07	3.4E+07	3.6E+07	3.9E+07	4.2E+07	4.5E+07	4.8E+07	5.0E+07	5.3E+07	5.6E+07	5.9E+07	6.2E+07	6.4E+07	6.7E+07	7.0E+07	7.3E+07	7.6E+07	7.8E+07	8.1E+07	8.4E+07	8.7E+07	9.0E+07	9.2E+07	9.5E+07	9.8E+07
156	30	1.4E+07	1.7E+07	2.0E+07	2.2E+07	2.5E+07	2.8E+07	3.1E+07	3.4E+07	3.6E+07	3.9E+07	4.2E+07	4.5E+07	4.8E+07	5.0E+07	5.3E+07	5.6E+07	5.9E+07	6.1E+07	6.4E+07	6.7E+07	7.0E+07	7.3E+07	7.5E+07	7.8E+07	8.1E+07	8.4E+07	8.7E+07	8.9E+07	9.2E+07	9.5E+07	9.8E+07
152	30	1.4E+07	1.7E+07	2.0E+07	2.2E+07	2.5E+07	2.8E+07	3.1E+07	3.3E+07	3.6E+07	3.9E+07	4.2E+07	4.5E+07	4.7E+07	5.0E+07	5.3E+07	5.6E+07	5.9E+07	6.1E+07	6.4E+07	6.7E+07	7.0E+07	7.2E+07	7.5E+07	7.8E+07	8.1E+07	8.4E+07	8.6E+07	8.9E+07	9.2E+07	9.5E+07	9.8E+07
148	30	1.4E+07	1.7E+07	1.9E+07	2.2E+07	2.5E+07	2.8E+07	3.1E+07	3.3E+07	3.6E+07	3.9E+07	4.2E+07	4.4E+07	4.7E+07	5.0E+07	5.3E+07	5.5E+07	5.8E+07	6.1E+07	6.4E+07	6.7E+07	6.9E+07	7.2E+07	7.5E+07	7.8E+07	8.0E+07	8.3E+07	8.6E+07	8.9E+07	9.2E+07	9.5E+07	9.7E+07
144	30	1.4E+07	1.7E+07	1.9E+07	2.2E+07	2.5E+07	2.8E+07	3.0E+07	3.3E+07	3.6E+07	3.9E+07	4.2E+07	4.4E+07	4.7E+07	5.0E+07	5.3E+07	5.5E+07	5.8E+07	6.1E+07	6.4E+07	6.7E+07	6.9E+07	7.2E+07	7.5E+07	7.8E+07	8.0E+07	8.3E+07	8.6E+07	8.9E+07	9.1E+07	9.4E+07	9.7E+07
140	30	1.4E+07	1.7E+07	1.9E+07	2.2E+07	2.5E+07	2.8E+07	3.0E+07	3.3E+07	3.6E+07	3.9E+07	4.1E+07	4.4E+07	4.7E+07	5.0E+07	5.3E+07	5.5E+07	5.8E+07	6.1E+07	6.4E+07	6.6E+07	6.9E+07	7.2E+07	7.5E+07	7.7E+07	8.0E+07	8.3E+07	8.6E+07	8.8E+07	9.1E+07	9.4E+07	9.7E+07
136	30	1.4E+07	1.7E+07	1.9E+07	2.2E+07	2.5E+07	2.8E+07	3.0E+07	3.3E+07	3.6E+07	3.9E+07	4.1E+07	4.4E+07	4.7E+07	5.0E+07	5.2E+07	5.5E+07	5.8E+07	6.1E+07	6.3E+07	6.6E+07	6.9E+07	7.2E+07	7.4E+07	7.7E+07	8.0E+07	8.3E+07	8.5E+07	8.8E+07	9.1E+07	9.4E+07	9.6E+07
132	30	1.4E+07	1.6E+07	1.9E+07	2.2E+07	2.5E+07	2.7E+07	3.0E+07	3.3E+07	3.6E+07	3.8E+07	4.1E+07	4.4E+07	4.7E+07	4.9E+07	5.2E+07	5.5E+07	5.8E+07	6.0E+07	6.3E+07	6.6E+07	6.8E+07	7.1E+07	7.4E+07	7.7E+07	8.0E+07	8.2E+07	8.5E+07	8.8E+07	9.1E+07	9.3E+07	9.6E+07
128	30	1.4E+07	1.6E+07	1.9E+07	2.2E+07	2.5E+07	2.7E+07	3.0E+07	3.3E+07	3.6E+07	3.8E+07	4.1E+07	4.4E+07	4.7E+07	4.9E+07	5.2E+07	5.5E+07	5.8E+07	6.0E+07	6.3E+07	6.6E+07	6.8E+07	7.1E+07	7.4E+07	7.7E+07	7.9E+07	8.2E+07	8.5E+07	8.8E+07	9.0E+07	9.3E+07	9.6E+07
124	30	1.4E+07	1.6E+07	1.9E+07	2.2E+07	2.5E+07	2.7E+07	3.0E+07	3.3E+07	3.5E+07	3.8E+07	4.1E+07	4.4E+07	4.6E+07	4.9E+07	5.2E+07	5.5E+07	5.7E+07	6.0E+07	6.3E+07	6.5E+07	6.8E+07	7.1E+07	7.3E+07	7.6E+07	7.9E+07	8.2E+07	8.4E+07	8.7E+07	9.0E+07	9.3E+07	9.5E+07
120	30	1.4E+07	1.6E+07	1.9E+07	2.2E+07	2.4E+07	2.7E+07	3.0E+07	3.3E+07	3.5E+07	3.8E+07	4.1E+07	4.3E+07	4.6E+07	4.9E+07	5.1E+07	5.4E+07	5.7E+07	6.0E+07	6.2E+07	6.5E+07	6.8E+07	7.0E+07	7.3E+07	7.6E+07	7.9E+07	8.1E+07	8.4E+07	8.7E+07	8.9E+07	9.2E+07	9.5E+07
116	30	1.4E+07	1.6E+07	1.9E+07	2.2E+07	2.4E+07	2.7E+07	3.0E+07	3.3E+07	3.5E+07	3.8E+07	4.0E+07	4.3E+07	4.6E+07	4.9E+07	5.1E+07	5.4E+07	5.7E+07	5.9E+07	6.2E+07	6.5E+07	6.8E+07	7.0E+07	7.3E+07	7.6E+07	7.9E+07	8.1E+07	8.4E+07	8.6E+07	8.9E+07	9.2E+07	9.4E+07
112	30	1.3E+07	1.6E+07	1.9E+07	2.2E+07	2.4E+07	2.7E+07	3.0E+07	3.2E+07	3.5E+07	3.8E+07	4.0E+07	4.3E+07	4.6E+07	4.8E+07	5.1E+07	5.4E+07	5.6E+07	5.9E+07	6.2E+07	6.5E+07	6.7E+07	7.0E+07	7.3E+07	7.6E+07	7.8E+07	8.1E+07	8.4E+07	8.6E+07	8.9E+07	9.1E+07	9.4E+07
108	30	1.3E+07	1.6E+07	1.9E+07	2.2E+07	2.4E+07	2.7E+07	3.0E+07	3.2E+07	3.5E+07	3.8E+07	4.0E+07	4.3E+07	4.6E+07	4.8E+07	5.1E+07	5.4E+07	5.6E+07	5.9E+07	6.2E+07	6.5E+07	6.7E+07	7.0E+07	7.3E+07	7.5E+07	7.8E+07	8.0E+07	8.3E+07	8.6E+07	8.8E+07	9.1E+07	9.4E+07
104	30	1.3E+07	1.6E+07	1.9E+07	2.1E+07	2.4E+07	2.7E+07	2.9E+07	3.2E+07	3.5E+07	3.7E+07	4.0E+07	4.3E+07	4.6E+07	4.8E+07	5.1E+07	5.4E+07	5.6E+07	5.9E+07	6.2E+07	6.4E+07	6.7E+07	7.0E+07	7.2E+07	7.5E+07	7.8E+07	8.0E+07	8.3E+07	8.6E+07	8.8E+07	9.1E+07	9.4E+07
100	30	1.3E+07	1.6E+07	1.9E+07	2.1E+07	2.4E+07	2.7E+07	2.9E+07	3.2E+07	3.5E+07	3.7E+07	4.0E+07	4.3E+07	4.5E+07	4.8E+07	5.1E+07	5.3E+07	5.6E+07	5.9E+07	6.1E+07	6.4E+07	6.7E+07	6.9E+07	7.2E+07	7.5E+07	7.7E+07	8.0E+07	8.3E+07	8.5E+07	8.8E+07	9.1E+07	9.3E+07
96	30	1.3E+07	1.6E+07	1.9E+07	2.1E+07	2.4E+07	2.7E+07	2.9E+07	3.2E+07	3.5E+07	3.7E+07	4.0E+07	4.2E+07	4.5E+07	4.8E+07	5.0E+07	5.3E+07	5.5E+07	5.8E+07	6.1E+07	6.4E+07	6.6E+07	6.9E+07	7.2E+07	7.4E+07	7.7E+07	8.0E+07	8.2E+07	8.5E+07	8.8E+07	9.0E+07	9.3E+07
92	30	1.3E+07	1.6E+07	1.8E+07	2.1E+07	2.4E+07	2.6E+07	2.9E+07	3.2E+07	3.4E+07	3.7E+07	3.9E+07	4.2E+07	4.5E+07	4.7E+07	5.0E+07	5.3E+07	5.5E+07	5.8E+07	6.1E+07	6.3E+07	6.6E+07	6.8E+07	7.1E+07	7.4E+07	7.7E+07	7.9E+07	8.2E+07	8.5E+07	8.7E+07	9.0E+07	9.2E+07
88	30	1.3E+07	1.6E+07	1.8E+07	2.1E+07	2.4E+07	2.6E+07	2.9E+07	3.1E+07	3.4E+07	3.7E+07	3.9E+07	4.2E+07	4.4E+07	4.7E+07	5.0E+07	5.2E+07	5.5E+07	5.8E+07	6.0E+07	6.3E+07	6.5E+07	6.8E+07	7.1E+07	7.3E+07	7.6E+07	7.8E+07	8.1E+07	8.4E+07	8.6E+07	8.9E+07	9.2E+07
84	30	1.3E+07	1.6E+07	1.8E+07	2.1E+07	2.3E+07	2.6E+07	2.9E+07	3.1E+07	3.4E+07	3.6E+07	3.9E+07	4.2E+07	4.4E+07	4.7E+07	4.9E+07	5.2E+07	5.5E+07	5.7E+07	6.0E+07	6.2E+07	6.5E+07	6.8E+07	7.0E+07	7.3E+07	7.5E+07	7.8E+07	8.1E+07	8.3E+07	8.6E+07	8.8E+07	9.1E+07
80	30	1.3E+07	1.6E+07	1.8E+07	2.1E+07	2.3E+07	2.6E+07	2.8E+07	3.1E+07	3.4E+07	3.6E+07	3.9E+07	4.1E+07	4.4E+07	4.7E+07	4.9E+07	5.2E+07	5.4E+07	5.7E+07	6.0E+07	6.2E+07	6.5E+07	6.7E+07	7.0E+07	7.2E+07	7.5E+07	7.7E+07	8.0E+07	8.3E+07	8.5E+07	8.8E+07	9.1E+07
76	30	1.3E+07	1.6E+07	1.8E+07	2.1E+07	2.3E+07	2.6E+07	2.8E+07	3.1E+07	3.4E+07	3.6E+07	3.9E+07	4.1E+07	4.4E+07	4.7E+07	4.9E+07	5.2E+07	5.4E+07	5.7E+07	5.9E+07	6.2E+07	6.4E+07	6.7E+07	6.9E+07	7.2E+07	7.4E+07	7.7E+07	7.9E+07	8.2E+07	8.4E+07	8.7E+07	9.0E+07
72	30	1.3E+07	1.5E+07	1.8E+07	2.1E+07	2.3E+07	2.6E+07	2.8E+07	3.1E+07	3.3E+07	3.6E+07	3.9E+07	4.1E+07	4.4E+07	4.6E+07	4.9E+07	5.1E+07	5.4E+07	5.7E+07	5.9E+07	6.2E+07	6.4E+07	6.7E+07	6.9E+07	7.2E+07	7.4E+07	7.7E+07	7.9E+07	8.2E+07	8.4E+07	8.7E+07	8.9E+07
68	30	1.3E+07	1.5E+07	1.8E+07	2.0E+07	2.3E+07	2.6E+07	2.8E+07	3.1E+07	3.3E+07	3.6E+07	3.8E+07	4.1E+07	4.3E+07	4.6E+07	4.8E+07	5.1E+07	5.3E+07	5.6E+07	5.8E+07	6.1E+07	6.3E+07	6.6E+07	6.9E+07	7.1E+07	7.4E+07	7.6E+07	7.9E+07	8.1E+07	8.4E+07	8.6E+07	8.9E+07
64	30	1.3E+07	1.5E+07	1.8E+07	2.0E+07	2.3E+07	2.5E+07	2.8E+07	3.0E+07	3.3E+07	3.6E+07	3.8E+07	4.1E+07	4.3E+07	4.6E+07	4.8E+07	5.0E+07	5.3E+07	5.5E+07	5.8E+07	6.0E+07	6.3E+07	6.5E+07	6.8E+07	7.1E+07	7.3E+07	7.6E+07	7.8E+07	8.1E+07	8.3E+07	8.6E+07	8.8E+07
60	30	1.3E+07	1.5E+07	1.8E+07	2.0E+07	2.3E+07	2.5E+07	2.8E+07	3.0E+07	3.2E+07	3.5E+07	3.8E+07	4.0E+07	4.3E+07	4.5E+07	4.8E+07	5.0E+07	5.2E+07	5.5E+07	5.7E+07	6.0E+07	6.2E+07	6.5E+07	6.7E+07	7.0E+07	7.2E+07	7.5E+07	7.7E+07	8.0E+07	8.2E+07	8.5E+07	8.7E+07
56	30	1.2E+07	1.5E+07	1.7E+07	2.0E+07	2.2E+07	2.5E+07	2.7E+07	3.0E+07	3.2E+07	3.5E+07	3.7E+07	4.0E+07	4.2E+07	4.5E+07	4.7E+07	5.0E+07	5.2E+07	5.5E+07	5.7E+07	5.9E+07	6.2E+07	6.4E+07	6.7E+07	6.9E+07	7.2E+07	7.4E+07	7.7E+07	7.9E+07	8.2E+07	8.4E+07	8.7E+07
52	30	1.2E+07	1.5E+07	1.7E+07	2.0E+07	2.2E+07	2.5E+07	2.7E+07	3.0E+07	3.2E+07	3.5E+07	3.7E+07	4.0E+07	4.2E+07	4.5E+07	4.7E+07	5.0E+07	5.2E+07	5.5E+07	5.7E+07	5.9E+07	6.2E+07	6.4E+07	6.7E+07	6.9E+07	7.2E+07	7.4E+07	7.7E+07	7.9E+07	8.2E+07	8.4E+07	8.7E+07
48	30	1.2E+07	1.5E+07	1.7E+07	2.0E+07	2.2E+07	2.5E+07	2.7E+07	2.9E+07	3.2E+07	3.4E+07	3.7E+07	3.9E+07	4.2E+07	4.4E+07	4.7E+07	4.9E+07	5.2E+07	5.4E+07	5.6E+07	5.9E+07	6.1E+07	6.4E+07	6.6E+07	6.9E+07	7.1E+07	7.4E+07	7.6E+07	7.9E+07	8.1E+07	8.3E+07	8.6E+07
44	30	1.2E+07	1.5E+07	1.7E+07	1.9E+07	2.2E+07	2.5E+07	2.7E+07	2.9E+07	3.2E+07	3.4E+07	3.6E+07	3.9E+07	4.1E+07	4.4E+07	4.6E+07	4.9E+07	5.1E+07	5.3E+07	5.6E+07	5.8E+07	6.1E+07	6.3E+07	6.6E+07	6.8E+07	7.1E+07	7.3E+07	7.6E+07	7.8E+07	8.0E+07	8.3E+07	8.5E+07
40	30	1.2E+07	1.4E+07	1.7E+07	1.9E+07	2.2E+07	2.4E+07	2.6E+07	2.9E+07	3.1E+07	3.4E+07	3.6E+07	3.8E+07	4.1E+07	4.3E+07	4.6E+07	4.8E+07	5.0E+07	5.3E+07	5.5E+07	5.8E+07	6.0E+07	6.2E+07	6.5E+07	6.7E+07	7.0E+07	7.2E+07	7.4E+07	7.7E+07	7.9E+07	8.2E+07	8.4E+07
36	30	1.2E+07	1.4E+07	1.7E+07	1.9E+07	2.1E+07	2.4E+07	2.6E+07	2.8E+07	3.1E+07	3.3E+07	3.6E+07	3.8E+07	4.0E+07	4.3E+07	4.5E+07	4.7E+07	5.0E+07	5.2E+07	5.5E+07	5.7E+07	5.9E+07	6.2E+07	6.4E+07	6.6E+07	6.9E+07	7.1E+07	7.3E+07	7.6E+07	7.8E+07	8.1E+07	8.3E+07
32	30	1.2E+07	1.4E+07	1.6E+07	1.9E+07	2.1E+07	2.3E+07	2.6E+07	2.8E+07	3.0E+07	3.3E+07	3.5E+07	3.7E+07	4.0E+07	4.2E+07	4.4E+07	4.7E+07	4.9E+07	5.1E+07	5.4E+07	5.6E+07	5.8E+07	6.1E+07	6.3E+07	6.5E+07	6.8E+07	7.0E+07	7.2E+07	7.5E+07	7.7E+07	7.9E+07	8.2E+07
28	30	1.1E+07	1.4E+07	1.6E+07	1.8E+07	2.1E+07	2.3E+07	2.5E+07	2.8E+07	3.0E+07	3.2E+07	3.4E+07	3.7E+07	3.9E+07	4.1E+07	4.4E+07	4.6E+07	4.8E+07	5.1E+07	5.3E+07	5.5E+07	5.7E+07	6.0E+07	6.2E+07	6.4E+07	6.7E+07	6.9E+07	7.1E+07	7.4E+07	7.6E+07	7.8E+07	8.0E+07
24	30	1.1E+07	1.4E+07	1.6E+07	1.8E+07	2.0E+07	2.2E+07	2.5E+07	2.7E+07	2.9E+07	3.1E+07	3.3E+07	3.5E+07	3.8E+07	4.0E+07	4.2E+07	4.5E+07	4.7E+07	4.9E+07	5.1E+07	5.3E+07	5.5E+07	5.7E+07	5.9E+07	6.2E+07	6.4E+07	6.6E+07	6.8E+07	7.0E+07	7.2E+07	7.4E+07	7.7E+07
20	30	1.1E+07	1.3E+07	1.5E+07	1.8E+07	2.0E+07	2.2E+07	2.4E+07	2.6E+07	2.9E+07	3.1E+07	3.3E+07	3.5E+07	3.7E+07	4.0E+07	4.2E+07	4.4E+07	4.6E+07	4.8E+07	5.1E+07	5.3E+07	5.5E+07	5.7E+07	5.9E+07	6.1E+07	6.4E+07	6.6E+07	6.8E+07	7.0E+07	7.3E+07	7.5E+07	7.7E+07
16	30	1.1E+07	1.3E+07	1.5E+07	1.7E+07	1.9E+07	2.1E+07	2.3E+07	2.6E+07	2.8E+07	3.0E+07	3.2E+07	3.4E+07	3.6E+07	3.8E+07	4.1E+07	4.3E+07	4.5E+07	4.7E+07	4.9E+07	5.1E+07	5.3E+07	5.5E+07	5.7E+07	5.9E+07	6.1E+07	6.3E+07	6.5E+07	6.8E+07	7.0E+07	7.2E+07	7.5E+07
12	30	1.0E+07	1.2E+07	1.4E+07	1.6E+07	1.8E+07	2.1E+07	2.3E+07	2.5E+07	2.7E+07	2.9E+07	3.1E+07	3.3E+07	3.5E+07	3.7E+07	4.0E+07	4.2E+07	4.4E+07	4.6E+07	4.8E+07	5.0E+07	5.2E+07	5.4E+07	5.6E+07	5.8E+07	6.0E+07	6.2E+07	6.4E+07	6.6E+07	6.8E+07	7.0E+07	7.2E+07
10	30	1.0E+07	1.2E+07	1.4E+07	1.6E+07	1.8E+07	2.0E+07	2.2E+07	2.4E+07	2.6E+07	2.8E+07	3.0E+07	3.2E+07	3.4E+07	3.6E+07	3.8E+07	4.0E+07	4.2E+07	4.4E+07	4.6E+07	4.8E+07	5.0E+07	5.2E+07	5.4E+07	5.6E+07	5.8E+07	6.0E+07	6.2E+07	6.4E+07	6.6E+07	6.8E+07	7.0E+07
8	30	9.7E+06	1.2E+07	1.4E+07	1.5E+07	1.7E+07	1.9E+07	2.1E+07	2.3E+07	2.5E+07	2.7E+07	2.9E+07	3.1E+07	3.3E+07	3.5E+07	3.7E+07	3.9E+07	4.1E+07	4.3E+07	4.5E+07	4.8E+07	5.0E+07	5.2E+07	5.4E+07	5.6E+07	5.8E+07	6.0E+07	6.2E+07	6.4E+07	6.6E+07	6.8E+07	6.9E+07
4	30	8.7E+06	1.0E+07	1.2E+07	1.4E+07	1.6E+07	1.7E+07	1.9E+07	2.1E+07	2.3E+07	2.4E+07	2.6E+07	2.8E+07	2.9E+07	3.1E+07	3.3E+07	3.5E+07	3.6E+07	3.8E+07	4.0E+07	4.2E+07	4.3E+07	4.5E+07	4.7E+07	4.9E+07	5.0E+07	5.2E+07	5.4E+07	5.6E+07	5.7E+07	5.9E+07	6.1E+07
0	30	8.7E+06	1.0E+07	1.2E+07	1.4E+07	1.6E+07	1.7E+07	1.9E+07	2.1E+07	2.3E+07	2.4E+07	2.6E+07	2.8E+07	2.9E+07	3.1E+07	3.3E+07	3.5E+07	3.6E+07	3.8E+07	4.0E+07	4.2E+07	4.3E+07	4.5E+07	4.7E+07	4.9E+07	5.0E+07	5.2E+07	5.4E+07	5.6E+07	5.7E+07	5.9E+07	6.1E+07

Table 7.3. Shedding frequency.

Elevation [m]	d(x) [m]	Shedding frequency vs. wind speed and building height																														
		5	6	7	8	9	10	11	12	13	14	15	16	17	18	19	20	21	22	23	24	25	26	27	28	29	30	31	32	33	34	35
200	30	0.026	0.032	0.037	0.042	0.047	0.053	0.058	0.063	0.068	0.074	0.079	0.084	0.089	0.095	0.100	0.105	0.110	0.116	0.121	0.126	0.131	0.137	0.142	0.147	0.152	0.158	0.163	0.168	0.173	0.179	0.184
196	30	0.026	0.031	0.037	0.042	0.047	0.052	0.058	0.063	0.068	0.073	0.079	0.084	0.089	0.094	0.100	0.105	0.110	0.115	0.121	0.126	0.131	0.136	0.142	0.147	0.152	0.157	0.163	0.168	0.173	0.178	0.184
192	30	0.026	0.031	0.037	0.042	0.047	0.052	0.058	0.063	0.068	0.073	0.079	0.084	0.089	0.094	0.099	0.105	0.110	0.115	0.120	0.126	0.131	0.136	0.141	0.147	0.152	0.157	0.162	0.168	0.173	0.178	0.183
188	30	0.026	0.031	0.037	0.042	0.047	0.052	0.057	0.063	0.068	0.073	0.078	0.084	0.089	0.094	0.099	0.104	0.110	0.115	0.120	0.125	0.131	0.136	0.141	0.146	0.151	0.157	0.162	0.167	0.172	0.178	0.183
184	30	0.026	0.031	0.036	0.042	0.047	0.052	0.057	0.062	0.068	0.073	0.078	0.083	0.089	0.094	0.099	0.104	0.109	0.115	0.120	0.125	0.130	0.136	0.141	0.146	0.151	0.156	0.162	0.167	0.172	0.177	0.182
180	30	0.026	0.031	0.036	0.042	0.047	0.052	0.057	0.062	0.068	0.073	0.078	0.083	0.088	0.094	0.099	0.104	0.109	0.114	0.120	0.125	0.130	0.135	0.140	0.146	0.151	0.156	0.161	0.166	0.172	0.177	0.182
176	30	0.026	0.031	0.036	0.042	0.047	0.052	0.057	0.062	0.067	0.073	0.078	0.083	0.088	0.093	0.099	0.104	0.109	0.114	0.119	0.125	0.130	0.135	0.140	0.145	0.150	0.156	0.161	0.166	0.171	0.176	0.182
172	30	0.026	0.031	0.036	0.041	0.047	0.052	0.057	0.062	0.067	0.072	0.078	0.083	0.088	0.093	0.098	0.104	0.109	0.114	0.119	0.124	0.129	0.135	0.140	0.145	0.150	0.155	0.160	0.166	0.171	0.176	0.181
168	30	0.026	0.031	0.036	0.041	0.046	0.052	0.057	0.062	0.067	0.072	0.077	0.083	0.088	0.093	0.098	0.103	0.108	0.114	0.119	0.124	0.129	0.134	0.139	0.145	0.150	0.155	0.160	0.165	0.170	0.176	0.181
164	30	0.026	0.031	0.036	0.041	0.046	0.052	0.057	0.062	0.067	0.072	0.077	0.082	0.088	0.093	0.098	0.103	0.108	0.113	0.118	0.124	0.129	0.134	0.139	0.144	0.149	0.155	0.160	0.165	0.170	0.175	0.180
160	30	0.026	0.031	0.036	0.041	0.046	0.051	0.057	0.062	0.067	0.072	0.077	0.082	0.087	0.092	0.098	0.103	0.108	0.113	0.118	0.123	0.128	0.134	0.139	0.144	0.149	0.154	0.159	0.164	0.170	0.175	0.180
156	30	0.026	0.031	0.036	0.041	0.046	0.051	0.056	0.061	0.067	0.072	0.077	0.082	0.087	0.092	0.097	0.102	0.107	0.112	0.118	0.123	0.128	0.133	0.138	0.143	0.148	0.153	0.158	0.164	0.169	0.174	0.179
152	30	0.026	0.031	0.036	0.041	0.046	0.051	0.056	0.061	0.066	0.072	0.077	0.082	0.087	0.092	0.097	0.102	0.107	0.112	0.117	0.122	0.128	0.133	0.138	0.143	0.148	0.153	0.158	0.163	0.168	0.173	0.178
148	30	0.025	0.031	0.036	0.041	0.046	0.051	0.056	0.061	0.066	0.071	0.076	0.082	0.087	0.092	0.097	0.102	0.107	0.112	0.117	0.122	0.127	0.133	0.138	0.143	0.148	0.153	0.158	0.163	0.168	0.173	0.178
144	30	0.025	0.030	0.036	0.041	0.046	0.051	0.056	0.061	0.066	0.071	0.076	0.081	0.086	0.091	0.097	0.102	0.107	0.112	0.117	0.122	0.127	0.132	0.137	0.142	0.147	0.152	0.158	0.163	0.168	0.173	0.178
140	30	0.025	0.030	0.035	0.041	0.046	0.051	0.056	0.061	0.066	0.071	0.076	0.081	0.086	0.091	0.096	0.101	0.106	0.111	0.116	0.121	0.126	0.131	0.136	0.141	0.147	0.152	0.157	0.162	0.167	0.172	0.177
136	30	0.025	0.030	0.035	0.040	0.045	0.051	0.056	0.061	0.066	0.071	0.076	0.081	0.086	0.091	0.096	0.101	0.106	0.111	0.116	0.121	0.126	0.131	0.136	0.141	0.146	0.151	0.156	0.161	0.166	0.171	0.176
132	30	0.025	0.030	0.035	0.040	0.045	0.050	0.055	0.060	0.065	0.071	0.076	0.081	0.086	0.091	0.096	0.101	0.106	0.111	0.116	0.121	0.126	0.131	0.136	0.141	0.146	0.151	0.156	0.161	0.166	0.171	0.176
128	30	0.025	0.030	0.035	0.040	0.045	0.050	0.055	0.060	0.065	0.070	0.075	0.080	0.085	0.090	0.095	0.100	0.105	0.110	0.115	0.120	0.125	0.131	0.136	0.141	0.146	0.151	0.156	0.161	0.166	0.171	0.176
124	30	0.025	0.030	0.035	0.040	0.045	0.050	0.055	0.060	0.065	0.070	0.075	0.080	0.085	0.090	0.095	0.100	0.105	0.110	0.115	0.120	0.125	0.130	0.135	0.140	0.145	0.150	0.155	0.160	0.165	0.170	0.175
120	30	0.025	0.030	0.035	0.040	0.045	0.050	0.055	0.060	0.065	0.070	0.075	0.080	0.085	0.090	0.095	0.100	0.105	0.110	0.115	0.120	0.125	0.130	0.135	0.140	0.145	0.150	0.155	0.160	0.165	0.170	0.174
116	30	0.025	0.030	0.035	0.040	0.045	0.050	0.055	0.060	0.065	0.070	0.075	0.079	0.084	0.089	0.094	0.099	0.104	0.109	0.114	0.119	0.124	0.129	0.134	0.139	0.144	0.149	0.154	0.159	0.164	0.169	0.174
112	30	0.025	0.030	0.035	0.040	0.045	0.049	0.054	0.059	0.064	0.069	0.074	0.079	0.084	0.089	0.094	0.099	0.104	0.109	0.114	0.119	0.124	0.129	0.134	0.139	0.144	0.148	0.153	0.158	0.163	0.168	0.173
108	30	0.025	0.030	0.035	0.039	0.044	0.049	0.054	0.059	0.064	0.069	0.074	0.079	0.084	0.089	0.094	0.099	0.104	0.108	0.113	0.118	0.123	0.128	0.133	0.138	0.143	0.148	0.153	0.158	0.163	0.168	0.173
104	30	0.025	0.029	0.034	0.039	0.044	0.049	0.054	0.059	0.064	0.069	0.074	0.079	0.083	0.088	0.093	0.098	0.103	0.108	0.113	0.118	0.123	0.128	0.133	0.137	0.142	0.147	0.152	0.157	0.162	0.167	0.172
100	30	0.024	0.029	0.034	0.039	0.044	0.049	0.054	0.059	0.064	0.068	0.073	0.078	0.083	0.088	0.093	0.098	0.103	0.108	0.112	0.117	0.122	0.127	0.132	0.137	0.142	0.147	0.152	0.156	0.161	0.166	0.171
96	30	0.024	0.029	0.034	0.039	0.044	0.049	0.054	0.058	0.063	0.068	0.073	0.078	0.083	0.088	0.092	0.097	0.102	0.107	0.112	0.117	0.122	0.127	0.131	0.136	0.141	0.146	0.151	0.156	0.161	0.165	0.170
92	30	0.024	0.029	0.034	0.039	0.044	0.048	0.053	0.058	0.063	0.068	0.073	0.078	0.082	0.087	0.092	0.097	0.102	0.107	0.111	0.116	0.121	0.126	0.131	0.136	0.140	0.145	0.150	0.155	0.160	0.165	0.170
88	30	0.024	0.029	0.034	0.039	0.043	0.048	0.053	0.058	0.063	0.067	0.072	0.077	0.082	0.087	0.092	0.096	0.101	0.106	0.111	0.116	0.121	0.125	0.130	0.135	0.140	0.145	0.149	0.154	0.159	0.164	0.169
84	30	0.024	0.029	0.034	0.038	0.043	0.048	0.053	0.058	0.062	0.067	0.072	0.077	0.082	0.086	0.091	0.096	0.101	0.106	0.110	0.115	0.120	0.125	0.130	0.134	0.139	0.144	0.149	0.153	0.158	0.163	0.168
80	30	0.024	0.029	0.033	0.038	0.043	0.048	0.052	0.057	0.062	0.067	0.072	0.076	0.081	0.086	0.091	0.095	0.100	0.105	0.110	0.114	0.119	0.124	0.129	0.134	0.138	0.143	0.148	0.153	0.157	0.162	0.167
76	30	0.024	0.028	0.033	0.038	0.043	0.047	0.052	0.057	0.062	0.066	0.071	0.076	0.081	0.085	0.090	0.095	0.100	0.104	0.109	0.114	0.119	0.123	0.128	0.133	0.138	0.142	0.147	0.152	0.157	0.161	0.166
72	30	0.024	0.028	0.033	0.038	0.042	0.047	0.052	0.057	0.061	0.066	0.071	0.075	0.080	0.085	0.090	0.094	0.099	0.104	0.108	0.113	0.118	0.123	0.127	0.132	0.137	0.141	0.146	0.151	0.156	0.160	0.165
68	30	0.023	0.028	0.033	0.037	0.042	0.047	0.052	0.056	0.061	0.066	0.070	0.075	0.080	0.084	0.089	0.094	0.098	0.103	0.108	0.112	0.117	0.122	0.126	0.131	0.136	0.141	0.145	0.150	0.155	0.159	0.164
64	30	0.023	0.028	0.033	0.037	0.042	0.047	0.051	0.056	0.060	0.065	0.070	0.074	0.079	0.084	0.088	0.093	0.098	0.102	0.107	0.112	0.116	0.121	0.126	0.130	0.135	0.140	0.144	0.149	0.154	0.158	0.163
60	30	0.023	0.028	0.032	0.037	0.042	0.046	0.051	0.055	0.060	0.065	0.069	0.074	0.079	0.083	0.088	0.092	0.097	0.102	0.106	0.111	0.115	0.120	0.125	0.129	0.134	0.139	0.143	0.148	0.152	0.157	0.162
56	30	0.023	0.027	0.032	0.037	0.041	0.046	0.050	0.055	0.060	0.064	0.069	0.073	0.078	0.082	0.087	0.092	0.096	0.101	0.105	0.110	0.115	0.119	0.124	0.128	0.133	0.137	0.142	0.147	0.151	0.156	0.160
52	30	0.023	0.027	0.032	0.036	0.041	0.045	0.050	0.055	0.059	0.064	0.068	0.073	0.077	0.082	0.086	0.091	0.095	0.100	0.104	0.109	0.114	0.118	0.123	0.127	0.132	0.136	0.141	0.145	0.150	0.154	0.159
48	30	0.022	0.027	0.031	0.036	0.040	0.045	0.049	0.054	0.058	0.063	0.0675	0.072	0.076	0.081	0.085	0.090	0.094	0.099	0.103	0.108	0.112	0.117	0.121	0.126	0.130	0.135	0.139	0.144	0.148	0.153	0.157
44	30	0.022	0.027	0.031	0.036	0.040	0.045	0.049	0.053	0.058	0.062	0.0668	0.071	0.076	0.080	0.085	0.089	0.094	0.098	0.102	0.107	0.111	0.116	0.120	0.125	0.129	0.134	0.138	0.142	0.147	0.151	0.156
40	30	0.022	0.026	0.031	0.035	0.040	0.044	0.048	0.053	0.057	0.062	0.066	0.070	0.075	0.079	0.084	0.088	0.092	0.097	0.101	0.106	0.110	0.114	0.119	0.123	0.128	0.132	0.136	0.141	0.145	0.150	0.154
36	30	0.022	0.026	0.030	0.035	0.039	0.043	0.048	0.052	0.057	0.061	0.065	0.070	0.074	0.078	0.083	0.087	0.091	0.096	0.100	0.104	0.109	0.113	0.117	0.122	0.126	0.130	0.135	0.139	0.143	0.148	0.152
32	30	0.021	0.026	0.030	0.034	0.039	0.043	0.047	0.051	0.056	0.060	0.064	0.069	0.073	0.077	0.081	0.086	0.090	0.094	0.099	0.103	0.107	0.111	0.116	0.120	0.124	0.129	0.133	0.137	0.141	0.146	0.150
28	30	0.021	0.025	0.029	0.034	0.038	0.042	0.046	0.051	0.055	0.059	0.063	0.067	0.072	0.076	0.080	0.084	0.088	0.093	0.097	0.101	0.105	0.110	0.114	0.118	0.122	0.126	0.131	0.135	0.139	0.143	0.147
24	30	0.021	0.025	0.029	0.033	0.037	0.041	0.045	0.050	0.054	0.058	0.062	0.066	0.070	0.074	0.078	0.083	0.087	0.091	0.095	0.099	0.103	0.107	0.112	0.116	0.120	0.124	0.128	0.132	0.136	0.140	0.145
20	30	0.020	0.024	0.028	0.032	0.036	0.040	0.044	0.048	0.052	0.056	0.061	0.065	0.069	0.073	0.077	0.081	0.085	0.089	0.093	0.097	0.101	0.105	0.109	0.113	0.117	0.121	0.125	0.129	0.133	0.137	0.141
16	30	0.020	0.023	0.027	0.031	0.035	0.039	0.043	0.047	0.051	0.055	0.059	0.063	0.067	0.070	0.074	0.078	0.082	0.086	0.090	0.094	0.098	0.102	0.106	0.110	0.114	0.117	0.121	0.125	0.129	0.133	0.137
12	30	0.019	0.023	0.026	0.030	0.034	0.038	0.041	0.045	0.049	0.053	0.056	0.060	0.064	0.068	0.072	0.075	0.079	0.083	0.087	0.090	0.094	0.098	0.102	0.105	0.109	0.113	0.117	0.120	0.124	0.128	0.132
8	30	0.018	0.022	0.026	0.029	0.033	0.037	0.040	0.044	0.048	0.051	0.055	0.059	0.062	0.066	0.070	0.073	0.077	0.081	0.084	0.088	0.092	0.095	0.099	0.103	0.106	0.110	0.114	0.117	0.121	0.125	0.128
4	30	0.018	0.021	0.025	0.028	0.032	0.035	0.039	0.043	0.046	0.050	0.053	0.057	0.060	0.064	0.067	0.071	0.075	0.078	0.082	0.085	0.089	0.092	0.096	0.099	0.103	0.106	0.110	0.114	0.117	0.121	0.124
0	30	0.016	0.019	0.022	0.025	0.029	0.032	0.035	0.038	0.041	0.045	0.048	0.051	0.054	0.057	0.060	0.064	0.067	0.070	0.073	0.076	0.080	0.083	0.086	0.089	0.092	0.095	0.099	0.102	0.105	0.108	0.111
		0.016	0.019	0.022	0.025	0.029	0.032	0.035	0.038	0.041	0.045	0.048	0.051	0.054	0.057	0.060	0.064	0.067	0.070	0.073	0.076	0.080	0.083	0.086	0.089	0.092	0.095	0.099	0.102	0.105	0.108	0.111

Appendix 8. RFEM acceleration simulation results

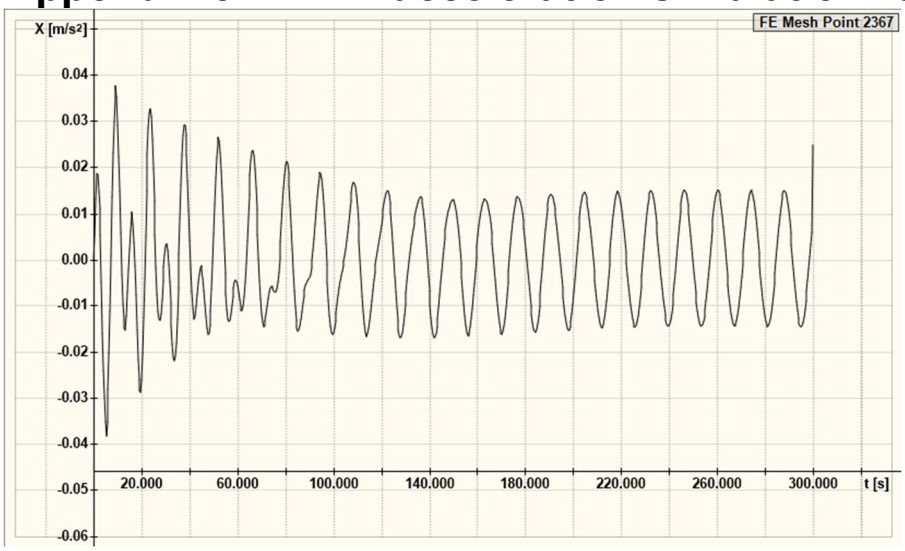

Figure 8.1. 14 m/s basic wind speed.

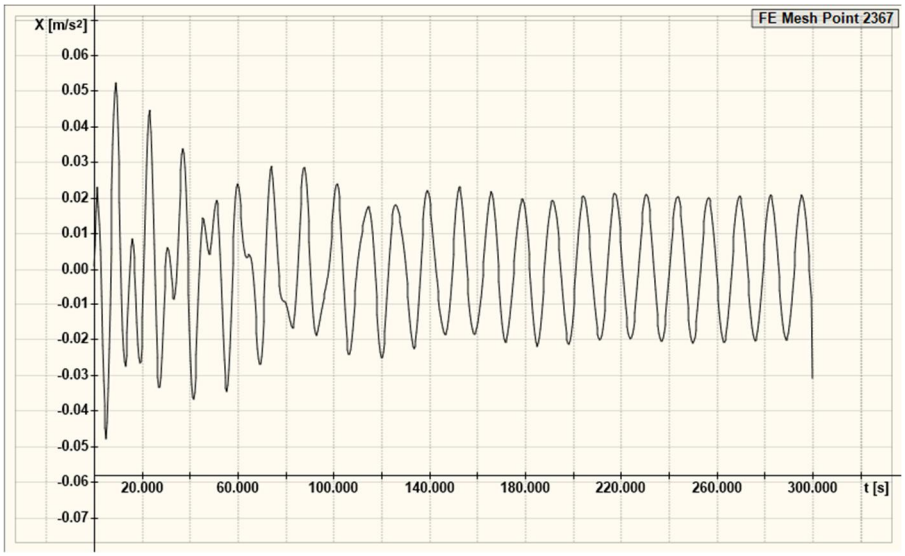

Figure 8.2. 15 m/s basic wind speed.

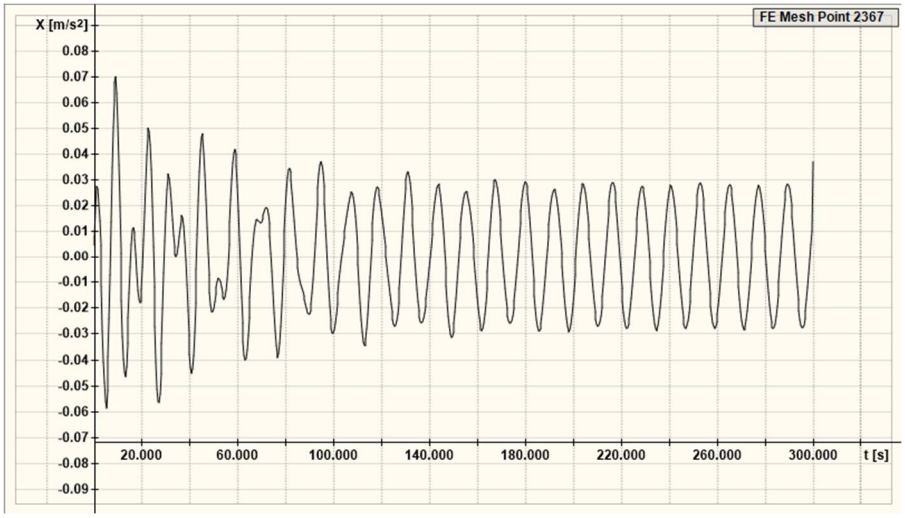

Figure 8.3. 16 m/s basic wind speed.

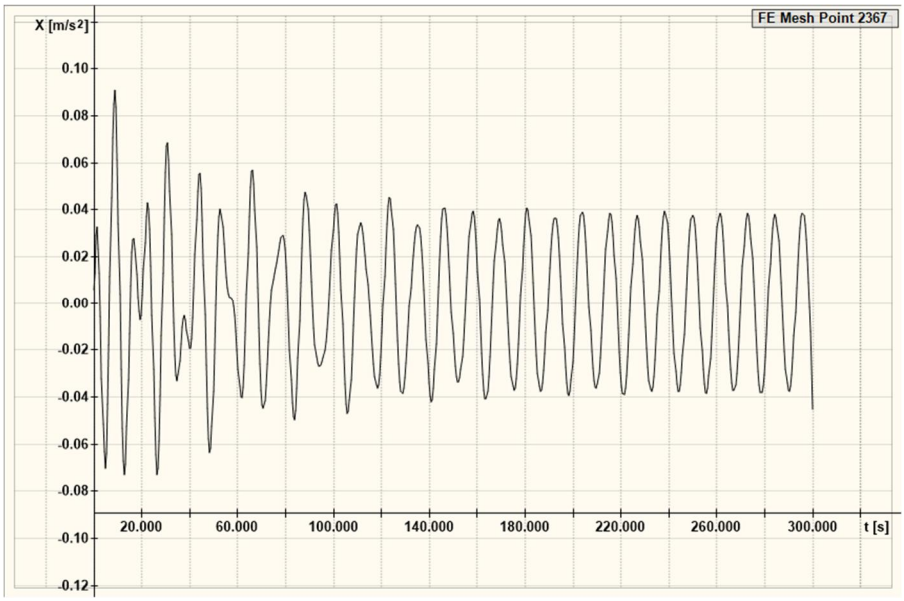

Figure 8.4. 17 m/s basic wind speed.

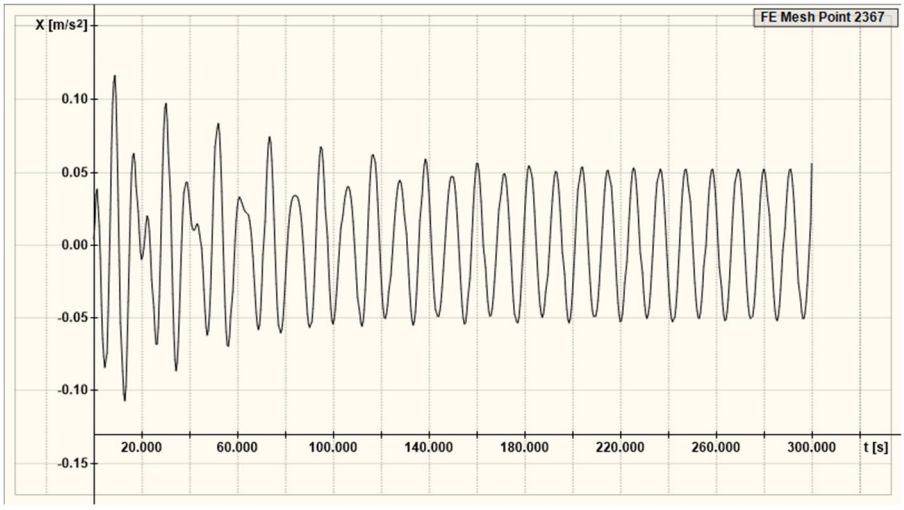

Figure 8.5. 18 m/s basic wind speed.

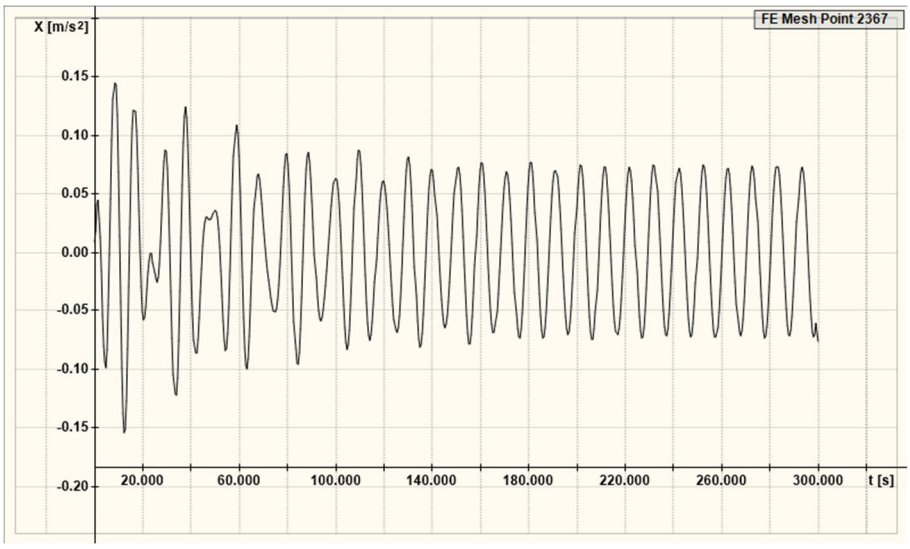

Figure 8.6. 19 m/s basic wind speed.

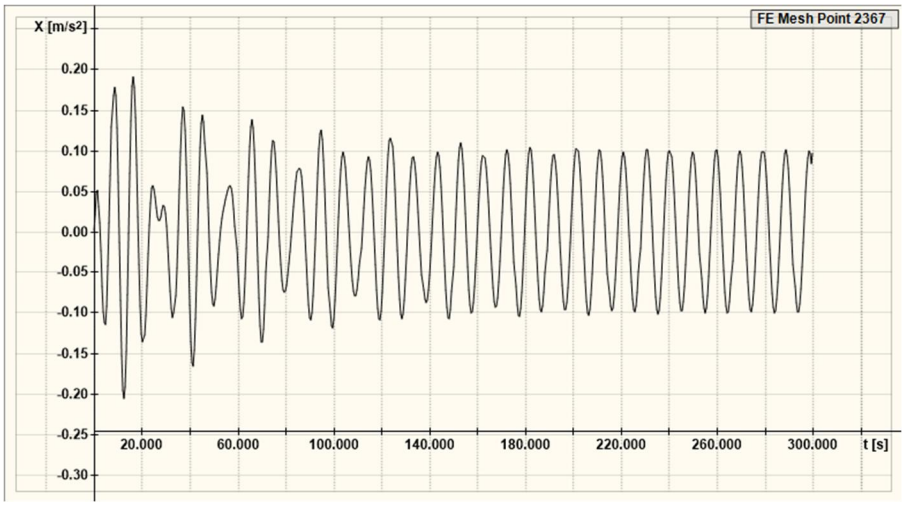

Figure 8.7. 20 m/s basic wind speed.

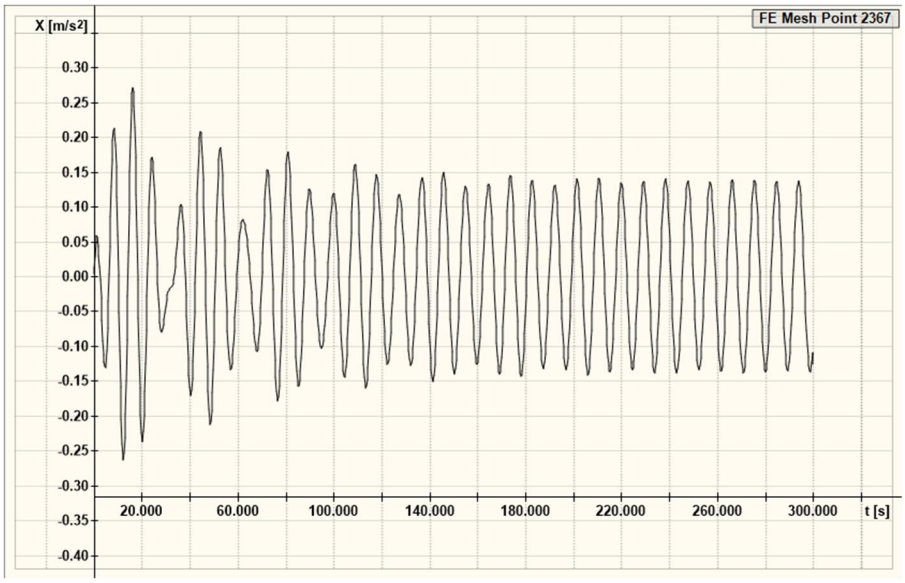

Figure 8.8. 21 m/s basic wind speed.

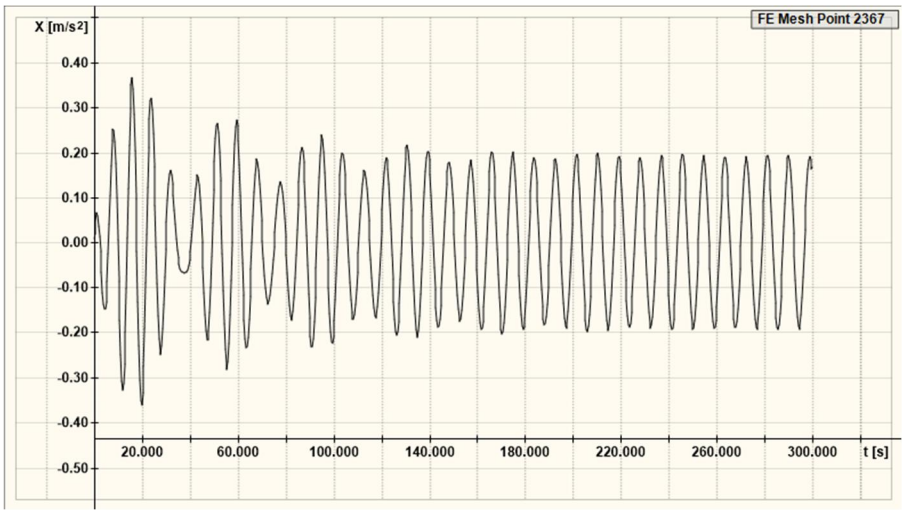

Figure 8.9. 22 m/s basic wind speed.

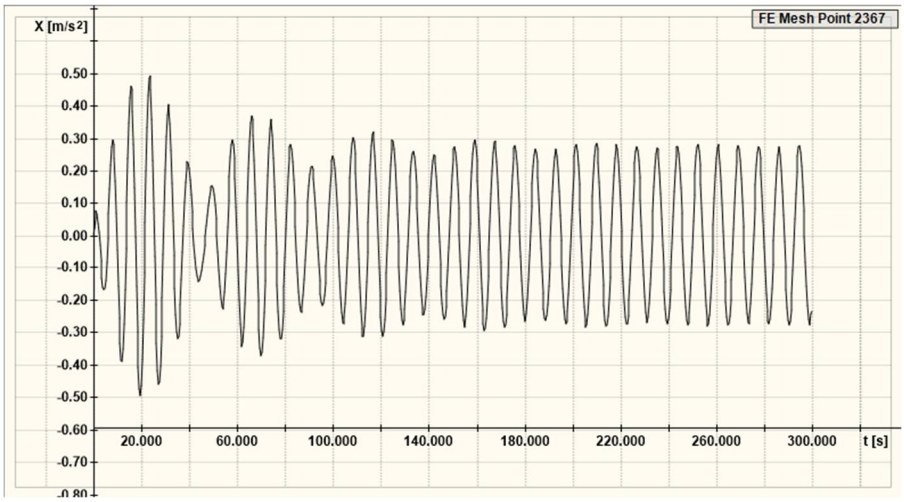

Figure 8.10. 23 m/s basic wind speed.

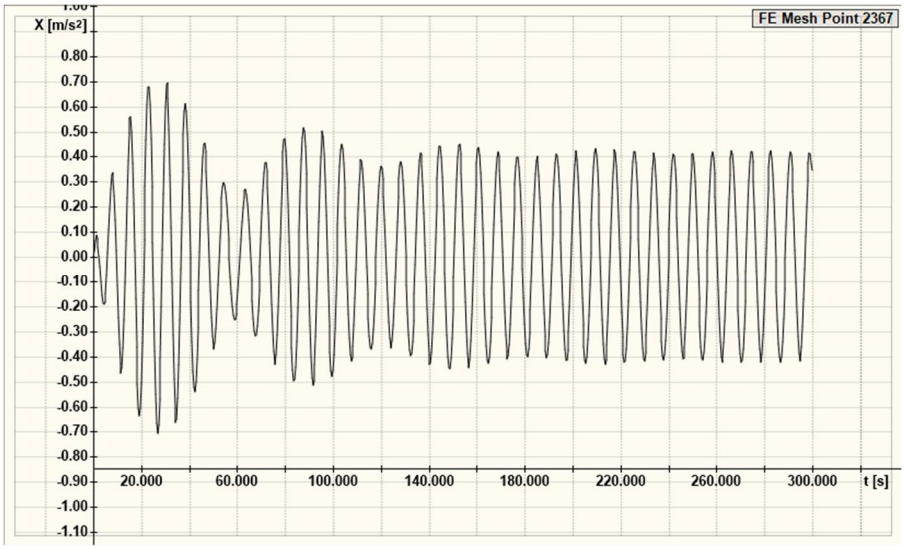

Figure 8.11. 24 m/s basic wind speed.

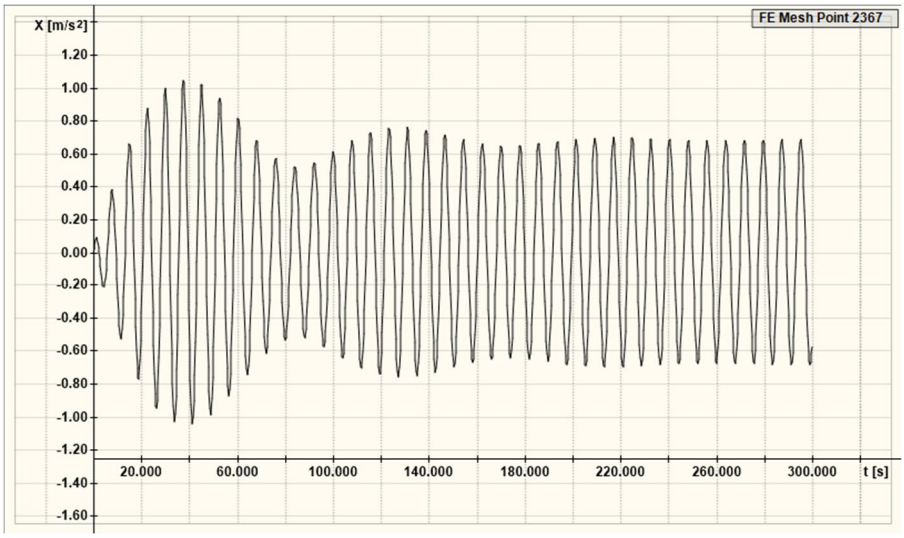

Figure 8.12. 25 m/s basic wind speed.

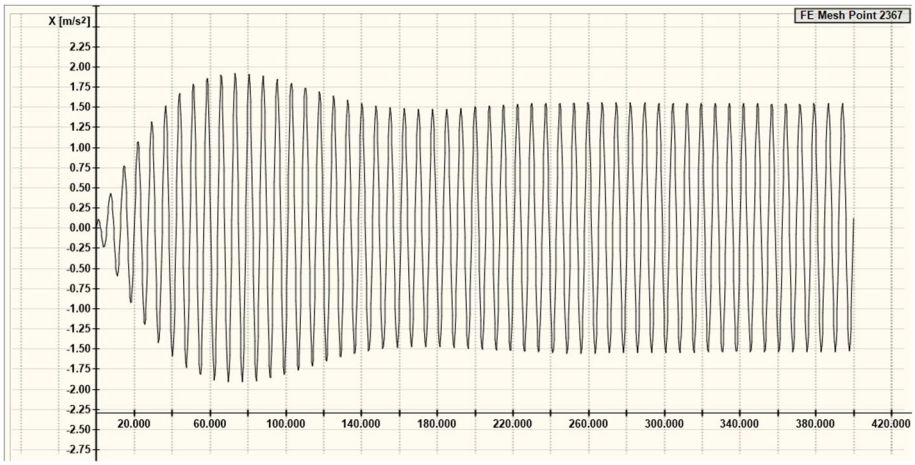

Figure 8.13. 26 m/s basic wind speed.

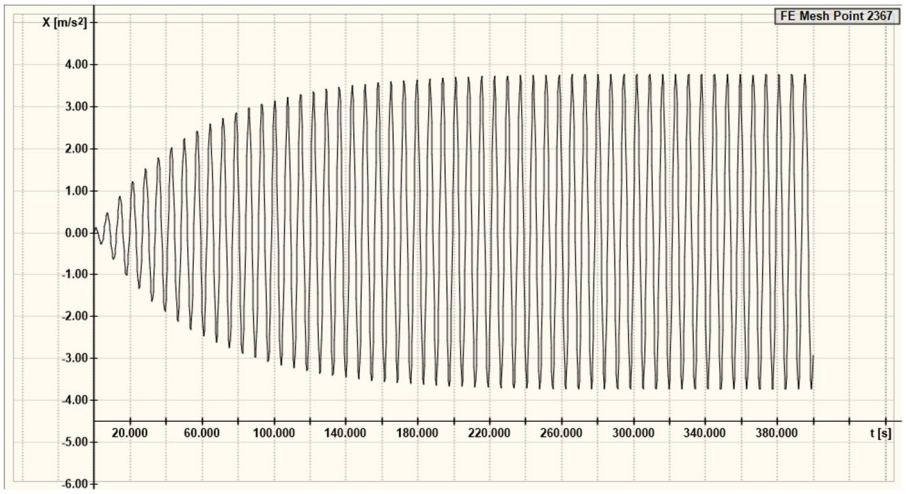

Figure 8.14. 27 m/s basic wind speed.